A model for temperature control in concrete dams

by

Johannes Lodewicus Schoeman

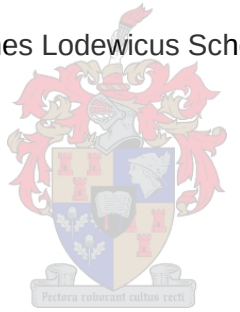

Thesis presented in fulfilment of the requirements for the degree of
Master of Engineering in the Faculty of
Engineering at Stellenbosch University

Supervisor: Prof J.A. Wium

March 2016

Declaration

By submitting this thesis electronically, I declare that the entirety of the work contained therein is my own original work, that I am the authorship owner thereof (unless to the extent explicitly otherwise stated) and that I have not previously in its entirety or in part submitted it for obtaining any qualification.

Date: March 2016

Abstract

Temperature control measures need to be implemented during the construction of concrete dams in order to avoid thermal cracking. Currently, only fragmented guidance is available to the engineer who wants to ensure that concrete temperatures remain within specified limits during the construction of such dams. The aim of this research was to develop a combined temperature control model to analyse concrete temperatures during concrete dam construction, and that includes tools and techniques developed by other researchers.

A temperature control model was subsequently developed using a literature based approach. The developed model is divided into three stages: (I) input, (II) analysis and (III) evaluation and optimisation. During the input stage, all of the required data is obtained. This data is then processed in stage II: A finite element mesh is created and thermal conductivities, specific heat capacities and densities calculated. Hydration heat characteristics are defined, solar radiation and convection boundaries are determined and initial concrete temperatures specified. The mentioned parameters are then included in a nonlinear finite element analysis, and the nodal temperature results extracted. Finally, in stage III, the input parameters are optimised in order to obtain a construction design that, when implemented, should ensure that concrete temperatures remain within specified limits throughout the construction period.

The analysis module contained in the developed model was validated using a case study. Data collected during the rehabilitation of the Stompdrift Dam was compared to the results obtained when replicating the construction process in the analysis module of the temperature control model.

The model itself was demonstrated using a simulative approach: The temperature control model was used to optimise the construction design of the rehabilitation works to Stompdrift Dam - after the fact. The data that was available prior to the construction of the rehabilitation works was used as input in the model. The model was then used to optimise the construction design. The result was a solution that ensured that concrete temperatures are kept within specified limits during construction. Following this the construction design determined by the temperature control model was demonstrated by a further analysis that incorporated both the optimised construction design and actual climate data collected during the construction period.

Finally, it was concluded that the model, as it was applied for the case of the Stompdrift Dam, is valid.

Opsomming

Temperatuurbeheermaatreëls moet toegepas word tydens die konstruksie van betondamme om temperatuurkrake te voorkom. Huidiglik is die leiding wat beskikbaar is vir ingenieurs om te verseker dat betontemperature binne gespesifiseerde perke bly gefragmenteerd. Die mikpunt van hierdie werk was om ‘n temperatuurbeheermodel te skep om betontemperature tydens die konstruksie van betondamme te analiseer. Die temperatuurbeheermodel moes ‘n kombinasie van verseie tegnieke en metodes wat deur ander navorser ontwikkel is insluit.

‘n Temperatuurbeheermodel is ontwikkel vanuit beskikbare literatuurbronne. Die model is verdeel in drie fases: (I) invoer, (II) analise en (III) evaluasie en optimering. In die invoerfase word al die benodigde data versamel. In fase II word hierdie data verwerk: ‘n eindige element maas word geskep, hittegeleidingsvermoeëns, spesifieke hittekapasiteite en digthede bepaal. Hidrasiehitte eienskappe word gedefiniëer, sonenergie radiasie en konveksie randwaardes word bereken en aanvanklike temperature vir vars beton word gespesifiseer. Hierna word ‘n nie-liniëre eindige element analise uitgevoer, en knooppunttemperature word onttrek. In fase III word die invoerdata geoptimeer om ‘n ontwerp te verkry wat behoort te verseker dat betontemperature binne gespesifiseerde limiete bly tydens konstruksie.

Die analise module wat vervat is in die ontwikkelde model is geverifieer deur gebruik te maak van ‘n gevallestudie. Data wat tydens die konstruksie van Stompdriftdam ingesamel is, is gebruik om te vergelyk met die resultate verkry wanneer die konstruksieproses in die analise nageboots word.

Die werking van die model word gedemonstreer deur van ‘n simulasie benadering gebruik te maak: Die temperatuurbeheermodel is eers gebruik om invoerdata wat voor die rehabilitasie van Stompdriftdam beskikbaar was te optimeer. Die resultaat was ‘n oplossing wat behoort te verseker dat temperature tydens konstruksie binne perke bly. Die geldigheid van die oplossing is ondersteun deur die geoptimeerde oplossing weer te analiseer – maar hierdie keer deur klimaat data te gebruik wat tydens konstruksie ingesamel is.

Laastens is daar tot die gevolgtrekking gekom dat die model, soos dit toegepas is in die geval van Stompdriftdam, geldig is.

Acknowledgements

My sincerest thanks to Anculien, who supported, motivated, inspired and encouraged me throughout, and for tolerating my lack of attention when I could not give it.

Thank you Deon, Johan and Vincent for your help in collecting the data. I could not have done it without you.

Thank you Dok Chris for motivating me to undertake this study, giving me the opportunity to do so and for being a great mentor.

I owe a debt of gratitude to the Department of Water & Sanitation for granting me the opportunity to use the rehabilitation of the Stompdrift Dam as a case study.

Thank you Professor Wium for your patience and guidance, and for reassuring me when I needed it.

To all the others who supported me – family and friends – you helped carry me.

Finally, thanks to God, through whom all things are possible.

Table of contents

List of figures

List of tables

Abbreviations

3-D	Three dimesnional
GGBS	Ground granulated blast-furnace slag
LST	Lump Sum Temperature
PCA	Portland Cement Association
RCC	Roller compacted concrete
w/c	Water / binder ratio

Chapter 1: Introduction

1.1 Background information

The Upper Stillwater Dam is located high in the Utah mountains where the annual average temperature is only 2.8° above freezing. During the construction of the dam a maximum concrete placement temperature of 10 °C was specified to minimise the effects of thermal contraction on the dam (Hansen & Forbes, 2012). After the dam's first filling, 23 vertical cracks developed in an upstream / downstream direction at an average spacing of 28 m. In addition to the cracks associated with thermal contraction, some cracks may have been initiated by a 10 mm horizontal downstream movement in the foundation after the reservoir load was applied to the dam. Figure 1-1 shows water leaking into the gallery through one of the cracks.

Figure 1-1 Water leaking into a gallery from a crack at Upper Stillwater Dam (Hansen & Forbes, 2012).

Cracking in concrete dams is undesirable - it can affect structural safety, water-tightness, durability, appearance and internal stresses (Townsend, 1981). As was illustrated in the case of the Upper Stillwater Dam, volumetric changes in concrete dams as a result of temperature change can, on its own or in combination with other loads, cause cracking of concrete (Hansen & Forbes, 2012). Two mechanisms related to thermal cracking are briefly described below:

Thermal contraction / expansion: Rise or fall in the average temperature in a concrete element causes an increase or decrease in the volume the element. If the average temperature in a concrete element drops, this will result in a reduction of the element's volume. If this volume change is restrained by, for instance, the foundation, stresses will be induced in the element (Conrad, 2006). If the induced stresses, on its own or in combination

with other factors, exceed the concrete's strength, cracking will result (Noorzaei, Bayagoob, Thanoon, & Jaafar, 2006).

Thermal gradients: During the hydration of cement, heat is generated. In thin concrete sections the generated heat dissipates to the atmosphere relatively quickly and the temperature of the concrete is not greatly influenced. In mass concrete elements, such as those encountered in most concrete dams, however, the internal temperature can reach high levels, while the temperature at the outer edges remain relatively low. The uneven temperature distribution throughout the concrete element is known as a thermal gradient, and results in a non-uniform volume change across the element 's cross section, thereby inducing stresses which can contribute to cracks forming (Klemczak & Knoppik-Wróbel, 2011).

1.2 Problem statement

To minimise or avoid thermal cracking of mass concrete members temperature control measures need to be implemented (Townsend, 1981). To this end it is common practice for engineers to specify a maximum and / or minimum allowable concrete temperature and possibly a maximum temperature differential between the centre and outside of a concrete element during construction (American Concrete Institute, 1999; Folliard et al., 2008).

Various methods exist to control concrete temperature to some extent. These methods, or interventions, can be as simple as using wooden shutters instead of steel shutters to better insulate fresh concrete (Ballim & Graham, 2004), or they can be as intricate as providing a cooling plant to cool aggregate before concrete batching (ACI Committe 207, 1993).

In the light of the need to control concrete temperatures during construction and the various interventions that can be implemented, the problem is how to decide which of these temperature control methods to implement, if any. This is a problem because it is sometimes not known to what extent certain temperature control mechanisms will influence the temperature distribution in mass concrete members over time. This uncertainty can lead to over- or underestimation of an intervention's effect on the temperature distribution. Overestimation of concrete temperature may lead to additional, unnecessary temperature control measures being implemented, thereby increasing costs. Underestimation can lead to concrete temperatures, temperature gradients or stresses higher or lower than specified by the engineer and might lead to thermal cracking. More accurate predictions of the effects of certain interventions will lead to cost effective dam construction to the specified performance standards.

1.3 Scope of study

Calculation procedures to determine the temperature distribution in concrete elements over time using various numerical methods are well documented in literature. The effects of certain temperature control measures and how to incorporate them into thermal analyses are also extensively described in published writings. This thesis aims to build on what has been done before by incorporating the existing knowledge on temperature calculation procedures and temperature control methods into a new temperature control model. The purpose of the proposed model is that it should be used to evaluate the effects of various temperature control interventions at design stage in order to decide which intervention, or combination of interventions, to impose during construction to achieve a desired temperature distribution throughout a concrete dam during and after construction.

In the light of the above, it is put forward as a premise that the temperature distribution in sequentially constructed concrete dams can be kept within specified limits during construction by implementing the proposed temperature control model during the design stage. To be clear: Controlling the temperature distribution is taken to mean that it is ensured that concrete temperatures remain within specified limits. The proposed temperature control model is shown in Figure 1-2.

This study focuses on temperature control in unreinforced concrete dams during construction. Hydration heat development, conduction, convection and solar radiation are dealt with as part of the study. Convective heat transfer between air and concrete is dealt with, but not between concrete and water, as impoundment normally takes place after peak temperatures are reached within the concrete body. Emphasis is placed on the South African context with regards to the materials and the construction techniques included in the study. The use of cooling pipes is excluded from the study, as its implementation is not very common in South Africa. Only portland cement and fly ash cementitious materials are included, as a combination of these two cementitious materials is frequently used in South African concrete dams.

1.4 Research objectives

Currently, only fragmented guidance is available to the engineer who wants to ensure that concrete temperatures remain within specified limits during the construction of concrete dams. Tools and techniques have been developed by other researchers that, when used in combination, can be used to ensure that concrete temperatures remain within specified limits. The aim of this research was to develop a combined model to calculate and control

concrete temperatures during the construction of concrete dams, that incorporates several tools and techniques developed by other researchers.

Three objectives were set to meet the aim stated above:

- Develop a temperature control model from the combined work of other researchers.
- Show that the analytical module included in the proposed model can be used to accurately model concrete temperature development during the construction of a concrete dam.
- Demonstrate that the proposed temperature control model can be used to ensure that concrete temperatures remain within specified limits during construction.

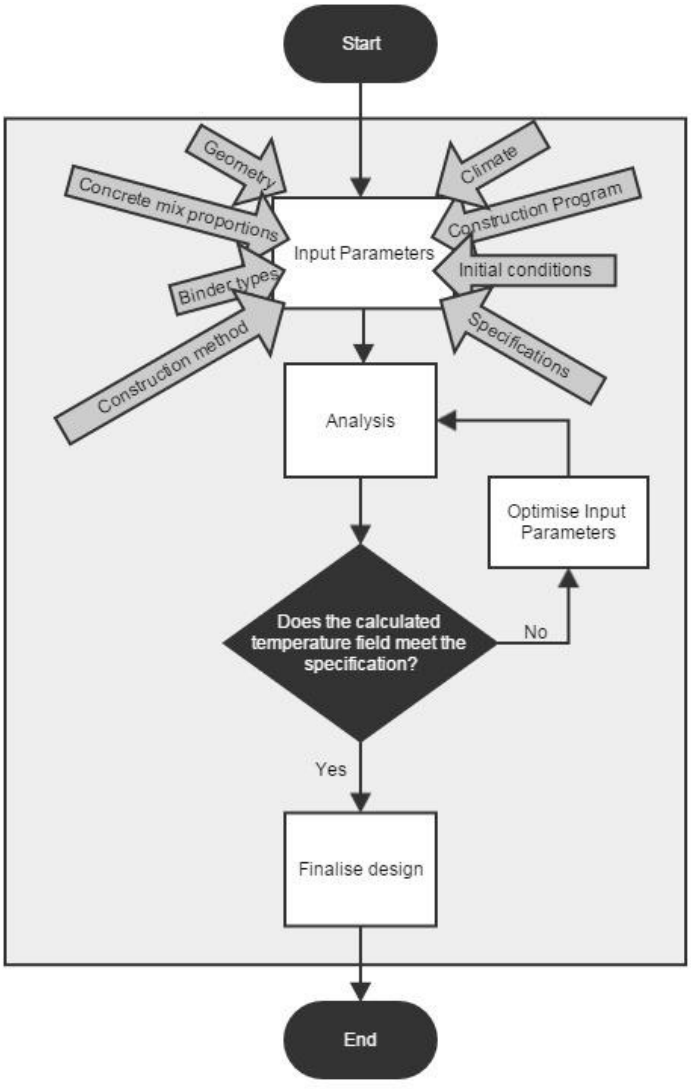

Figure 1-2 A flow-diagram of the proposed temperature control model.

If it is shown that the proposed model can be used to ensure that concrete temperatures remain within specified limits during construction, then the aim of the study would have been met.

1.5 Thesis structure

The theoretical basis and underlying assumptions used in the development of the proposed model are described in the Chapter 2. This chapter provides an overview of available literature on the theory related to heat transfer, thermal analysis and factors that influence temperature development over time.

In Chapter 3 the methods that were followed to achieve the objectives of this study are elaborated on. Different research methods that could be used to achieve the goals of the study are discussed. After suitable methods are selected, details on how these methods were implemented in this study are provided. Emphasis is placed on the methods by which data was collected, the quality of the data, as well as how the data was analysed in subsequent chapters.

Chapter 4 deals with the development of the temperature control model. Here, the model is presented, elaborating on which techniques and methods obtained from literature were selected for inclusion into the model.

In chapter 5 a case study – the rehabilitation of the Stompdrift Dam - is presented. The focus of this chapter is to demonstrate how accurate the model is. This is done by comparing in-situ concrete temperature data with the results obtained from analysing the construction process of one of the blocks using the analysis module contained in the temperature control module.

Chapter 6 describes the implementation of the model at the hand of an example – also the rehabilitation of the Stompdrift Dam. In this chapter data that was available prior to the construction of the rehabilitation works is taken as input into the model. The model is then used to optimise the input data, thereby determining a solution that should conform to pre-set specifications. Finally, the model is demonstrated by simulating a combination of the optimised input parameters and the actual climate conditions encountered during the construction of the rehabilitation works.

The final chapter of the thesis deals with conclusions that can be drawn from this study and recommendations for future research.

Chapter 2: Literature Review

2.1 Introduction

This chapter presents a review of available literature on the principles of heat transfer and illustrates how these principles can be used to manage the thermal behaviour of concrete dams. The ultimate goal of assembling this information is to implement it in the proposed temperature control model.

The principles of heat transfer forms the basis of the analysis procedure required as part of the proposed temperature control model, and are described first: It will be shown how conduction, internal heat generation, convection and radiation can be described mathematically by the Fourier heat transfer equation (commonly known as the heat flow equation), with accompanying boundary conditions. In the proposed model the results obtained from solving the heat flow equation are used to evaluate if the analysed design conforms to prescribed specifications.

Solving the heat flow equation, however, is not a trivial matter when considering complex problems. Several numerical methods can be used to solve the heat flow equation. The most suitable numerical methods for the current application are considered to be the finite difference and finite element methods. The finite element method is the preferred over the finite difference method, mainly because (i) the finite element method has greater flexibility in terms of the geometries that can be evaluated and (ii) that commercial finite element analysis software packages for transient temperature analysis are more widely available. As the technique that is used to solve the heat flow equation greatly affects the results obtained, the use of the finite element method to solve the heat flow equation is evaluated in terms of its ability to accurately model transient concrete temperature profiles.

Next, factors that affect heat transfer in concrete dams are elaborated upon. Both internal and external factors are discussed. Internal factors refer to thermal diffusivity and internal heat generation, while external factors refer to aspects that influence the amount of energy that is transferred to or from the concrete from atmospheric conditions due to convection and radiation. These above mentioned internal and external factors need to be taken into account when solving the heat flow equation. The models of various authors on how to take these factors into account during analysis are consequently reviewed. In addition to describing factors that influence heat transfer in concrete dams, ways are also described by which these internal and external factors can be controlled and managed during construction.

Finally, temperature specifications are briefly discussed. Specifications form the final part of the temperature control model: the measure by which the adequacy of a design is judged.

2.2 Heat transfer

The modelling of heat transfer lies at the centre of the temperature control methodology developed as part of this study. This sub-section focuses on the theoretical basis of heat transfer analysis, which forms the foundation of the analysis method that is used in the proposed methodology.

In general heat transfer deals with solids, liquids and gasses. Solids are of prime interest for the purpose of this thesis (although concrete does contain liquid phases before and during hydration). Heat flows within a solid by conduction, while it is transferred to and from a body by convection and radiation. Heat may also be generated internally as a result of internal heat generation.

Mathematically, the mechanisms mentioned above can be described by a boundary value problem. The governing equation for three-dimensional (3-D) unsteady heat flow, which can be derived from the Fourier law of heat conduction and the energy conservation principle, is shown in differential form in Equation 2.2.1. This equation is commonly referred to as the heat flow equation (Ballim, 2004a; Kuzmanovic, Savic, & Stefanakos, 2010; Luna & Wu, 2000; Zill & Cullen, 2006).

$$\rho \cdot C \cdot \frac{\partial T}{\partial t} = k\left(\frac{\partial^2 T}{\partial x^2} + \frac{\partial^2 T}{\partial y^2} + \frac{\partial^2 T}{\partial z^2}\right) + \frac{\partial Q_w}{\partial t} \qquad 2.2.1$$

Where:

	ρ	=	Density of the object (kg/m^3)
	C	=	Specific heat capacity of the object (J/kg·K)
	T	=	Temperature (K; °C is used when radiation is not involved)
	k	=	Isotropic thermal conductivity of the object (W/m·K)
	x, y & z	=	Cartesian coordinates at a particular point in the object (m)
	Q_w	=	Heat evolved at a particular point in the object (J/m^3)
	$\frac{\partial Q_w}{\partial t} = q_w$	=	Time rate of heat evolution at point (x, y, z) (W/m^3)

Four types of boundary conditions are applied to the heat transfer equation:

- Dirichlet boundary conditions;
- Neumann boundary conditions;
- Robin boundary conditions; and
- Nonlinear, mixed boundary conditions.

2.2.1 Dirichlet boundary conditions

The initial temperature of fresh concrete at the time of placement is an important parameter that needs to be taken into account when considered in the context of the proposed temperature control model. For transient thermal analyses the initial temperature of the subject being analysed needs to be specified over its entire volume at the start of the analysis (TNO DIANA BV, 2014).

Dirichlet, or essential, boundary conditions are applied to a differential equation when the solution (temperature) on the volumetric domain is specified. In the case of Equation 2.2.1 this implies that the temperature is specified (Cheng & Cheng, 2005; Nikishkov, 2010).

$$T_{S1} = T(x, y, z, t) \qquad 2.2.2$$

Where: $S1$ = Domain where temperature is specified

2.2.2 Neumann boundary conditions

The intention of the proposed temperature control methodology is that it should be applicable to concrete dams of various shapes and sizes, including roller compacted concrete (RCC) dams. Consider the concrete temperature distribution during the construction of a RCC gravity dam with a length (left bank to right bank) much greater than its width or height. RCC is generally placed in continuous horizontal layers across the length of a dam (Luna & Wu, 2000). As the length of the dam under consideration is much greater than its width and height, it can reasonably be assumed that heat flow in the length direction (z-direction) will approach zero (Kuzmanovic et al., 2010). Perfectly insulated conditions are implied on the xy-plane $\left(\frac{\partial T}{\partial z} = 0\right)$.

Neumann, or natural, boundary conditions specify the normal derivative of a solution along the boundary region. In the context of heat flow analysis this implies specifying the heat flow across the outer surface of the body (Cheng & Cheng, 2005; Nikishkov, 2010; Van Rooyen, 2008). In mathematical form:

$$q_{S2} = -k\left(\frac{\partial T}{\partial x} \cdot n_x + \frac{\partial T}{\partial y} \cdot n_y + \frac{\partial T}{\partial z} \cdot n_z\right) \qquad 2.2.3$$

Where: q_{S2} = Heat flux (W/m^2) on boundary where heat flow is specified.

n_x, n_y, n_z = Coordinates of the unit vector normal to the boundary at point (x, y, z)

2.2.3 Robin boundary conditions

As part of the proposed temperature control methodology the effect of insulation on the amount of heat that is transferred to and from the concrete body by convection and radiation can be evaluated. Robin, or mixed, boundary conditions specified on the boundary domain specify a weighted, linear combination of Dirichlet and Neumann boundary conditions. Robin boundary conditions are used to model convection.

Heat flow across a convection boundary is assumed to follow Newton's law of cooling, which states that the heat flow between a surface and the ambient region is proportional to the temperature difference between the surface and the ambient temperatures (Cook, Malkus, Plesha, & Witt, 2002; Kuzmanovic et al., 2010; Nikishkov, 2010). Mathematically, this relationship is described by:

$$q_{S3} = h\left(T_{S3} - T_{eff}\right) = -k\left(\frac{\partial T}{\partial x}\cdot n_x + \frac{\partial T}{\partial y}\cdot n_y + \frac{\partial T}{\partial z}\cdot n_z\right) \qquad 2.2.4$$

Where: q_{S3} = Convective heat transfer rate (W/m^2) on boundary $S3$ where convection is specified

T_{eff} = Effective environmental temperature at time t

h = Convection coefficient (W/m^2·K)

When the upstream face of a dam that is exposed to water is considered, Equation 2.2.4 can also be used to model convection between the water and the concrete. If the downstream face of the dam is considered, the rate of heat transfer at the boundary is dependent on a combination of convection between the air and concrete, as well as solar radiation.

2.2.4 Nonlinear, mixed boundary conditions

As mentioned above, heat transfer by radiation plays a significant role when evaluating the effects of some temperature control interventions. A radiation boundary can be described by a weighted, nonlinear combination of Dirichlet and Neumann boundary conditions (Cook et al., 2002; Nikishkov, 2010). The expression for radiation boundary conditions is:

$$\sigma\cdot\varepsilon\cdot T_{S4}^4 - \alpha\cdot q_r = -k\left(\frac{\partial T}{\partial x}\cdot n_x + \frac{\partial T}{\partial y}\cdot n_y + \frac{\partial T}{\partial z}\cdot n_z\right) \qquad 2.2.5$$

Where: σ = Stefan-Boltzmann constant ($\sigma = 5.670 \times 10^{-8}$ W/m^2·K^4)

ε = Surface emission coefficient

T_{S4} = Temperature on boundary where radiation is specified

α = Surface absorption coefficient

q_r = Incident radiant heat flow per unit area at time t

2.3 Numerical analysis: finite element analysis

It is impossible to find explicit formulas for solutions to all differential equations (Trench, 2013). As the typical geometry of dams that are to be modelled tends to be relatively complex, a numerical method to solve Equation 2.2.1 is preferred for use in the proposed temperature control model.

The popularity of six different numerical techniques to solve partial differential equations is illustrated in a study by Cheng & Cheng (2005). A bibliographic database search performed showed that the finite element method was the most popular method of the six methods, mentioned in 67% of the entries. The finite difference method was the second most mentioned method, mentioned in 18% of the entries.

The application of the finite element method to the heat flow equation as it applies to the proposed temperature control model is discussed below. The focus of this sub-section is on the validity of utilizing the finite element method to model the temperature distribution in concrete dams during and after construction, rather than on the underlying theoretical background of the method or how it is implemented in any specific commercially available software package. The reader is referred to any of the various manuals available on the topic for information on the method's theoretical background (Amirouche, 2006; Cook et al., 2002).

A question that can be asked is: how well is finite element analysis suited to evaluating the thermal problems that need to be solved in order to evaluate the effects of different temperature control interventions?

A precedent has been set for the use of finite element analysis to evaluate various aspects related to temperature control at dams. Examples that can be cited are the study by da Silva, Šmilauer, & Štemberk (2015) that describes a novel way of modelling hydration heat development which is applicable to various binder types; Chen, Wang, Li, & Chen's (2003) study evaluates the influence of concrete placement temperature, construction commencement date and construction rate; and the study by Cervera, Oliver, & Prato (2000) that evaluate the effects of thermal properties of different concrete mixes. This list is by no means exhaustive, but the point has been made that, quantitatively, the use of finite element analysis to evaluate different aspects that affect the temperature distribution in concrete dams over time is well established.

How do the results of finite element analyses of temperature control interventions applied to concrete dams during construction compare with actual, experimentally verified data? As an illustration results obtained from da Silva et al. (2015) are presented in Figure 2-1. The goal

of the study by da Silva et al. (2015) was to investigate the use of semi-adiabatic measurements for simulating the rise in concrete temperature resulting from hydration heat liberation. Different concrete mixes containing different ratios of supplementary cementing materials were used in the two experiments of which the temperature distribution at several positions over time is given in Figure 2-1.

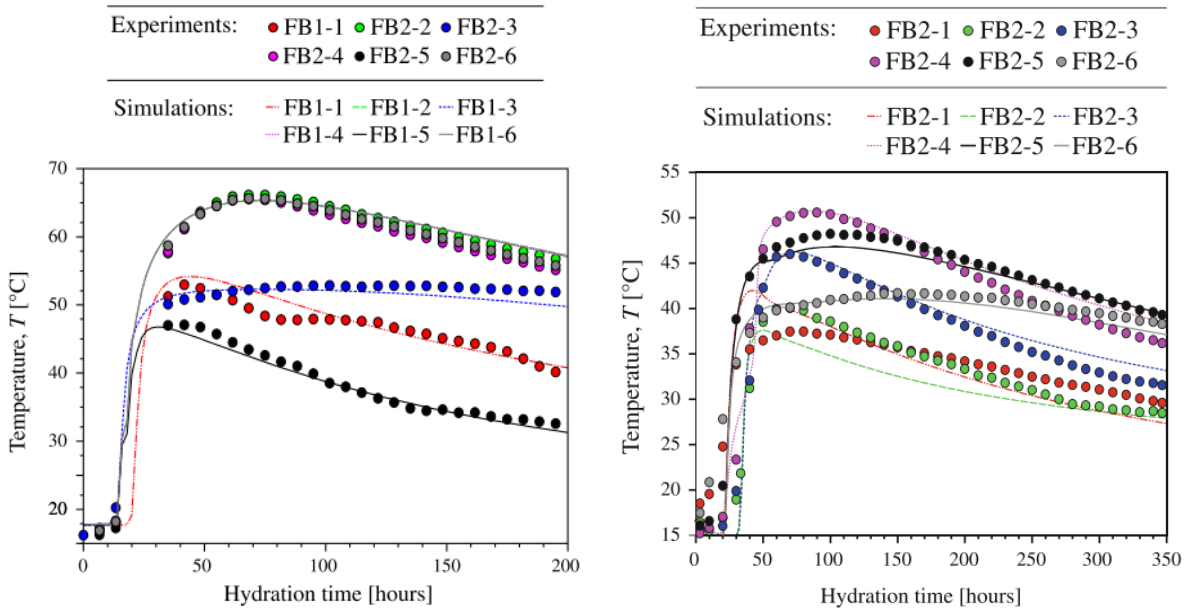

(a) 511 m^3 mass concrete foundation block **(b) 1050 m^3 mass concrete foundation block**

Figure 2-1 A comparison of measured concrete temperatures with values simulated using finite element analysis (da Silva et al., 2015).

The results presented in Figure 2-1 show good correlation between the measured and modelled early age temperature close to centre of construction lifts (FB1 - 2, 4 & 6 and FB2 - 3, 4 & 5), while a comparison of the results closer to the sides of the blocks generally show some deviation (up to 15 % for FB2 – 1) between modelled and measured values.

The deviation between the modelled and measured results near the concrete elements' sides can be explained by the approach the study followed to model convection, conduction and radiation. Convection and conduction were modelled using constant values. The effect of radiation was not modelled. Evaluation of the measured results close to the elements' edges show that the concrete temperature field in these regions is sensitive to these boundary conditions. The inadequacy of this linear approach to model these phenomena is illustrated later in this chapter where the nonlinearities associated with each of these effects are discussed.

External boundary conditions have relatively little influence on the concrete temperature closer to the centre of mass concrete elements at early ages – according the ACI Committee

207 (1993) the temperature rise at the centre of mass concrete elements with heights greater than 1.5 m is essentially adiabatic. Consequently the good correlation between measured and modelled results close to the centres of both mass concrete blocks can be used as motivation for utilising finite element analysis to model concrete temperature rise resulting from hydration, notwithstanding the deviation between the modelled and measured results closer to the edges of the concrete blocks. The aim of the cited study was to establish whether semi-adiabatic calorimetry could be used to accurately model temperature rise in mass concrete elements – not to accurately model convection, conduction or radiation.

The use of a finite element analysis to model temperature rise resulting from heat liberation during the hydration of cement, as well as for evaluating the hydration characteristics of different concretes has been qualitatively validated above. The validity of using finite element analysis to model other temperature control interventions will be dealt with implicitly throughout the rest of this chapter, where each of the mechanisms that contribute to the proposed temperature control model are discussed.

2.4 Thermal diffusivity

The first internal factor affecting heat transfer which is considered is thermal diffusivity. Thermal diffusivity is a material specific parameter that describes how fast temperature changes in a material would occur under a thermal gradient. The thermal diffusivity of a material is dependent on its thermal conductivity, density and specific heat capacity. The parameter is expressed mathematically as (ACI Committe 207, 1997):

$$F = \frac{k}{\rho \cdot C} \qquad 2.4.1$$

Where: F = Thermal diffusivity (m^2/s)

k = Isotropic thermal conductivity of the object (W/m·K)

ρ = Density of the object (kg/m^3)

C = Specific heat capacity of the object (J/kg·K)

Each of the three parameters that are amalgamated into the thermal diffusivity concept affects how the temperature of a region within a concrete element will react when there is a temperature difference between adjoining regions.

Large thermal gradients within a concrete body can lead to thermal cracking (Riding, Poole, Schindler, Juenger, & Folliard, 2007a). The use of low thermal diffusivity concrete to control thermal gradients is illustrated as part of the parametric study presented in Chapter 6 of this document. On the other hand, high diffusivity in combination with a relatively slow

construction rate could reduce the maximum temperature rise resulting from hydration heat liberation. The influence of thermal diffusivity in combination with construction rate is also illustrated as part of the parametric study in Chapter 6. The accurate modelling of each of the parameters used to calculate thermal diffusivity is thus essential for the proper working of the proposed temperature control model.

Literature available on the estimation of these three parameters is described below, with the ultimate aim of utilising the presented estimation methods or techniques as part of the analysis procedure in the proposed temperature control model.

2.4.1 Thermal conductivity

Conduction is the process whereby heat is transmitted through a material when it is subjected to a temperature gradient. Thermal conductivity, simply put, is a basis for comparison of the ability of a material to conduct heat (energy) under a temperature gradient. A volume of concrete with a high thermal conductivity will consequently transfer heat (energy) at a greater rate under the same thermal gradient than would be the case for a volume of concrete with a low thermal conductivity.

Factors affecting the thermal conductivity of concrete

Various factors influence the thermal conductivity of concrete. These dependencies can be summarised as follows:

Mix proportions: Concrete is made from ingredients that have dissimilar thermal conductivities. It is clear from various sources that the thermal conductivity of concrete is proportional to the ratio in which the different ingredients are present in the concrete (Choktaweekarn, Saengsoy, & Tangtermsirikul, 2009b; Khan, 2002; K. Kim, Jeon, J. Kim, & Yang, 2003). Table 2-1 illustrates the difference in conductivity between the different concrete ingredients considered in the experimental study by Choktaweekarn et al. (2009b).

Table 2-1 Thermal conductivities of ingredients found in concrete (Choktaweekarn et al., 2009b; Wang & Aki, 1996).

Ingredient	Limestone	Grey-wacke	Quartz sand	Air	Water	Portland cement	Fly ash	Hydrated product
Thermal conductivity (W/m.K)	2.56	2.5 – 3.4	3.49	0.03	0.59	1.55	0.76	1.16

Type of aggregate used: Researchers generally agree that concrete made with aggregate with a lower thermal conductivity will yield concrete with lower conductivity, while the use of more conductive aggregates will yield a more conductive concrete (Ballim & Graham, 2009; Khan, 2002; K. Kim et al., 2003).

Table 2-1 shows the difference between the thermal conductivity of two types of rocks – limestone and quartz. Khan (2002) notes that not only is thermal conductivity dependant on the type of rock, but that it is also dependant on the degree of crystalisation of the rock itself: Rocks with crystaline structure have higher conductivities than amorphous or vitreous rocks of the same type. Figure 2-2 shows data published by Čermák & Rybach (1982; in Conrad, 2006) for values of the thermal conductivities of commonly used concrete aggregates.

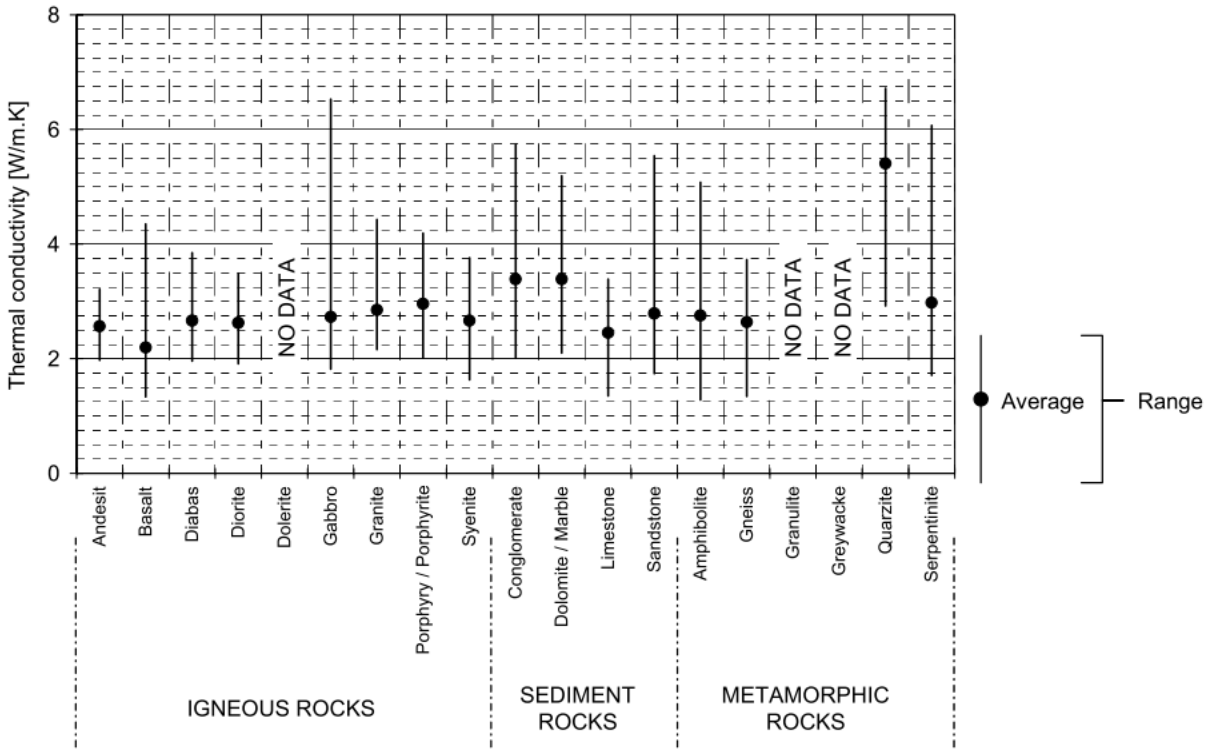

Figure 2-2 Range of thermal conductivities for different types of rocks used as aggregate in concrete (Čermák & Rybach, 1982 reproduced in Conrad, 2006).

Ballim & Graham (2009) suggest that aggregate type is the factor with the largest influence on thermal conductivity. The authors published average values for the thermal conductivity of concrete based only on the type of aggregate used. These values, which are intended to be used as a first estimate for conductivity, are reproduced here in Table 2-2.

Table 2-2 Thermal conductivity of concrete made with a range of common aggregates (Ballim & Graham, 2009).

Type of aggregate	Thermal conductivity of concrete (W/m.K)
Quartzite	3.5
Dolomite	3.2
Limestone	2.6 – 3.3
Granite	2.6 – 2.7
Rhyolite	2.2
Basalt	1.9 – 2.2

Degree of saturation (moisture content): The thermal conductivity of air is much lower than that of water. Concrete that is fully saturated will consequently have a higher conductivity (Choktaweekarn et al., 2009b; Demirboğa, Türkmen, & Karakoç, 2007; Khan, 2002).

According to Khan (2002) the conductivity of fully saturated concrete is between 44 and 64 % greater than an oven dry sample, depending on the type of aggregate used.

Temperature: Thermal conductivity of concrete decreases nearly linearly with an increase in temperature (K. Kim et al., 2003). However, the effect is small over the range of temperatures that mass concrete is normally exposed to (Ballim & Graham, 2009).

Age (degree of hydration): There is disagreement amongst researcher as to the effect of concrete age on thermal conductivity. Some researchers have reported a drop of up to 30 % in thermal conductivity during the first seven days of hydration (Brown & Javaid, 1970), while others report no influence at all (K. Kim et al., 2003) or a slight increase during the first three to six days (van Breugel, 1998 in Ballim & Graham, 2009; Choktaweekarn et al., 2009b).

Choktaweekarn et al. (2009b) suggest that the disagreement between the results of the previous researchers can be attributed to the different curing conditions, moisture contents and testing procedures used in these studies.

Supplementary cementing materials: Several authors (Choktaweekarn et al., 2009b; Demirboğa et al., 2007; Kim et al., 2003) have shown that replacing a portion of the cementitious content with fly ash reduces concrete's thermal conductivity. The same effect has been observed for blast-furnace slag by Kim et al. (2003).

Research by Demirboğa et al. (2007) has shown a reduction in the thermal conductivity of mature concrete (28+ days) by up to 39% by replacing 70% of the cement content with fly ash. The study by Demirboğa et al. (2007) is only applicable to a specific concrete mix (167.5 kg water, 350 kg cementitious content, 1755 kg of aggregate of an unknown type), but it can be argued that large errors can be made by applying the values in Table 2-2,

which are only based on aggregate type, without due consideration for the influences of the amount and type of ingredients used in concrete apart from aggregate type.

Prediction of concrete thermal conductivity

One of the older prediction models for concrete's thermal conductivity was suggested by Campbell-Allen & Thorne (1963, in Khan, 2002). The model considers the effects of mortar (water, cement and fine aggregate) and coarse aggregates, based on these two components' conductivities and volumetric fractions. Saturation is taken into account by taking different values for the thermal conductivities of mortar and aggregate in dry and saturated states. Comparing experimentally obtained results with those predicted by the Campbell-Allen & Thorne formula, Khan (2002) found that the prediction model overestimates conductivity in the dry state by 13 % to 32 % while predicted values in the saturated state were between -13 % to 8 %. The predicted results reportedly decrease in accuracy with an increase in the thermal conductivity of the aggregate.

One of the limitations of the Campbell-Allen & Thorne model is that mortars made with different mix proportions or mix constituents will have different thermal properties. Physical testing is therefore required, making the method inappropriate as a desktop estimation tool.

Guo, Guo, Zhong, & Zhu (2011) recommend that a mass weighted average of the unreacted constituents be used to calculate the thermal conductivity of concrete. This approach does not account for changes in hydration degree, or for the degree of saturation, but can still be considered reasonably accurate based on the accuracy of the measured versus calculated concrete temperatures presented in their article.

The study by Choktaweekarn et al. (2009b), which investigates the thermal conductivity of concrete containing fly ash, proposes a model for predicting the thermal conductivity of concrete based on the volumetric fraction of its ingredients over time. Significantly the authors take the effects of mix proportions, aggregate type, degree of hydration and the influence of supplementary cementing materials into account.

The methodology Choktaweekarn et al. (2009b) followed to develop and validate the model entailed performing a literature survey as well as an experimental study. Validation of the model was done by comparison of the results predicted by the model with the authors' own experimental research as well as results from other authors. While the method proposed to calculate the thermal conductivity of concrete by Choktaweekarn et al. (2009b) appears to be highly accurate, it is elaborate, with some input parameters requiring a separate analysis to be performed.

2.4.2 Specific heat capacity

Specific heat capacity refers to the amount of heat that is required to increase the temperature of a unit mass of a material by 1 °C. The temperature within a volume of concrete with a high specific heat capacity will consequently react slower to a temperature gradient (and internal heat generation) than a volume of concrete with a low specific heat capacity.

Factors affecting specific heat capacity

The specific heat capacity of concrete is dependent on the following factors:

Mix proportions: It is normally sufficient to calculate the specific heat capacity of concrete by taking a mass-weighted average of the constituent raw materials' specific heat capacities. The specific heat capacity of Portland cement and supplementary cementing materials (over all temperatures) is taken as 880 J/kg.K and that of water as 4187 J/kg.K by Gibbon, Ballim, & Grieve (1997).

Temperature: Specific heat capacity can vary significantly (± 7.5 %) with temperature according to Ballim & Graham (2009). This observation is confirmed in principle by Riding et al. (2007a).

Aggregate type: Values for the specific heat capacity of commonly used aggregates in South Africa are shown in Table 2-3. The values in the table suggest that specific heat capacity generally increases with increased temperature.

Table 2-3 Specific heat capacity of common South African aggregates Ballim & Graham (2009).

Aggregate type	Specific heat capacity (J/kg.K)		
	10 °C	21 °C	32 °C
Quartzite	875	910	945
Dolomite	940	965	995
Limestone	925	935	960
Granite	920	920	935
Basalt	945	945	960
Rhyolite	920	945	970

Reyes reports that Greywacke, an aggregate type frequently encountered in the Western Cape province of South Africa, has a specific heat capacity of 920 J/kg.K. No data on its temperature dependence is given.

Age (maturity): Riding et al. (2007a) and Choktaweekarn, Saengsoy, & Tangtermsirikul (2009a) note that the specific heat capacity of concrete is dependent on the degree of

hydration. Of the ingredients contained in concrete, water has the highest specific heat capacity. As the hydration reaction proceeds, free water decreases and consequently so does the specific heat capacity of concrete (Choktaweekarn et al., 2009a). The study by Choktaweekarn et al. (2009a) shows a reduction in specific heat capacity of up to 50 % over the first five days for one of the pastes that were tested.

The study by Choktaweekarn et al. (2009a) raises questions with regards to the validity of simply taking a mass weighted approach to calculate specific heat capacity as the effect of the phase change of water on specific heat capacity is not taken into account.

Supplementary cementing materials: Choktaweekarn et al. (2009a) show that the specific heat capacity of fly ash cement pastes are higher at early ages when compared to those of cement pastes, but that the specific heat capacity of fly ash pastes' approaches that of cement pastes over the long term. This result is to be expected, based on the fact that the pozzolanic reaction is significantly slower than cement hydration (Beushausen, Alexander, & Ballim, 2012), which leads to a slower reduction in the amount of free water in the paste.

Prediction of specific heat capacity

Addis (1986, in Ballim, 2004a) suggests that the specific heat capacity of concrete should simply be calculated by taking the mass weighted average of the specific heat capacities of its ingredients.

Choktaweekarn et al. (2009a) propose a mass-weighted relationship for the determination of the specific heat capacity of concrete over time that accounts for the effect of the phase change in water. A comparison between experimentally obtained values and those modelled using by Choktaweekarn et al. (2009a) is shown in Figure 2-4. A reasonably good correlation between modelled and measured values can be observed. Note that the results obtained at "Age of paste = 0" is equivalent to taking a mass weighted average of the paste's raw ingredients' thermal conductivities. The specific heat capacity of Portland cement, fly ash and cement gel were taken as 753, 711 and 419 J/kg.K respectively.

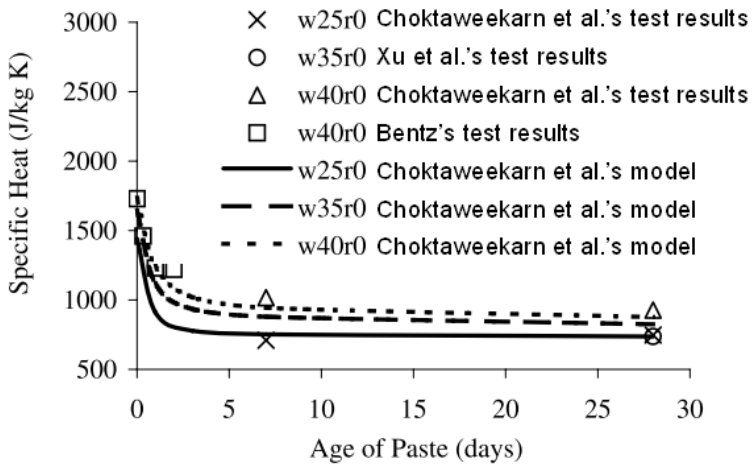

Figure 2-3 A comparison between experimentally obtained values for the specific heat capacity of cement pastes with those modelled using the model by Choktaweekarn et al (2009a).

Including the degree of hydration in the calculation procedure to determine specific heat capacity might lead to it being taken into account twice. The change in specific heat capacity with the change in the degree of hydration is taken into account implicitly during adiabatic calorimetry (Gibbon & Ballim, 1996). Including the variation in specific heat capacity with a change in the hydration degree in thermal analysis without adjusting the heat output curve obtained from calorimetry would constitute taking its effect into account twice.

2.4.3 Density

Density, when viewed in combination with specific heat capacity (density multiplied by specific heat capacity), is a measure of how much heat is required to raise the temperature of a unit volume of material by 1 °C. The temperature of a volume of concrete with a high density will consequently react slower to temperature gradients (or internal heat generation) than a volume of concrete with a low density.

The density of concrete is mainly affected by the density of the raw materials it is made from (mass weighted average), water content, degree of compaction and air content (Kellerman & Crosswell, 2009). The density of mass density commonly ranges between 2240 kg and 2600 kg / m^3 according to Conrad (2006). Table 2-4 and Figure 2-4 provides a summary of the relative densities of concrete ingredients.

Table 2-4 Relative densities of cementitious materials commonly found in South Africa.

Concrete ingredient	Relative density	Reference
Cement (CEM I)	3.14	(Addis & Goodman, 2009)
Fly ash	2.3	
Ground granulated blast-furnace slag	2.9	

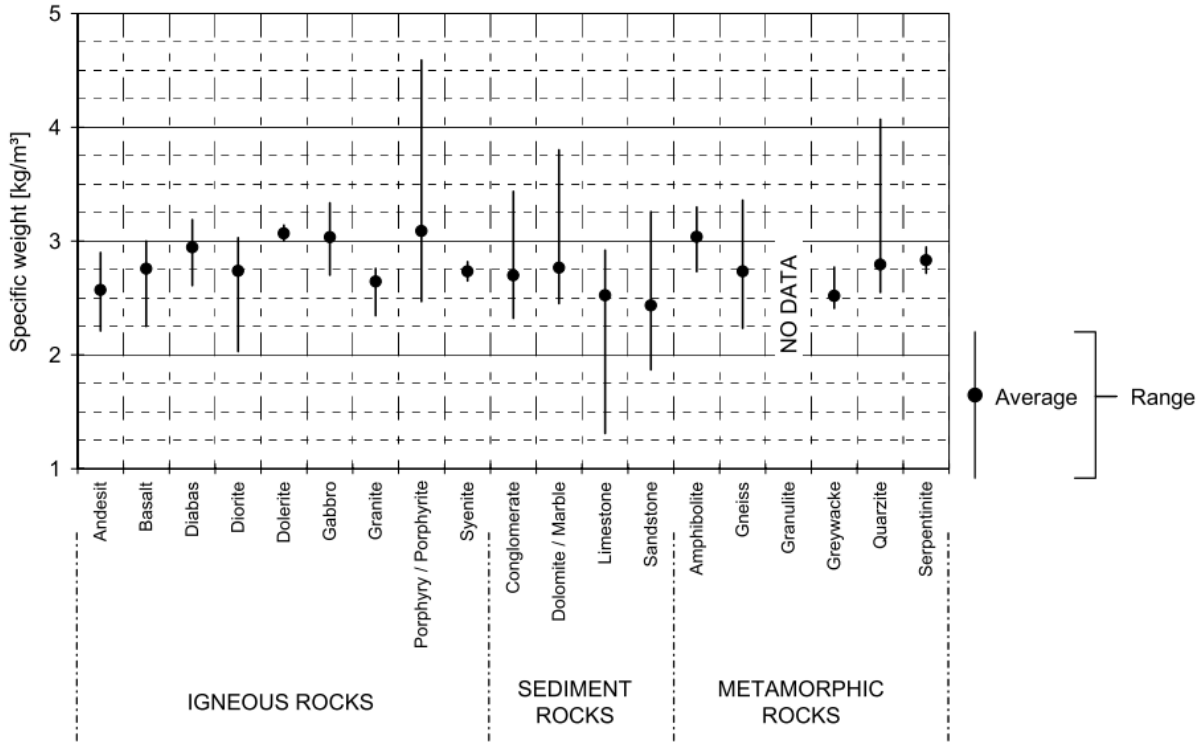

Figure 2-4 A comparison of the specific weights of different aggregates used in concrete. From Lama & Vutukuri (1978) and Čermák & Rybach (1982), both in Conrad (2006).

Conrad (2006) notes that, given the typical variation of ± 7 % for the density of placed concrete (average density = 2400 kg/m^3), this results in a variation of ± 6 % in the adiabatic temperature rise that would be measured.

According to Reyes (2007), the density of Greywacke is in the order of 2650 kg/m^3.

2.5 Internal heat generation

Internal heat generation is the second internal factor considered. Internal heat generation is a term used to describe the generation of heat during the hydration of cementitious materials. The liberated heat, if not dissipated, results in an increase in concrete temperature that is dependent on both the density and specific heat capacity of concrete, as described in section 2.4.

Various authors describe the mechanisms associated with internal heat generation and techniques by which it can be modelled for various types of cementing materials – this is

dealt with below. The contribution of this work lies in incorporating the collected information into the proposed temperature control model, thereby allowing the use of the hydration characteristics of a concrete mix to be used as one of the parameters that can be manipulated in order to achieve a desired temperature distribution during and after concrete dam construction.

The term “cementing materials” refers to Portland cement (clinker), ground granulated blast-furnace slag, ground granulated corex slag, pozzolanic materials, fly ash, limestone, burnt shale and silica fume. “Supplementary cementing materials” is used when referring to any cementing material other than Portland cement. This discussion will be limited to Portland cement, fly ash and ground granulated blast-furnace slag (GGBS).

2.5.1 Theoretical basis: Cement chemistry

The hydration of cementing materials, when examined in great detail, is a complex subject. Only a basic overview of the theory behind these reactions is described below. The aim is to provide context for the discussions on factors affecting internal heat generation and how it can be characterised and modelled. The interested reader is referred to the works by Illstone & Domone (2010), Czerin (1980) and Swamy (1986) should more information be required on the chemical reaction themselves, or the chemical composition of cements.

When water is added to Portland cement the hydration reactions that ensue have several by-products, two that are of concern for this topic: Calcium silicate hydrate (abbreviated as $C_3S_2H_3$) and Calcium hydroxide (CH). $C_3S_2H_3$ is the hydration product responsible for most of the strength of the hardened cement paste (Grieve, 2009).

Grieve (2009) further states that South African fly ash contains 48 – 55 % SiO_2 and less than 10% CaO. When used as a supplementary cementing material, the SiO_2 reacts with water in combination with CH formed during the hydration of Portland cement to form$C_3S_2H_3$. This reaction is known as a pozzolanic reaction. Class C fly ash, which has a CaO content greater than 20 %, also has self-cementing properties.

GGBS, when alkali activated, reacts with water on its own, and in combination with CH from the hydration of Portland cement, to form $C_3S_2H_3$.

The term “hydration” is used inclusively throughout the rest of this work to refer to the hydration of Portland cement, GGBS and any pozzolanic reaction unless explicitly stated otherwise.

2.5.2 Factors affecting internal heat generation

Two aspects should be considered when evaluating internal heat generation: The rate at which the hydration reaction takes place and the total amount of heat that is generated. These two aspects are affected by the following factors:

Temperature: It is an accepted fact that the rate of hydration is largely dependent on temperature (Ballim, 2004a; Gaspar, Lopez-Caballero, Modaressi-Farahmand-Razavi, & Gomes-Correia, 2014; Schindler, 2004). Experimental results from several authors have shown that there is good agreement between hydration reaction rate (rate of heat liberation) and the Arrhenius theory for reaction rate (Ballim, 2004b; Gawin, Pesavento, & Schrefler, 2006; Schindler & Folliard, 2003).

Mix proportions: The amount of heat that can be generated from hydration is limited by the amount and type of cementitious materials present, as well as the amount of water available for hydration. The limiting effect of water is illustrated in Figure 2-5. Figure 2-5 shows the extent of hydration of concrete mixes with different w/c ratios at 7, 28 and 90 days.

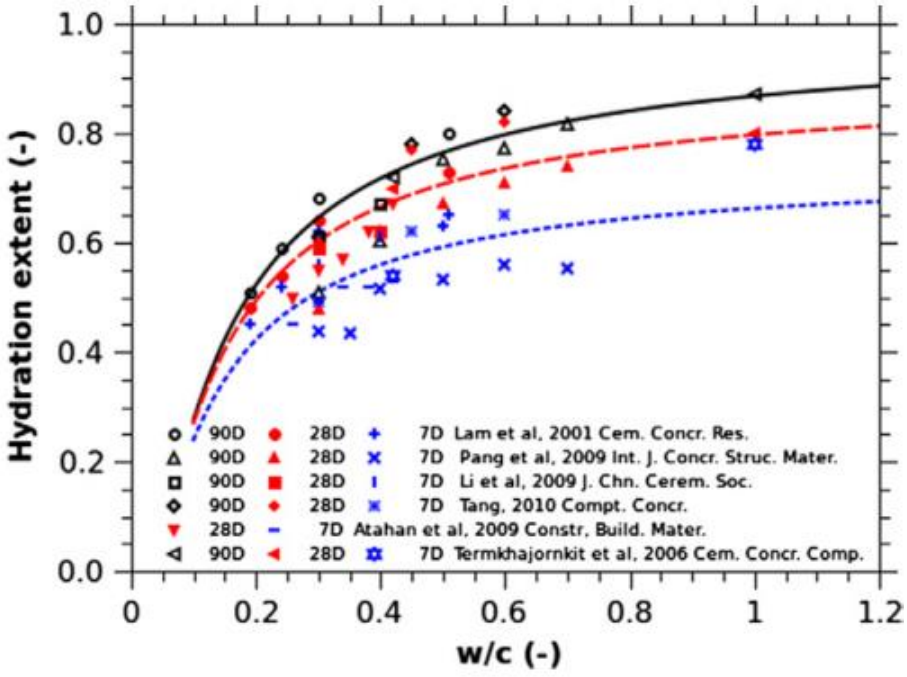

Figure 2-5 A relationship between degree of hydration and w/c ratio for cement pastes at different ages (Zeng, Li, Fen-Chong, & Dangla, 2012).

Note that, while a degree of hydration of 1 (100%) is not reached at any w/c ratio by 90 days, low w/c ratios (< 0.42) stoichiometrically limit the ultimate degree of hydration (Grieve, 2009). The presence of large cement grains and unreacted supplementary cementing materials also limit the extent to which the reaction progresses, according to da Silva et al. (2015).

Filler effect: Some authors have noted an increase in reaction rate of Portland cement at early ages due to the physical presence of fly ash or ground granulated blast-furnace slag in cement (Berodier & Scrivener, 2014; Zajac & Ben Haha, 2013). Berodier & Scrivener (2014) assert that the observed effect is the result of the increased space between Portland cement particles, providing more space for the growth of $C_3S_2H_3$ crystals. This is in contrast to previous thinking that postulated that the increased reaction rate is the result of increased nucleation sites for the growth of $C_3S_2H_3$ crystals (Gutteridge, 1990 in Berodier & Scrivener 2012).

Cement fineness: Researchers generally agree that the rate and amount of heat generated during the early stages of hydration of Portland cement is strongly influenced by the fineness to which the cement clinker is ground according to a literature survey on the matter by Hooton, Boyd, & Bhadkamkar (2004). Graham, Ballim, & Kazirukanyo (2011) published an article on the effect of the fineness of two South African Portland cements for controlling the early-age temperature development in concrete. The results of the study indicated that both the reaction rate and total heat liberated of both of the Portland cements studied are influenced by the fineness to which the clinker is ground. The effect of increasing cement fineness for these two types of clinker on the total amount of heat liberated is shown in Figure 2-6. Table 2-5 quantifies the same effect on reaction rate. Note that time in Table 2-5 is expressed as t_{20} (maturity) hours – this concept is described in section 2.5.3.

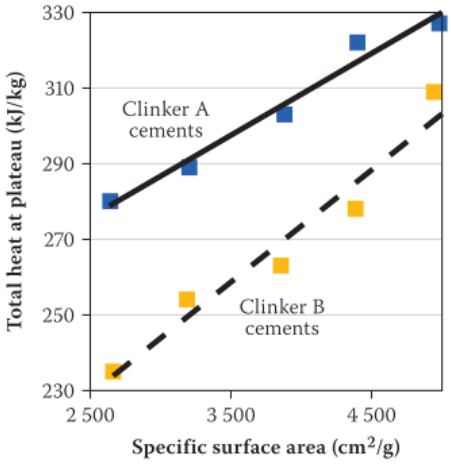

Figure 2-6 A comparison of the effects of increasing cement fineness on the amount of heat liberated (Graham et al., 2011).

Graham et al. (2011) conclude that increasing the fineness of cement from 2 650 to 5 000 cm^2 / g resulted in an increase in the total measured heat output of 17 % for clinker A and 32 % for clinker B. The explanation given for the increased total heat output is an increased degree of hydration over time for finer clinkers, while the difference between the

total heat outputs of the two clinkers is attributed to mineralogical differences between the two types of clinker.

Table 2-5 A comparison of the effects of increasing cement fineness on the peak heat rate and time to peak heat rate from Graham et al. (2011).

Clinker		Nominal Specific Area (cm^2 / g)				
		2600	3200	3800	4400	5000
A	Peak heat rate (W / kg)	2.08	2.23	2.58	3.18	3.85
	Time to peak heat rate (t_{20} hrs)	12.0	10.4	10.3	9.0	9.0
B	Peak heat rate (W / kg)	1.83	2.51	2.74	2.97	4.2
	Time to peak heat rate (t_{20} hrs)	12.	11.0	10.0	10.0	10.6

Mineralogical differences: Graham (2003) performed a study on the heat evolution characteristics of different South African cements. Cements sourced from different production facilities have different mineralogical make-ups, with different constituents occurring in different ratios (Grieve, 2009). To illustrate the effect that variation in mineralogical composition has on Portland cement's hydration heat characteristics, Graham (2003) presented the maturity heat rate graphs of different cements superimposed on top of each other. This comparison is reproduced here in Figure 2-7.

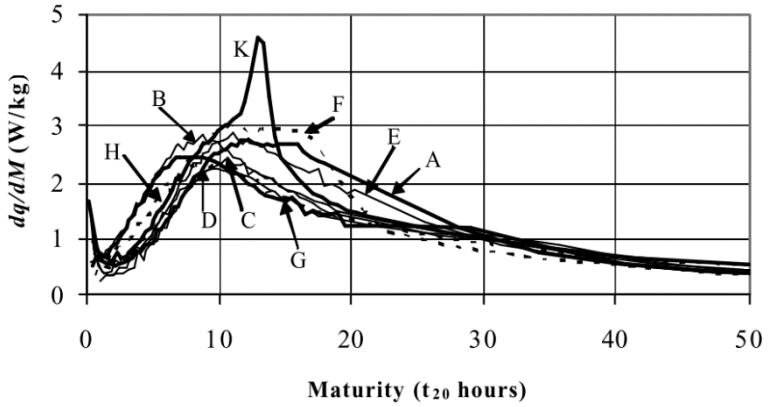

Figure 2-7 A comparison between the maturity heat rates sourced from different production facilities in South Africa after Graham (2003).

It can clearly be seen from Figure 2-7 that Portland cements sourced from different locations have significantly different hydration characteristics.

Figure 2-8 illustrates the same effect between Class C and Class F (less than 20% CaO) fly ash.

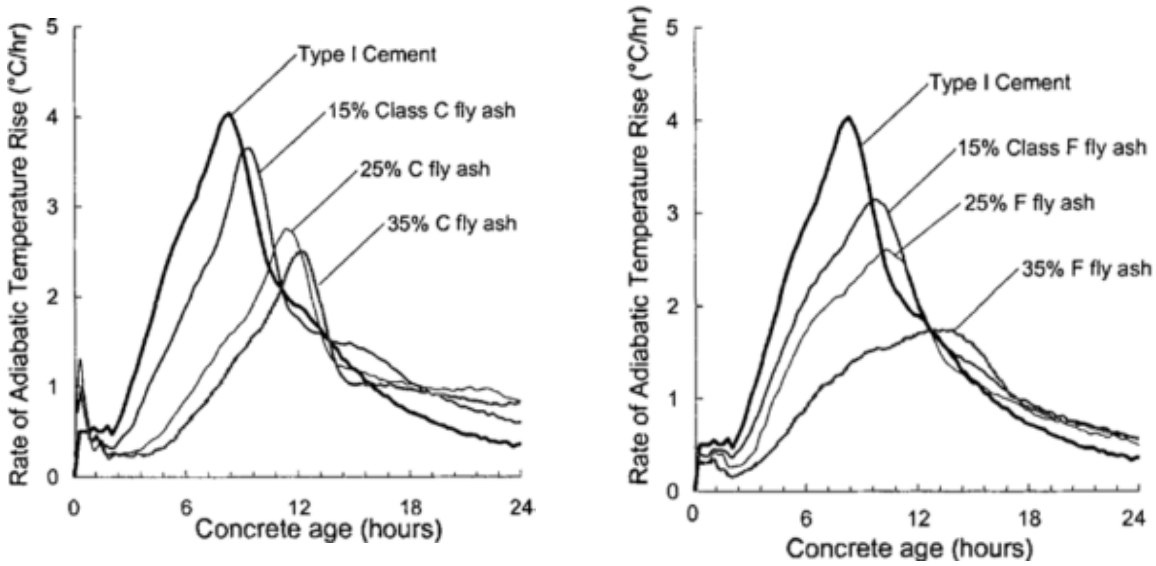

Figure 2-8 Comparison between the hydration heat characteristics of Class C and Class F fly ash concrete blends at different replacement ratios (Schindler & Folliard, 2003).

A comparison between the two sets of results shown in Figure 2-8 generally indicates that Class C fly ash cements have higher early age heat rates at the same replacement levels when compared to Class F fly ash cements.

Curing temperature: Cement hydration is accelerated at high temperatures, as is shown in Figure 2-9. Several authors claim that hydration rate can be scaled according to the Arrhenius equation for the temperature dependence of reaction rates (Cervera, Oliver, & Prato, 1999; Martinelli, Koenders, & Caggiano, 2013; Thomas, 2012).

2.5.3 Quantifying hydration

Historic approaches

In their paper on the evaluation of temperature prediction methods for mass concrete members, Riding et al. (2007a) discuss three different concrete temperature prediction methods: The modified Portland Cement Association (PCA) method; the ACI 207.2R graphical method; and the Schmidt method. The significance of the study was to determine if these three methods, all of them developed more than 50 years ago, are still valid. The results of the study showed that all three methods failed to accurately predict both the maximum concrete temperature rise, as well as the time it takes to achieve the maximum concrete temperature rise.

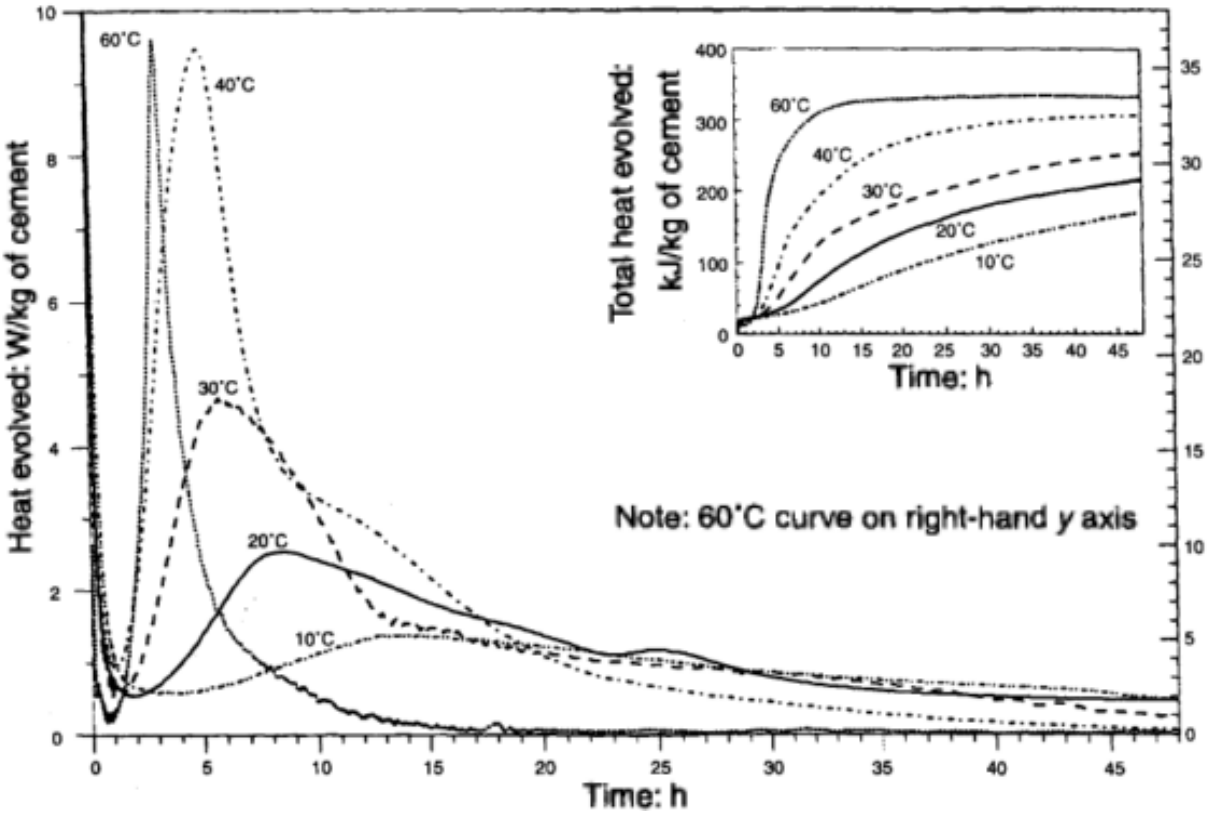

Figure 2-9 The effect of curing temperature on hydration heat development (S. G. Kim, 2010).

Weighted clinker phase approach

Conrad (2006) describes a two-phased approach for modelling hydration heat development. The first part of the approach entails estimating the mass weighted fractions of the clinker phases from the mass weighted fraction of the oxide phases present in the Portland cement. This is done using so-called Bogue calculations. Knowledge of the mass percentage of the oxide phases present in Portland cement, fly ash and slag are readily available on mill certifications from manufacturers.

The second part of the method involves calculating the total heat developed per kilogram of binder over time as the sum the total heat liberated by each clinker phase after full hydration with a time dependant weighting factor. Both of these parameters (the heat developed by each clinker phase after full hydration as well as the time dependant weighting factor for each clinker phase) are obtained from literature.

Conrad (2006) plotted values predicted by the weighted clinker approach described above against laboratory results and values back-calculated from monitoring results obtained at two different dams. The experimentally obtained values correlate reasonably well (±15 %) with the predicted values over the timespan shown.

The method, as outlined above, is only applicable to concretes containing 100 % Portland cement as binder. It fails to take into account the effects of the w/c ratio, curing temperature and cement fineness. It is considered suitable as a desktop scoping method, but not for detailed analysis.

Conrad (2006) goes on to describe a method to include the effect of fly ash in the weighted clinker approach described above: The heat generation contribution of supplementary cementing materials is assumed to be half of that of the contribution of Portland cement. This is in accordance with the modified PCA approach (A 40 % fly ash replacement ratio returns a hydration heat for the blend as 80% of that of pure Portland cement). The mass fraction of the Portland cement is reduced proportionally in the concrete for the purpose of calculating the total heat generated per cubic metre of concrete. The same hydration heat curve calculated using the weighted clinker approach above is then used in the analysis. A comparison between calculated values and values obtained from literature for different blended cements show that this approach is inadequate: Up to 85 % errors can be observed from the presented data in Conrad (2006).

Physical testing

The literature based methods described above are not considered accurate enough for implementation in the proposed temperature control model. Internal heat generation is the main reason why thermal analysis is required and needs to be modelled accurately for this work to have any relevance.

On the characterisation of the hydration characteristics of concrete, Conrad (2006) states that physical testing during detail design is inevitable if accurate modelling of heat evolution is required.

Ballim, on his own and in combination with Graham, published several works relating to the numerical modelling of time-temperature profiles in concrete structures due to the hydration of cementitious materials (Ballim & Graham, 2004, 2009; Ballim, 2004a, 2004b). On determining the hydration heat of a binder these two authors repeatedly propose physical testing by means of adiabatic calorimetry according to the procedure described by Gibbon et al. (1997). The emphasis placed on physical testing by these authors, as opposed to generalised predictive modelling, might be attributed to the relatively significant variation that has been observed between the hydration characteristics of different cements, as shown in Figure 2-7. An advantage of physical testing is that many of the effects affecting hydration heat development, such as w/c ratio, cement fineness and the influence of supplementary cementing materials, are taken into account directly without having to rely on assumptions.

Various test methods have been developed to determine the rate of heat liberation during the hydration of cement. These methods can be grouped into three categories: Adiabatic, semi-adiabatic and isothermal.

Adiabatic tests measure the temperature rise in a sample of concrete that is perfectly insulated. Semi-adiabatic testing also measures temperature rise, but the sample is imperfectly insulated. Isothermal methods are aimed at measuring the heat developed while the sample is kept at a constant temperature.

Each of these methods has advantages and disadvantages associated with them. The interested reader is referred to the works by Gibbon et al. (1997) and S. G. Kim (2010) for more detail on the testing procedures themselves.

The results obtained from physical testing can be incorporated in finite element analysis, leading to accurate modelling of concrete temperatures rise resulting from hydration heat liberation, as will be demonstrated for the two methods described below.

Concrete maturity

Figure 2-9 illustrates the effect of temperature on the rate of heat development during the hydration of cement: Cements cured at higher temperatures react faster than cements cured at lower temperatures. To account for the varying degree of hydration throughout the volume of a concrete element at a specific time the concept of “maturity” can be used.

There are two widely accepted forms are used to describe maturity: The Nurse-Saul and Arrhenius forms. Both forms describe the age (or maturity) of concrete, relative to the same concrete cured at a constant temperature, based on its temperature history.

The Nurse-Saul form is the more basic of the two: Maturity age at a point in the structure is defined as (Martinelli et al., 2013):

$$M_{T_{ref}}(t) = \int_0^t T(t)dt \qquad 2.5.1$$

Where: $M_{T_{ref}} =$ Equivalent age or maturity relative to concrete cured at a constant temperature of T_{ref} (days or hours)

The Arrhenius form takes the influence of hydration rate into account in addition to the influence of temperature variation over time. Ballim & Graham (2009) propose a modified version of the Arrhenius equation for discrete timesteps:

$$M_{T_{ref}} = \sum_{i=0}^{i=n} \exp\left[\left(\frac{E}{R}\right) \cdot \left(\frac{1}{273 + T_{ref}} - \frac{1}{273 + 0.5 \cdot (T_i - T_{i-1})}\right)\right] \cdot (t_i - t_{i-1}) \qquad 2.5.2$$

Where: E = Activation energy parameter (J / mole)

R = Universal gas constant = 8.314 J / mole

T_i = Temperature at the end of the i^{th} time interval (°C)

t_i = Clock time at the end of the i^{th} time interval (h)

Taking the activation energy as a constant equal to 33.5 kJ / mole in Equation 2.5.2, as suggested by Ballim & Graham (2009), it can be shown as an example that cement cured at 25 °C reacts 26% faster than cement cured at 20 °C over a fixed period. In other words, hydrating cement cured at 25 °C for 10 hours releases the same amount of energy as the same cement cured at 20 °C for 12.6 hours.

According to Gaspar et al. (2014) the activation energy parameter can vary between 29.4 kJ / mole to 66.5 kJ / mole. Several parameters influence the activation energy and laboratory testing is advised if, for instance, high amounts of pozzolana are incorporated into the concrete mix.

Figure 2-10 illustrates the difference between maturity time and clock time when considering the hydration of cement. The total amount of heat developed over the long term remains unaffected. The rate at which heat develops is, however, normalised to isothermal conditions.

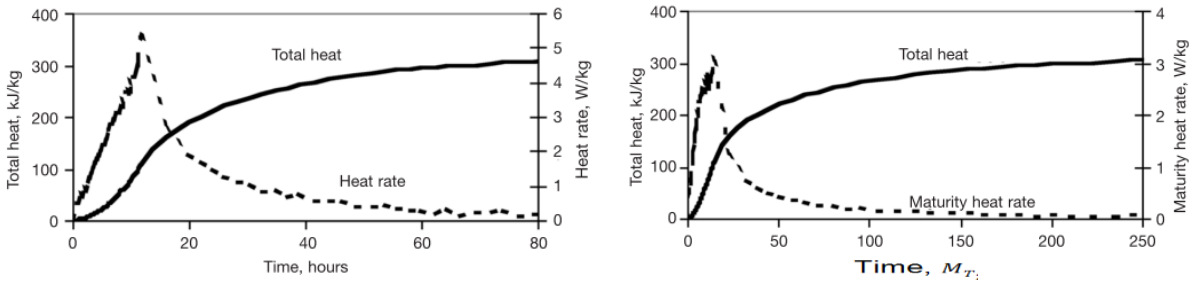

Figure 2-10 Heat of hydration curves for a typical binder in (a) clock time and (b) equivalent maturity time. Note the difference between the time scales of the two graphs (Ballim & Graham, 2009).

Normalising a heat rate curve obtained from adiabatic testing to an equivalent maturity form is done using Equation 2.5.3 (Ballim, 2004a):

$$\frac{\partial Q}{\partial t} = \frac{\partial Q}{\partial M_{T_{ref}}} \cdot \frac{\partial M_{T_{ref}}}{\partial t} \qquad 2.5.3$$

Where: Q = Heat developed by the hydrating cement

Equation 2.5.3 shows that it is necessary to monitor maturity as well as the rate of change in maturity at each point in the structure during analysis.

Adiabatic testing of a binder, in combination with Equations 2.5.2 and 2.5.3 can be implemented directly in a finite element analysis (TNO DIANA BV, 2014). This was validated as shown in Figure 2-11 (Ballim, 2004a). The analysis was done using a finite difference method approach and includes effects other than only internal heat generation, such as the influence of the foundation, thermal diffusivity and ambient conditions. Notwithstanding all of the other effects included in the analysis, a comparison between the measured and predicted values close to the centre of the mass concrete block show adequate correlation for validation of the outlined approach.

A major advantage of the approach described above is that a spreadsheet containing maturity heat rate data for various South African cements containing pure Portland cement or Portland cement blended with fly ash and GGBS at various replacement ratios was published along with the Fulton's Concrete Technology Handbook (Gill Owens, 2009). The availability of this data makes it possible to effectively evaluate the effects of various binder contents and binder blends on the temperature in the proposed temperature control model.

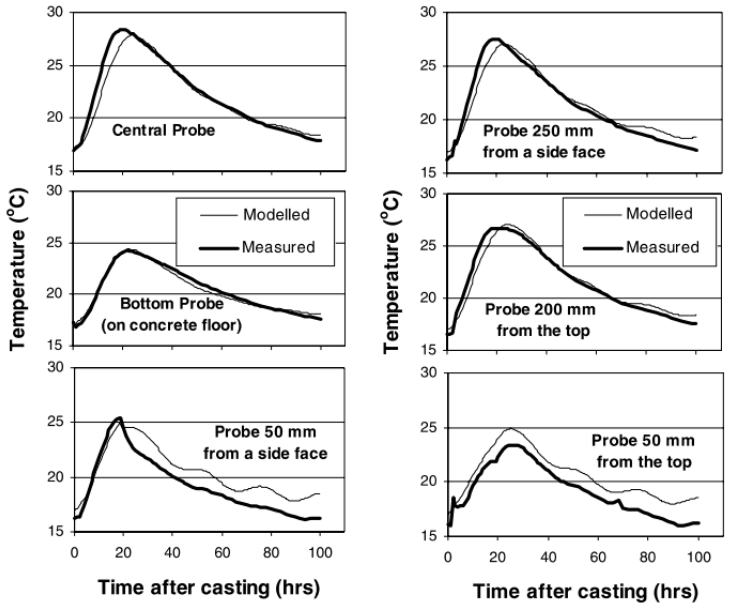

Figure 2-11 A comparison between modelled and measured temperature values at six different positions in a mass concrete block (Ballim, 2004a).

Affinity hydration model

Cervera et al. (1999) introduced a thermo-chemo-mechanical approach for modelling heat development that is worth mentioning. Gawin et al. (2006) suggested some modifications to the method, which was finally further simplified by da Silva et al. (2015). The model is based on the concept of chemical affinity. Affinity can be likened to a driving force behind a

chemical reaction. Normalised chemical affinity is defined as the derivative of hydration degree with respect to time at a constant concrete reference temperature. A general, analytical form of the normalised affinity is given by

$$\tilde{A}_{T_{ref}}(\alpha_h) = k_1 \left(\frac{k_2}{\alpha_{max}} + \alpha_h\right) \cdot (\alpha_{max} - \alpha_h) \cdot \exp\left(-\eta \frac{\alpha_h}{\alpha_{max}}\right) \quad 2.5.4$$

Where: $\tilde{A}_{T_{ref}}(\alpha_h)$ = Normalised chemical affinity relative to isothermal temperature T_{ref} (1 / time)

k_1 = Regression coefficient 1

k_2 = Regression coefficient 2

η = Regression coefficient 3 representing the micro diffusion of free water through formed hydrates

α_h = Degree of hydration (%)

α_{max} = Ultimate degree of hydration

The regression coefficients required for Equation 2.5.4 can be obtained from isothermal, adiabatic or semi-adiabatic calorimetry.

The degree of hydration of cementitious materials describes the extent to which the hydration reaction has progressed. According to Gawin et al. (2006) the hydration degree is defined as:

$$\alpha_h = \frac{m_{hydr}}{m_{hydr\infty}} = \frac{Q_w}{Q_{w,max}} \quad 2.5.5$$

Where: m_{hydr} = Mass of hydrated water at time (g)

$m_{hydr\infty}$ = Ultimate mass of hydrated water after hydration reaction stops (g)

Q_w = Total heat liberated from start of hydration to time t (J / g)

$Q_{w,max}$ = Total heat potentially available for liberation that is present in the concrete mix under consideration (J / g)

As previously stated, the degree of hydration never reaches 1 (Gawin et al., 2006) and is mainly dependant on the w/c ratio (Cervera et al., 1999). Cervera et al. (1999) suggest the use of the following formula, originally proposed by Pantazopoulo & Mills (1995, in Cervera et al., 1999) for estimating the ultimate degree of hydration of a concrete mixture:

$$\alpha_{max} = \frac{1.031 \cdot w/c}{0.194 + w/c} \quad 2.5.6$$

Where: w/c = Water / binder ratio (kg / kg)

If hydration proceeds under varying internal temperatures, as is normally the case, the affinity $\tilde{A}_{T_{ref}}$ is scaled to an arbitrary temperature using the Arrhenius equation:

$$\tilde{A}_T = \tilde{A}_{T_{ref}} \cdot \exp\left[\frac{E}{R} \cdot \left(\frac{1}{273.15 + T_{ref}} - \frac{1}{273.15 + T}\right)\right] \quad 2.5.7$$

Where: $\tilde{A}_T$ = Affinity at temperature T (1 / time)

Da Silva et al. (2015) validated the use of the affinity type hydration model described above by comparing actual hydration heat developed at isothermal temperature ($T_{ref} = 25$ °C) with values obtained from the affinity hydration model. As can be seen in Figure 2-12, the model performs quite well. It is noted that only results from pure Portland cement and Portland cement / ground granulated slag cements are included in Figure 2-12. CEM IV (pozzolanic cement) was, however, used to obtain the results shown in Figure 2-1.

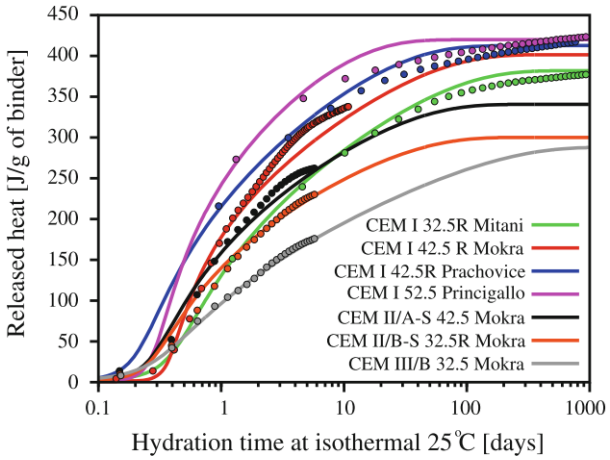

Figure 2-12 Comparison between actual hydration heat development at isothermal temperature and values predicted by an affinity type hydration model from da Silva et al. (2015).

2.6 Boundary conditions

The environment in which a dam is constructed as well as the methods used to construct a dam play a significant role on the energy that is transferred to and from a concrete element. Folliard et al. (2008) state that, when performing heat transfer analyses for concrete members, boundary conditions are often the most difficult parameters to quantify. Different external factors that influence concrete temperature are described below.

2.6.1 Foundation

Heat is transferred to and from the foundation by conduction. Two aspects are of concern when considering the effect of the foundation on concrete temperature: Its thermal diffusivity and initial temperature.

As described in section 2.4, thermal diffusivity is a measure used to describe how fast a material reacts to temperature gradients. The same properties assigned to concrete based on a certain aggregate type are usually also applied to the foundation (Ballim & Graham, 2009).

The temperature of the foundation at the time of concrete placement is site specific and engineering judgement should be applied when assuming an initial value. Ballim (2004b) suggests that the minimum temperature occurring on the previous day be used as the initial foundation temperature. The good correlation between monitored vs predicted results near the foundation contact shown in Figure 2-11 would suggest that this approach is adequate.

For arch dams the influence of the foundation is relatively small, as the foundation interface of this dam type is small in comparison with other heat transfer interfaces (Sheibany & Ghaemian, 2004). Sheibany & Ghaemian (2004) do not consider it worth wile to include foundation temperature in their thermal stress analysis of an arch dam. It should be mentioned that their study focused on the long term modelling of an arch dam – not the construction thereof, where the influence of the foundation could well have a significant effect during the early phases of construction.

2.6.2 Existing concrete and sequential construction

Heat transfer between fresh and existing concrete is similar to heat transfer between the foundation and fresh concrete. Distinction should, however, be made between existing concrete that is still hydrating, as would be encountered in multiple lift construction, and existing concrete that is inert, as would be encountered when performing rehabilitation.

The temperature of existing concrete that is still hydrating and in the process of cooling down (or heating up) is affected by the placement of subsequent lifts: Heat loss through convection at the top surface of the lower construction lift is prevented / reduced by the upper lift. Additionally, heat generated in the upper lift might also be conducted into the lower lift. The effect of the placement of a second construction lift on top of an existing construction lift on the temperature in the lower lift is illustrated in Figure 2-13.

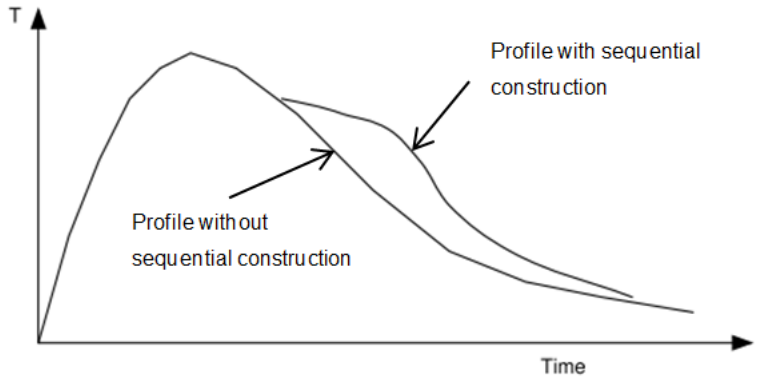

Figure 2-13 Temperature profile of a point in a lower construction lift with and without sequential construction. Adapted from Fowkes, Mamboundou, Makinde, Ballim, & Patini (2004).

The extent of the effect of sequential construction on the temperature distribution inside the concrete is largely dependent on construction rate: Chen et al. (2003) performed a parametric study on the effects of construction designs on the time-based temperature field in a RCC dam. As an example, they evaluated the effect of shortening the construction period for the dam under consideration from 48 to 33 to 15 months. The result was an increase in the maximum concrete temperature inside the dam from 33.8 to 35.8 to 41.3 °C.

2.6.3 Fresh concrete initial temperature

Given a specific concrete mix, limiting the placement temperature of concrete will automatically limit the adiabatic temperature rise of the concrete mix. This is a logical conclusion, given the fixed amount of energy that is available during hydration at a specific w/c ratio (Gawin et al., 2006). This concept is illustrated by Chen et al. (2003) as part of their parametric study for optimising the construction design of Long-Tan Dam: By placing a limit of 15 °C on the concrete placement temperature as opposed to taking the concrete placement temperature as equal to the ambient temperature, the maximum modelled concrete temperature inside the dam throughout the construction period is reduced from 35.8 to 28.6 °C.

The temperature of a fresh concrete mixture can be taken as the mass weighted average of the average temperatures of its constituents (Ballim & Graham, 2009).

$$T_c = \frac{\sum_{i=l}^{n} m_i C_i T_i}{\sum_{i=l}^{n} m_i C_i} \qquad 2.6.1$$

Where: T_c = Temperature of the concrete mixture (°C)

m_i = Mass of the i^{th} component (kg)

C_i = Specific heat capacity of the i^{th} component (J/kg.K)

T_i = Temperature of the i^{th} component (°C)

From Equation 2.6.1 it follows that controlling the temperature of any of the concrete mix's ingredients will consequently also help to control the temperature of the concrete mixture. Methods to cool concrete and / or concrete ingredients are listed below. The discussion will be limited to listing the different interventions that can be imposed to control concrete placement temperature. The reader is referred to the "Cooling and insulation systems" manual by ACI Committee 207 (1993) for details on how to implement and calculate the effect of each of the interventions listed on the final concrete temperature achieved. Table 2-6 lists different interventions that can be implemented to control the initial temperature of concrete.

By applying the principles set out in the manual by ACI Committee 207 (1993), virtually any desired initial concrete temperature can be achieved. ACI Committee 207 (1997) claim that concrete can be produced at less than 7 °C in practically any summer weather, given the efficient equipment currently available for concrete production.

It is worth noting that the process of mixing concrete also imparts energy into the concrete mix, leading to an increase in initial concrete temperature (ACI Committe 207, 1993).

Table 2-6 A list of methods to cool concrete ingredients after ACI Committee 207 (1993).

Ingredient	**Intervention**
Mixing water	Chilled mixing water Replace some mixing water with ice
Aggregates	Shaded stockpiles Processing and stockpiling during the cold season Processing in a classifier using chilled water (fine aggregates) Evaporative cooling by sprinkling stockpiles with water Spraying chilled water on aggregates on slow moving belts Immersion of aggregates in baths with chilled water (coarse aggregates) Cooling by means of liquid nitrogen Blowing chilled air through batching bins Evaporative cooling by means of a vacuum
Cements	Introducing liquid nitrogen into storage silos during transfer from tankers Insulation of storage silos Painting storage silos with a reflective (white) coating
Concrete	Introducing liquid nitrogen during mixing

2.6.4 Boundary heat flux

Heat transfer at exposed concrete faces occurs through convection and radiation. These two mechanisms can significantly influence the temperature distribution inside a concrete over time. Measures can be taken to control the effects of convection and radiation, such as using wooden shutters instead of steel shutters, but convection and radiation are natural phenomena which are mostly dependent on site specific atmospheric conditions. Methodologies used to model these two phenomena are described below with the aim of incorporating suitable estimation methods in the proposed temperature control model.

Convection

Convection is the process whereby energy is transported from a surface to a surrounding fluid by diffusion (Riding, Poole, Schindler, Juenger, & Folliard, 2007b). The two factors of interest when attempting to model convection are the (1) difference between the ambient and concrete temperature and (2) the convection or film coefficient.

Various authors make use of historic climatic data to estimate ambient air temperatures. Riding et al. (2007b), whose research was carried out in the USA, makes use of a climatic database containing hourly average weather data to model the ambient temperature. This approach is commendable, as good historic data reduces the amount of uncertainty that is inherently included in attempting to predict future climatic conditions. Where only average daily maximum and minimum temperatures are known (or estimated), sinusoidal variation of the ambient temperature throughout a day can be assumed, as suggested by Gaspar et al. (2014) and Ballim (2004a).

Several approaches have been followed in literature to calculate the convection coefficient:

Riding et al. (2007b) calculate the convection coefficient for bridge members based on wind velocity, inclination of the surface being considered relative to a horizontal plane, ambient temperature, surface temperature and roughness of the surface. Roughness values for exposed concrete and steel shutters are provided, but no provision is made for wooden shutters or insulation. The results of the modelled temperature close to element edges correlate well with monitored values. The approach of Riding et al. (2007b) to model convection appears to be very accurate, and is well suited to the application (modelling bridge members) for which it was applied. The approach is difficult to implement in finite element analysis, as the formula used to calculate the convection coefficient changes based on whether the surface temperature is less or more than ambient temperature. This effectively makes modelling convection in finite element analysis a manual, iterative process, which can be very time consuming.

The U.S. Army Corps of Engineers (1997, p. A–16) distinguishes between surfaces with forms and / or insulation and those without forms in their film coefficient calculation method. A basic convection coefficient is calculated for surfaces free from forms based only on wind velocity. The difference between forced and free convection is taken into account by having separate formulas for wind velocities higher and lower than 17.5 km/h. The film coefficient for surfaces free from formwork is calculated by

$$h = 2.6362 \cdot V^{0.8} \qquad V > 17.5 \text{ km/h} \tag{2.6.2}$$

$$h = 5.662 + 1.086 \cdot V \qquad V < 17.5 \text{ km/h} \tag{2.6.3}$$

Where: h = Convection coefficient (W/m^2.K)

V = Wind velocity (km/h)

The convection coefficient for surfaces with forms or insulation in place is calculated from the thickness and thermal conductivities of the form and insulation as well as the basic convection coefficient for surfaces free from forms (U.S. Army Corps of Engineers, 1997):

$$h' = \frac{1}{\left(\frac{b_f}{k_f}\right) + \left(\frac{b_f}{k_f}\right) + \left(\frac{1}{h}\right)} \tag{2.6.4}$$

Where: h' = Revised convection coefficient (W/m^2.K)

b_f = Thickness of the formwork (m)

k_f = Thermal conductivity of the formwork (W/m.K)

b_i = Width of the insulation (m)

k_i = Thermal conductivity of the insulation (W/m.K)

The approach of the U.S. Army Corps of Engineers (1997) to model convection is easy to implement and widely used in the dam engineering field (Husein Malkawi, Mutasher, & Qiu, 2003).

Similar approaches to that of the basic formula by the U.S. Army Corps of Engineers (1997), based only on wind velocity, are used by Duffie & Beckman (1980, in Nzuza, 2012) and Noorzaei, Bayagoob, Thanoon, & Jaafar (2006), but these formulas do not account for the difference between forced and free convection.

Guo et al. (2011) suggest a formula for calculating the film coefficient based on wind velocity and relative humidity. The approach shows promise, but more experimental verification is required.

Various authors simply use constant values for the convection coefficient (Ballim & Graham, 2009; Husein Malkawi et al., 2003; Sheibany & Ghaemian, 2004), thereby assuming a

constant wind velocity throughout the construction period. The validity of using a constant value throughout the construction period is demonstrated in a study by Gaspar et al. (2014). They developed a probabilistic analysis methodology applicable to RCC dam construction. The authors included the convection coefficient as one of the random variables considered as part of their study. They found that the effect of the variability of the convection coefficient was so small that they suggested a constant value be used for the convection coefficient.

Ballim & Graham (2009) suggest using $h = 25$ W/m^2.K for steel shutters and concrete faces free from formwork, and $h = 5$ W/m^2 where wooden formwork is present as a first estimate for the film coefficient. The 25 W/m^2 value corresponds to an average wind speed of 17.8 km/h when back-calculated using Equation 2.6.3. This estimate appears to be a realistic average wind speed applicable to South Africa when compared to average wind velocity data from Hagemann (2013). It is also clear from the average wind velocity data from Hagemann (2013) that there is considerable variation in the average wind speed throughout South Africa, which leads to the conclusion that if a constant value for the convection coefficient is to be used, it should at least be based on the site specific average wind speed.

Solar Radiation

Radiation refers to the emission of electromagnetic energy. The term irradiation is used to describe the flux of radiant energy onto a surface, while radiosity is used to describe the flux of radiant energy leaving a surface due to emission and reflection of electromagnetic radiation (Mills, 1992).

On the topic of radiation as it relates to modelling of concrete temperature, work by previous authors work can be categorised into three groups:

1. Radiation is taken into account directly. That is to say, the terms for radiation appear in the constitutive modelling equations. The works of Riding et al. (2007b) and Koenders & van Breugel (1995) can be cited as examples.
2. Radiation is modelled as part of the convection load. Conrad (2006) describes an approach whereby a combination of irradiation and radiosity is converted to an increase or decrease in the ambient temperature used to model convection. In an analogues approach, Gaspar et al. (2014) modify the convection coefficient to accommodate the effect of radiation.
3. Radiation is not taken into account at all by some authors (Ballim, 2004b; da Silva et al., 2015).

Results from an analysis by Koenders & van Breugel (1995) on the temperature development in a freshly cast concrete wall, where radiation was taken into account directly, illustrates the effect of solar radiation on concrete temperature as well as the magnitude of the error that can be made if its effect is ignored. It also serves to validate direct modelling of solar radiation. The results of the analysis are shown in Figure 2-14.

Up to a 10 °C difference between modelled and measured values can be observed in Figure 2-14(b) where radiation was not included in the analysis. This result makes ignoring radiation when performing thermal analysis questionable when accurate modelling of concrete temperatures close to exposed concrete faces is desired.

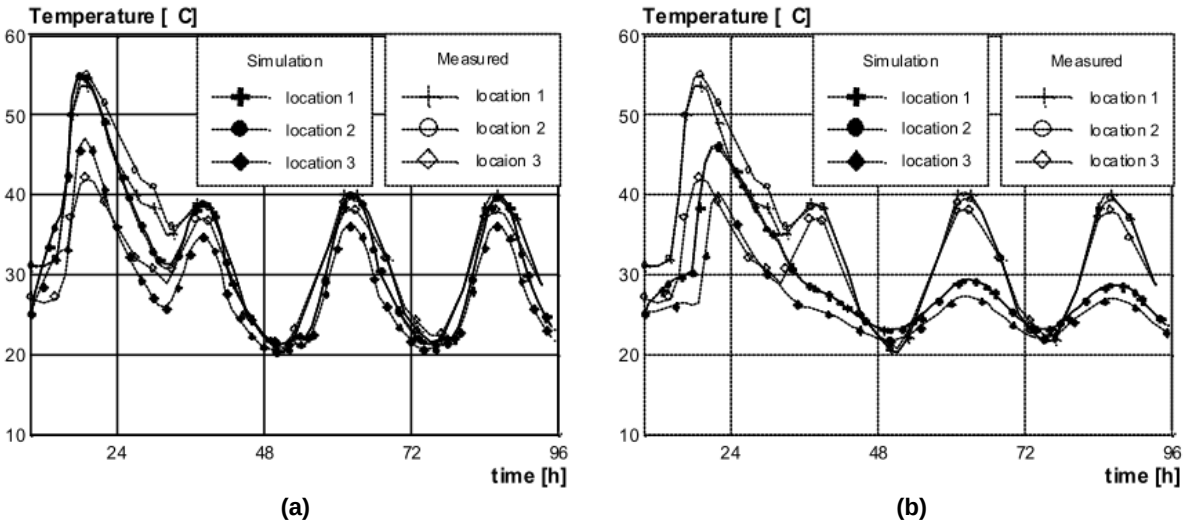

Figure 2-14 A comparison between measured concrete temperatures in a freshly cast wall and modelled values where solar radiation was (a) taken into account and (b) ignored (Koenders & Van Breugel, 1995).

Whether modelling solar radiation directly or as part of the convection load, the inclination of the radiation source (sun) relative to the surface being modelled (concrete face) over time plays an important role in determining the solar radiation flux. Procedures for determining the inclination and intensity of solar radiation over time are described by Koenders & van Breugel (1995), Conrad (2006), and Riding et al. (2007b) and will not be presented here. Factors that are taken into account include the inclination angle (relative to a horizontal plane) and orientation (direction) of a concrete surface, as well as the sun's position in the sky according to its declination, elevation and hour angle. Differentiation is also made between the effects of direct and diffuse solar radiation.

As stated above, Conrad (2006) suggests a procedure for taking radiation into account implicitly by adding a lump sum temperature representing solar radiation to the ambient temperature used in convection calculations:

$$T_{eff} = T_{amb} + \Delta T_{rad} \qquad 2.6.5$$

Where: T_{eff} = Effective ambient temperature (°C)

T_{amb} = Ambient temperature (°C)

ΔT_{rad} = Temperature lump-sum from solar radiation (°C)

The lump-sum temperature from solar radiation is calculated by

$$\Delta T_{rad} = \frac{Q_{S,glob}}{c \cdot m} = \frac{\int_{-12h}^{12h} q_{S,glob} dt}{c \cdot \rho \cdot 0.2} \qquad 2.6.6$$

Where: $Q_{S,glob}$ = Global solar radiation energy (J/m^2)

$q_{S,glob}$ = Global solar radiation heat flux (W/m^2)

c = Specific heat capacity of concrete (J/kg.K)

m = Superficial mass of 1 m^2 of concrete. The characteristic penetration depth of the diurnal temperature cycle is taken as 0.2 m.

ρ = Concrete density (kg/m^3)

t = Clock time (h)

The basic adequacy of Conrad's (2006) approach to model radiation is illustrated in Figure 2-15 where the concrete temperature close to the downstream face of the Mujib Dam is plotted against computed effective ambient temperature values over a three year period. The computed effective ambient temperature and the concrete's face temperature correlate reasonably well over the monitoring period..

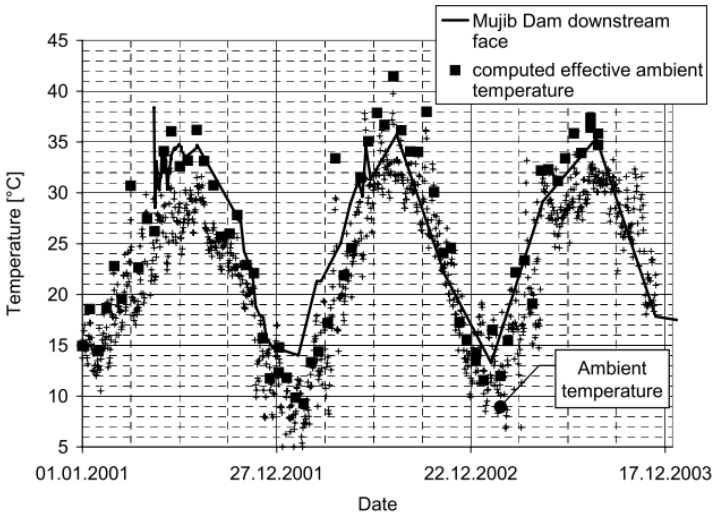

Figure 2-15 A plot of the concrete temperature close to the downstream face of Mujib Dam and computed effective ambient temperature values over a three year period (Conrad, 2006).

The advantage of taking radiation into account implicitly as suggested by Conrad is that it simplifies the analysis procedure when implemented in finite element analysis.

2.7 Construction considerations

The influence of some construction aspects on concrete temperature has been dealt with indirectly in previous sections of this chapter: The influence of controlling the placement speed of fresh concrete on the maximum temperature achieved as well as the influence of using wooden shutters instead of steel shutters are cited as examples. The effects of construction considerations that affect concrete temperature which were not previously addressed are described below.

2.7.1 Curing practice

The curing practice employed during construction can influence concrete temperature, but the quantification of its effect is not well documented.

ACI Committee 207 (1993) state that evaporative cooling with a fine water spray, the use of cool curing water as well as shading may provide some cooling benefit. The authors also noted that the results of these curing practices are variable. The results do not greatly affect the internal concrete temperature when the ratio of the surface area, where one of the abovementioned curing methods is used, to the volume of the concrete lift being considered is less than 1.0 m^{-1}.

ACI Committee 207 (1997) note that curing concrete with water provides a cooling benefit in warm weather, but the extent of the effect thereof is not quantified.

2.7.2 Start date of construction

The time of year when construction is started can have a significant effect on concrete temperature distribution in a dam (U.S. Army Corps of Engineers, 1997). To illustrate this, the modelled vertical temperature distribution at the centre of Long-Tan Dam is shown in Figure 2-16 for four different start dates.

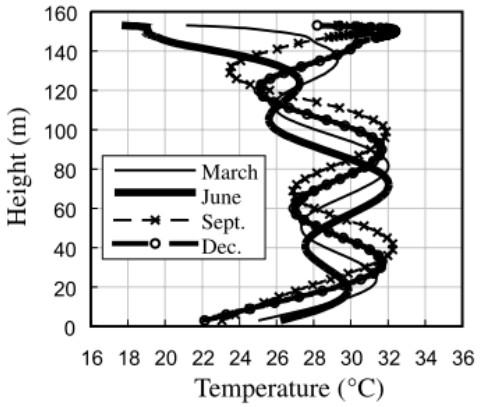

Figure 2-16 Modelled temperature distribution at the centre of the Long-Tan Dam for four different start dates after construction is completed (Chen et al., 2003).

It can be seen from Figure 2-16 that the absolute maximum concrete temperature achieved throughout the 33 month construction period is not greatly affected, with a 2 °C difference that can be observed between June and December start dates. The temperature peaks that can be observed at various heights throughout the dam for all of the start dates corresponds to concrete that was placed during the warmer months. This is in agreement with the statement by the U.S. Army Corps of Engineers (1997) that "different starting dates may yield temperature problems at different locations." The effect of the construction start date is also investigated as part of this study, but shorter construction periods are investigated than was done in the study by Chen et al. (2003).

2.7.3 Cooling pipes

The inclusion of embedded cooling pipes in the concrete body is an effective way of controlling concrete temperature during hydration (Liu, Duan, Zhou, & Chang, 2012; Sheibany & Ghaemian, 2004; U.S. Army Corps of Engineers, 1997). It is not common practice to make use of cooling pipes in South Africa. Its use has consequently not been further investigated in this study and will not be elaborated on further.

2.8 Specifications

An important part of the temperature control model developed as part of this study is the evaluation of a calculated temperature field: Specifications are the basis on which a decision can be made if a given temperature distribution is adequate or not.

Distinction can be made between two types of temperature specifications:

1. Generalised specifications based on past experience
2. Site specific specifications based on analysis

2.8.1 Generalised specifications based on past experience

Maximum absolute temperature

Concretes cured at temperatures higher than 70 °C (160 °F) are susceptible to delayed ettringite formation, which causes a reduction in compressive strength (Acquaye, 2006). To avoid this phenomena, several state highway agencies in the U.S.A. limit the maximum in-place concrete temperature to 70 °C (Riding et al., 2007a).

Two of the U.S.A. state highway authorities specify a limit of 24 °C on the placement temperature of concrete (Riding et al., 2007a). Schindler & McCullough (2002) further argue that it is impractical to place this limit on the placement (or ambient) temperature, as the effects of low wind speeds and humidity are not taken into account, which might permit higher ambient and concrete temperatures up to 38 °C without increasing the risk for delayed ettringite formation.

Schindler & McCullough (2002) recommend that a maximum in-place concrete temperature be specified instead of a maximum placement temperature, as this would motivate contractors to use supplementary cementing materials to keep the ultimate concrete temperature low instead of forcing them to utilize expensive cooling procedures to achieve a set maximum fresh concrete temperature.

Maximum temperature gradients

If length and volume changes associated with decreasing temperatures could take place freely, no tensile strain or stress would develop in a concrete member (ACI Committe 207, 1997). When potential contraction of a concrete member is restrained tensile stress and strain will result. Typical areas where restraint is encountered are between a concrete member and its rock foundation (or previous construction lift), adjacent concrete members as well as internally within a concrete member.

According to Acquaye (2006) the Florida Department of Transportation places a limit of 20 °C (35 °F) on the temperature differential between the core and the exterior of mass concrete elements (not dams). This is also the case for six other state highway authorities in the U.S.A according to Riding et al. (2007a). Folliard et al. (2008) notes that the 20 °C limit is placed on the temperature differential to avoid thermal cracking, but that the research behind this specification is "ambiguous."

Townsend (1981) suggests that a temperature drop of between 14 and 17 °C can be allowed from the maximum temperature achieved during hydration to the long term stable temperature before tensile cracking would develop in gravity-type dams. Townsend's suggestion is based on previous experience.

Conrad (2006) notes that temperature gradients of approximately 2.5 – 3 °C/m at concrete faces could lead to cracking, while a temperature differential between the dam core and dam exterior of more than 15 °C is believed to cause cracking.

2.8.2 Site specific specifications based on analysis

In a coupled thermal-stress analyses the actual site specific structural and construction designs as well as the ambient conditions can be modelled. In addition to temperature effects, other loading conditions can also be considered. This leads to a situation where temperature limits can be imposed based on the site specific risk of cracking as opposed to a generalised assumption.

For the construction of the Deep Creek RCC Dam, a limit of 21.1 °C was placed on the maximum concrete placement temperature based on the results of a coupled analysis. The designers did, however, recognise that the 24 hour average placement temperature was more technically correct than a strict RCC placement temperature. A concession was made to allow the placement temperature to reach 22.8 °C for up to four hours as long as the weighted average did not exceed 21.1 °C (Hansen & Forbes, 2012).

Other examples where coupled thermal-stress analyses were performed to assess the risk of cracking for concrete dams include Noorzaei et al. (2006) and Husein Malkawi et al. (2003).

This study is limited to the use of generalised specifications, as structural analysis does not form part of the scope of the thesis.

2.9 Chapter conclusion

This chapter presented an overview of available literature on heat transfer as it relates to the analysis of concrete dams. Aspects that were covered ranged from the purely theoretical (the mathematical formulation of the heat transfer equation), onto how this theory is implemented to model real-world transient concrete temperature development, and finally to how insight into the mechanisms of heat transfer can be used to control concrete temperature in practice. The presentation includes works that reflect the latest thinking on these subjects, as well as those that have practical significance.

The concepts described in this chapter form the building blocks of the proposed temperature control model to be used in this study. In essence the proposed temperature control model takes these building blocks and combines them into a tool that can be used to optimise a given design in terms of temperature related requirements. How these building blocks are included in the proposed temperature control model is discussed further in Chapter 4.

Chapter 3: Methodology

3.1 Introduction

It was the aim of this study to develop a temperature control model that can be used to ensure that concrete temperatures remain within specified limits during construction. Step one in meeting the abovementioned aim was to develop the model. The second step was to show that the temperature analysis module contained in the model accurately models concrete temperatures during the construction of concrete dams. Being able to model concrete temperature accurately is essential, as without confidence in the accuracy of the results no subsequent decisions can be based thereon. The final step was to establish if concrete temperature can be kept within specified limits by implementing the proposed model. If it is shown that, by implementing the model, concrete temperatures can in fact be kept within specified limits during construction, then this study would have accomplished its goal. The set of procedures, or methodology, followed to achieve the goals of this study are described in this chapter.

Various methods could have been used to develop the model, validate the analytical module and confirm if the model can be used to ensure that concrete temperatures are kept within specified limits during construction. In section 3.2 different research methods are critically reviewed. Appropriate methods are then selected, and ways in which to limit the inherent limitations of these methods are put forward.

Section 3.3 is devoted to describing how the selected research methods were implemented in this study. Emphasis is placed on the research instruments used to collect data, the quality of the data that was collected and how the data was analysed to turn it into information from which conclusions could be drawn.

The final part of the chapter deals with the overall limitations of the methodology followed.

3.2 Research design

Research can be described as a logical procedure that is systematically approached with the aim of finding new and useful information on a topic (Rajasekar, Philominathan & Chinnathambi, 2006 in Theart, 2014). This section describes the logic behind the procedures followed to achieve the goals of this study.

The process followed to achieve the objectives of the study is divided into three steps:

- The first step was to develop the temperature control model. It was developed by combining several methods and techniques proposed by previous researchers.
- The next step deals with establishing whether the analytical module contained in the developed model produces accurate results. For the model to be able to predict time-based temperature profiles in concrete with any degree of certainty it must first be shown that the analysis procedure used provides accurate results. If it is shown that the analysis module provides accurate result when modelling a scenario with known input parameters, it follows that the same analytical procedure will produce accurate results when modelling other scenarios.
- In the final step it is shown how concrete temperatures can be kept within specified limits by demonstrating the implementation of the model.

Figure 3-1 shows a flow diagram of the procedure described above.

All research methods have strengths and limitations. No one is applicable to all situations. The research methods considered suitable for each of the above steps is summarised sub-section 3.2.1 - 3.2.3.

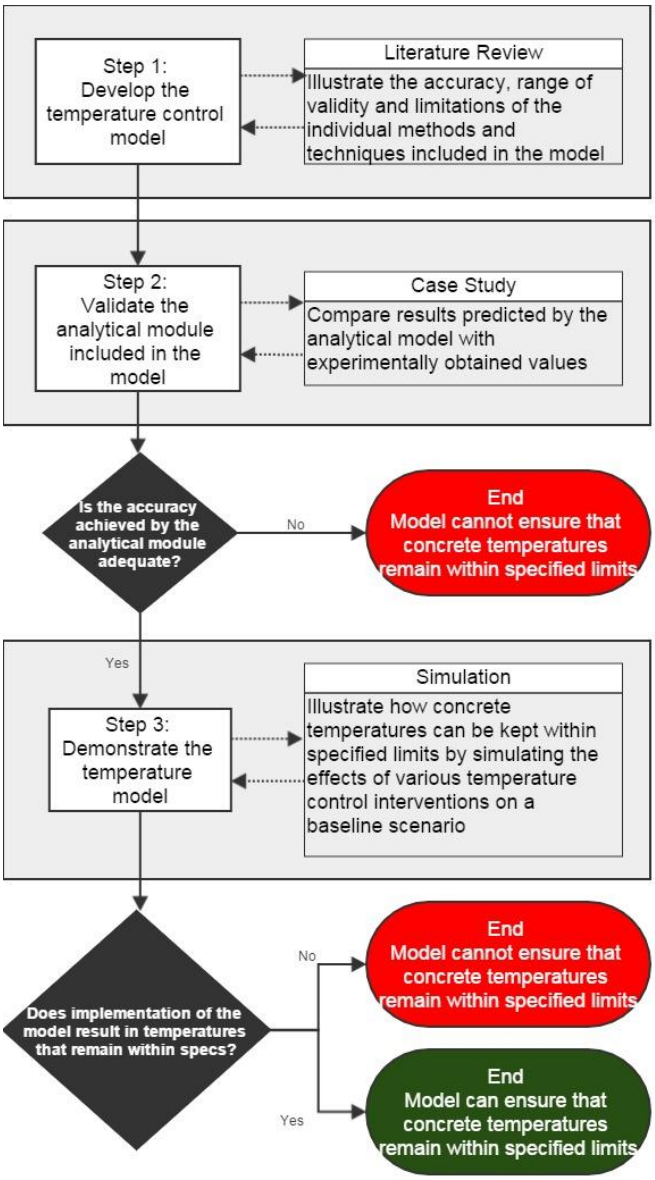

Figure 3-1 An overview of the approach followed to reach the objectives of the study.

3.2.1 Step 1: Develop the temperature control model

The temperature control model was developed using a literature based approach. The literature review can thus be viewed as the research method used to develop it. The strengths and weaknesses of this approach are summarised in Table 3-1.

Table 3-1 A summary of the advantages and disadvantages associated with developing the temperature control model from a literature review.

Research method	Discussion
Literature review	**Positives** (1) It can be shown that the techniques and methods included in the model are up-to-date with the current 'state of the art' to a large extent. (2) Limits on the validity if the model can be established by excluding all of the limitations of the procedures and methods it contains from the model's range of validity. **Negatives** (1) The results obtained from the literature review are subject to the bias and the ability of the researcher (Bartolucci & Hillegass, 2010).

It is shown in Table 3-1 that one of the drawbacks of a literature review is that it is subject to the bias and ability of the researcher. Therefore another validation of the model is also necessary. Such validation was done by comparing data collected during the rehabilitation of the Stompdrift Dam with results determined by the analytical module of the proposed model, as is elaborated on in sub-section 3.2.2.

3.2.2 Step 2: Validate the analytical module included in the temperature control model

Two research methods were considered applicable for validating the analysis module included in the temperature control model. These two methods are summarised in Table 3-2, elaborating on their strengths and limitations as they relate to the current validation step.

Table 3-2 Research methods considered suitable to validate the model's temperature analysis ability

Research method	Discussion
Experimental Laboratory study	**Positive** (1) During laboratory studies, in order to evaluate the effect of one variable (or set of variables), other variables are kept constant (Hofstee, 2006). This is the ideal situation when developing theories and determining causative relationships. **Negatives** (1) Laboratory studies can be limiting in that evaluating a combination of all of the variables involved is not very feasible. As the goal of the current study is not to develop causative relationships, but rather to implement a combination of causative relationships that have been developed by other researchers, a laboratory study would perhaps not be the best option. (2) Experiments can usually only be carried out on a small scale. Replicating the effect of a phenomenon like sequential construction can become questionable under these circumstances.
Case study	**Positives** (1) Case studies are effective when considering complex inter-variable relationships – which is the case for the current application. (2) It can be used to test the robustness of theories and causative relationships developed through laboratory experiments (Hodkinson & Hodkinson, 2001). (3) Case study research is grounded in reality. The effect of sequential construction, for instance, is reflected directly in the data obtained from the construction of an actual dam, while replicating its effect in a laboratory can only be done at a small scale at best, drawing its results into question. (4) An opportunity was granted by the Department of Water & Sanitation to use the rehabilitation of the Stompdrift Dam as a case study for the current research. **Negatives** (1) The comparison between collected and predicted data can be difficult. For instance, it is difficult to differentiate between the effects of hydration heat development and changes in specific heat capacity with hydration degree when the only parameter that is measured is the concrete temperature. Both of these

	factors affect the adiabatic temperature rise of a unit weight of concrete will be, but neither is measured explicitly. The result is that the interpretations made from the data can be subject to the bias of the researcher (Merriam, 2009). (2) The amount of data collected as part of a case study reduces the ease by which the data can be analysed (Hodkinson & Hodkinson, 2001). (3) The conclusions drawn from the research is, in general, not easy to generalise (Hodkinson & Hodkinson, 2001).

It was decided to perform a case study to validate the analytical module. Performing a case study was selected because funding was received for this part of the study, but mostly because a case study, in combination with the literature review performed to develop the model is deemed to be the most effective way to validate the analytical module of the temperature control model.

Two of the limitations of case study research relate to the ease by which data can be interpreted. This was addressed in the current study by the careful selection of locations where instruments were installed. The instruments were installed at locations where daily climate variations would have minimal effect, thereby limiting the extent to which the variables associated with the climate have an impact on the data collected, and consequently making the data easier to interpret.

The final limitation of case study research that was mentioned, i.e. the difficulty to generalise conclusions drawn from the results, is addressed by the complementary nature of the literature study. As other researchers have already established the limitations and range of validity of the methods incorporated into the proposed model, generalising the conclusions drawn from the case study is not considered to be a problem.

3.2.3 Step 3: Demonstrate temperature control model

Two research methods were considered appropriate for demonstrating how concrete temperatures can be kept within specified limits through the implementation of the model: Simulation or a case study. As was done for the previous validation step, these two methods are compared in Table 3-3 with regards to their strengths, limitations and applicability.

Table 3-3 Research methods considered suitable to demonstrate that the model can be used to keep concrete temperatures within specified limits

Research method	Discussion
Case study	**Positives** (1) The results from the case study are tangible. Establishing if the model can be used to keep concrete temperatures within specified limits would be as easy as answering the question – did the temperatures or did they not remain within the specified limits? (2) Case studies are effective when considering complex inter-variable relationships. (3) An opportunity was granted by the Department of Water & Sanitation to use the rehabilitation of the Stompdrift Dam as a case study. **Negatives** (1) The comparison between collected and predicted data can be difficult. (2) High amounts of data collected as part of a case study reduces the ease by which data can be analysed. (3) The consequences if the model does not perform as expected are real and could lead to undesirable cracking. (4) The temperature control model could not be developed in time for use during the rehabilitation of Stompdrift Dam. No other case study was available.
Simulation	**Positives** (1) It is well suited to the nature of the problem. The model that was developed can also be viewed as a prediction tool which aims to answer the question: "What would happen if approach A was followed instead of approach B." By comparing different outputs obtained from modelling different temperature control interventions it can be inferred what would happen in the real world if such interventions were to be implemented. (2) Simulation can be used as a substitute for experimentation (Dooley, 2002). (3) It is much less expensive than experimentation or case studies. (4) There are no real world consequences if the model is not able to achieve its goal. **Negatives** (1) The predictions made by the model are only valid if the model itself is valid

	(Dooley, 2002). So too are any conclusions drawn from the simulation. (2) One of the risks associated with simulation is the well-known GIGO rule of computing – garbage in equals garbage out. Simulated results might be analytically 100% correct, but devoid of any truth if the input parameters used are not realistic. Take the binder hydration characteristics of the two different cement clinkers in Figure 2-7 as an example: If simulation is done using the total heat output of Clinker B, but the actual clinker characteristics corresponds to those of Clinker A, the calculated adiabatic temperature rise would be 3.8 °C lower than what could be expected in reality (depending on concrete density and specific heat capacity). (3) Another risk associated with simulation is that the relationship between simulation and reality can become blurred. For instance, optimisation of a design using the proposed model might show that the selection of a certain aggregate type is the best choice, based on the resulting temperature distribution, but said aggregate might not occur naturally within 1000 km of the construction site, thereby making the aggregate type selected unrealistic.

Simulation was selected as the research method to show that the proposed model is able to ensure that concrete temperatures are kept within specified limits during the construction of concrete dams. It was selected both because the temperature prediction model was not ready to implement during the rehabilitation of the Stompdrift Dam, and because simulation is well suited to come to a conclusion regarding the validity of the proposed model.

Three limitations were identified when implementing a simulative approach for the current problem. Two of these relate to the quality of the input data – the fact that predictions can be made using unrealistic input data. In order to guard against this, the Stompdrift Dam rehabilitation was used as the basis for the simulations made, along with all of the constraints associated with the project. This effectively prohibited unrealistic inputs.

The final concern regarding simulation is that results obtained from simulations are only valid if the model used to make the simulations is valid. This is why it was important to test the accuracy of the analysis module contained in the proposed model before demonstrating the model as a whole.

3.3 Methodology

The logic behind the approach followed to come to a conclusion regarding the validity of the proposed model was described in the previous sub-section. The research methods selected

were described based on their strengths, limitations and applicability. How the limitations of the selected research methods restricted was also discussed. In this sub-section details are given on how the three selected research methods were implemented. The focus here is on the quality of the data that was collected, challenges encountered and on the limitations of the data.

3.3.1 Literature review

A review of literature on the thermal analysis of concrete dams was performed. Works reviewed ranged from the underlying theory base required to perform thermal analyses, up to the current state of the art as it relates to the analysis of concrete dams during construction. Works obtained from various sources were reviewed, including the following sources:

- Peer reviewed Journals
- Conference proceedings
- Books
- Manuals
- Online content:
    - Published dissertations and theses
    - Manuals of concrete practice from the American Concrete Institute (ACI)
    - Manuals of practice from the Unites States Bureau of Reclamation (USBR)
    - Other research reports

The works included in the review were selected from the sources above based on their availability, applicability and quality. Preference was given to newer works, as these inevitably reflect the latest thinking on the subjects covered. The data contained in the selected sources were reviewed critically with the aim of establishing which factors affect concrete temperature development and how these factors can be incorporated into a thermal analysis procedure for concrete dams.

The validity of the data and techniques found in literature was checked, mostly by comparing results obtained from analyses using said data or techniques with results from experiments or case studies, if such results could be obtained. Alternatively data and methods obtained from various sources were compared qualitatively. It was also checked under which circumstances the data and methods that were reviewed are applicable.

As mentioned in the previous section, data collected in a literature review can be limited in two ways: the data can be incomplete (important works containing new and valid techniques

omitted during the review) or biased. Care was taken in the literature review that neither of these two limitations took effect. An effort was made to include current works, helping to ensure that the data used in the proposed model reflected the latest thinking on the relevant matters. When choosing between different, valid techniques for inclusion in the model, the decision was based on the accuracy of the results provided by the different techniques, and not on the preferences of the researcher (such as ease of implementation).

The above measures consequently ensured that the data obtained from the literature view is as complete as possible.

3.3.2 Case study

The rehabilitation of the Stompdrift Dam was used as case study. Data collected during the rehabilitation was used to test if the analytical module of the proposed model can accurately model concrete temperature during concrete dam construction. The discussion below aims to elucidate how data was collected, what the limitations of the collected data are and how this data was analysed to come to a conclusion regarding the analytical module's validity. Table 3-4 summarises the different types of data that was collected during the rehabilitation.

Quality of the data collected

Climate data: Data was collected using a Campbell Scientific GRWS100 during the rehabilitation. It is generally of a high quality. The record length is continuous, apart from a gap from 22 to 28 June 2012 due to a power failure. Besides this short gap in the collected climate data, another limitation in the data is the wind speed data collected. The wind speed data collected on the crest of the dam cannot be considered representative of the wind speed at the locations where new concrete was placed. This is because the existing structure provided shelter from the wind for most wind directions. The actual wind speed, which is a driving force for convection, was much lower. Apart from the inapplicable wind speed data, the climate data is of sufficient length and quality to use the data as input in the proposed temperature control model to evaluate climate driven heat transfer effects.

Fresh concrete temperature: The fresh concrete temperature for each batch of concrete was recorded by the site laboratory technician on a quality control sheet. This data was then digitized by the site's administration personnel. There are no gaps in the data. The human factor does make it possible that errors might have been made in the recording or digitizing of the data, but no unrealistic values were observed in the dataset. The realistic temperatures recorded, along with the good work ethic of the laboratory technician, led to

the conclusion that the data on the initial temperature of the fresh concrete is of a high quality.

In-situ concrete temperature: In-situ concrete temperatures were measured using 3 kΩ NTC thermistors. The installation of and data collecting from the in-situ instruments did not go entirely as planned. Procurement difficulties and personnel error led to some instruments not being installed. Temperature measurements had to be taken and recorded manually as a result of the datalogger system only being installed near the end of the project. During the early stages of the project, data from the in-situ thermistors were recorded three times per day. Later, the sheer amount of instruments installed made it impossible to read every instrument within a two week cycle using the available resources. Additionally, access to the instrumentation gallery was blocked for a two month period, making it impossible to record any measurements during this period.

The in-situ concrete temperature data collected during the rehabilitation of the Stompdrift Dam is not perfect, as described above. But it also does not need to be: While the frequency of the manually collected data is not high enough to evaluate whether the proposed model predicts hydration heat development accurately over the first 24h, it is high enough to evaluate whether the model accurately models the total temperature rise achieved as well as the period of cooling after most of the hydration heat has been liberated. Continuous data is not essential for comparing the measured and predicted temperature values during the cooling period, because the cooling process happens relatively slowly.

Comparison between case study and the analytical module of the proposed temperature control model

The case study data collected, as described above, was ultimately compared with a back-analysis of the construction process. The known construction programme, fresh concrete temperatures and climate data collected are used as input into the analysis module of the model. Other parameters, such as the specific heat capacity, thermal conductivity of the concrete and hydration characteristics were based on literature values. All of this input data was then processed into a finite element model that simulates the actual conditions and materials encountered during construction as close as possible. A finite element analysis was then carried out.

Table 3-4 Data collection during the rehabilitation of the Stompdrift Dam.

Type of data		Method of data collection	Data collection location
Climatic data	Air temperature	Campbell Scientific GRWS100 general-purpose weather station. All data types were measured and logged automatically at hourly intervals.	The weather station was installed on the crest of the existing dam, close to the position where the concrete was placed during the rehabilitation.
	Wind speed		
	Wind direction		
	Relative humidity		
	Barometric pressure		
	Precipitation		
	Solar radiation		
Concrete temperature	Fresh concrete	A Sinometer DM6801B digital thermometer was used to measure the fresh concrete temperature after batching. The data was recorded manually by the site laboratory technician.	Measurements were taken at the batching plant, 250 m from the final point of delivery (concrete pump) on the sample used to determine the slump of the concrete.
	In-situ temperature	Concrete temperatures were measured using RS Components' 3 kΩ NTC thermistors that were installed inside 15 mm copper pipe casings filled with polyurethane epoxy. Measurements were taken manually at infrequent intervals during the first part of the project using a Major Tech MTD10 digital multimeter. Measurements were taken and stored automatically at 1 hour intervals using a Campbell Scientific data-logger system (CR1000 data logger) during the latter part of the project.	Thermistor-type instruments were installed at the centres of concrete blocks (plan view), at the bottom of construction lifts. Instruments were also installed 300 mm from the edges of selected blocks, also at the bottom of construction lifts.

Results from the finite element analysis were then extracted at nodes which correspond to the positions where in-situ temperature measurement devices were installed. A comparison between the measured and calculated temperature values was then made.

The input into the model was subsequently calibrated in order to obtain a reasonably accurate solution. Based on the comparison between measured and calculated temperatures, as well as a reflection on the nature of the calibration that was required, a conclusion is then drawn regarding the validity of the analysis module.

3.3.3 Parameter study

A parameter study was performed to establish if the proposed model can be used to ensure that concrete temperatures can be kept within specified limits. In the parameter study, several aspects were varied, individually and in combination, in order to arrive at a solution that complies with pre-set specifications.

The main research instrument used in the parameter study was the proposed temperature control model itself. A description of what the proposed temperature model entails and under which circumstances it is applicable has been provided above.

The data collected as part of the parameter study is essentially the nodal concrete temperatures that were calculated during each analysis performed as part of the study. Regarding the quality of the data, it can only be considered as good as the model itself and the input provided. Input data, which is an important part of the proposed model, can have a large effect on the quality of the data produced. Consequently, parameters were only varied within reason: All of the constraints that were applicable during the rehabilitation of the Stompdrift Dam were made applicable to the parameter study. This helped ensure that only realistic scenarios were evaluated.

The approach followed to come to a conclusion regarding the validity of the model is outlined in Figure 3-2.

3.4 Limitations

The research methods used have certain limitations. The way this study was approached determines the reliability of the findings made, as well as the extent to which they can be generalized. These limitations are highlighted below.

The reliability of the conclusions drawn regarding the accuracy and generalizability of results generated by the model can be improved. If several case studies were considered, taking into account different concrete mixes, climate conditions and construction programs, more

reliable conclusions could have been drawn. Due to time and financial constraints, generalising the findings made from the case study was done based on secondary data obtained from literature. While still a valid approach, generalising these findings could have been made more reliable by using several case studies instead.

Conclusions drawn about the validity of the model could have been made more reliable by supporting the predictions made by the model with experimental or case study data. Again, due to financial and time constraints this was not done. Findings regarding the proposed temperature control model are based solely on the assumption that the model produces valid results. The assumption regarding the accuracy of the model is tested as part of the research design and therefor does not invalidate conclusions drawn from the simulated results.

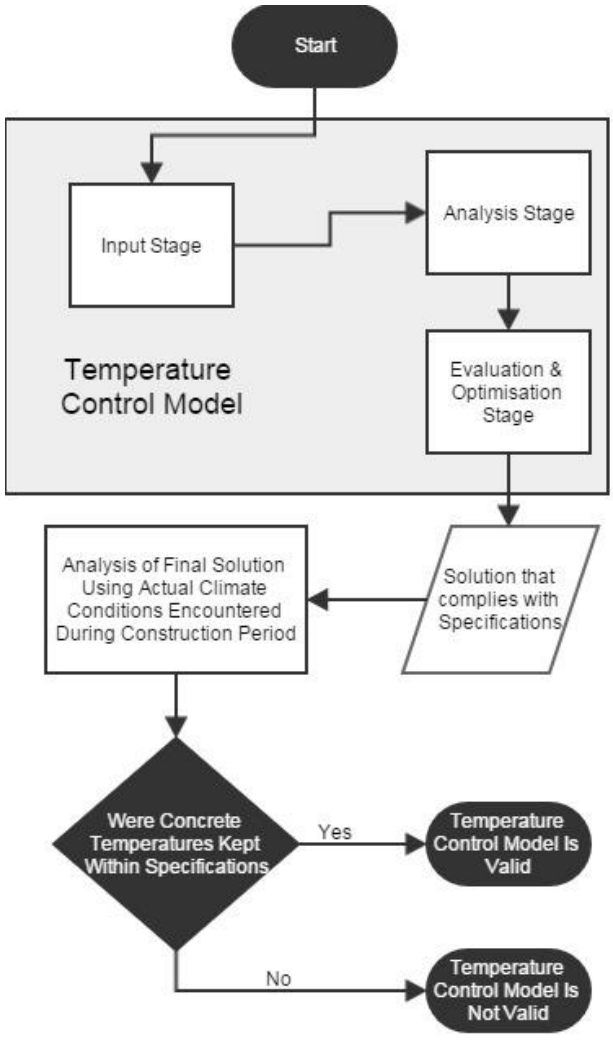

Figure 3-2 A flow diagram showing the logic followed during the parameter study to come to a conclusion regarding the validity of the proposed temperature control model.

Generalising the findings made from the parameter study could have been made more effective by incorporating every possible temperature control intervention in the study. This was not done, as the research objectives could be achieved without considering every possible alternative.

Chapter 4: Development of the temperature control model

4.1 Introduction

This chapter elaborates on the development of the temperature control model. The proposed model is in essence a logical set of procedures that can be followed to obtain a construction design that conforms to pre-set temperature related specifications. This set of procedures has been divided into three stages – the design, analysis and evaluation & optimisation stages.

The input stage is described first. Here all of the un-processed data required as input into the model is described.

Section 4.3 is used to describe the analysis stage. This stage is also divided into three parts - pre-processing, analysis and post-processing. It is in this section where selected techniques and methods from other researchers are incorporated into the model.

Next, the evaluation & optimisation stage is described. In this stage input parameters are optimised in order to obtain a construction design that, when implemented, should ensure in concrete temperatures remain within specified limits throughout the construction period.

Finally, the model's limitations are discussed.

4.2 Input stage

The basic structural and construction designs of a concrete dam are used as input into the model. After a decision has been taken to build a dam at a specific site, the dam type to be constructed is selected. If a concrete-type dam is to be built, the design process aims to establish the required geometrical layout of the dam, concrete strength class and construction method. It is this basic design, in combination with a preliminary implementation plan, which is used as input into the proposed model.

The accuracy of the parameters used as input in the model determines the accuracy of the time-based concrete temperature profiles calculated by the model. There are a multitude of factors that affect the time-based temperature distribution in concrete, as has been elaborated on in Chapter 2. Site and project specific testing and sampling results are the first choice when it comes to parameter estimation. If such results are unavailable literature-based values can be used, but this reduces the confidence levels associated with the results. High quality input leads to high quality output.

The following aspects are taken into account by the proposed model and are required as input:

- **Geometry of the dam:** In addition to the geometry of the dam itself, this includes the positions of construction joints, galleries and any major features that could significantly affect the calculated temperature field.
- **Concrete mix proportions:** This includes the amount and type of ingredients used, along with their thermal properties (conductivity, specific heat capacity and density).
- **Binder type(s), quantity and hydration characteristics:** Due to the significant variation between the hydration characteristics of binders obtained from different sources, physical testing is highly recommended for determining the adiabatic temperature rise curve. Additionally, if experimental data is available on the activation energy parameter, this can also be included. If physical testing cannot be carried out, the maturity heat rate data for various Portland cement / supplementary cementing material blends that can be found in the "Ballim Temp Model.xls" spreadsheet which accompanies Owens (2009) can be used.
- **Construction method:** Distinction is made between RCC construction and mass concrete construction, as different analysis techniques can be employed when determining the resultant time-based temperature distribution. All other post-placement temperature control interventions to be implemented during construction, apart from cooling pipes, are also included here. These interventions include the type of shutter used (steel vs wood and / or insulation), the time shutters are kept in place before stripping as well as curing practice.
- **Construction programme:** This entails specifying the planned start date, construction rate and any planned stoppages during construction.
- **Site climate conditions:** The estimated average daily air temperature, daily air temperature variation, wind velocity, relative humidity and solar radiation heat flux throughout the construction duration is required as input here.
- **Initial conditions:** The initial fresh concrete temperature as well of that of the foundation and, if applicable, other existing concrete is required.
- **Specifications:** The specifications included as input form the basis on which it will be decided whether the calculated time-based temperature field resulting from an analysis incorporating all the other input parameters is acceptable or not.

The flow diagram shown in Figure 4-1 provides an overview of what the "Input stage" of the temperature control model entails.

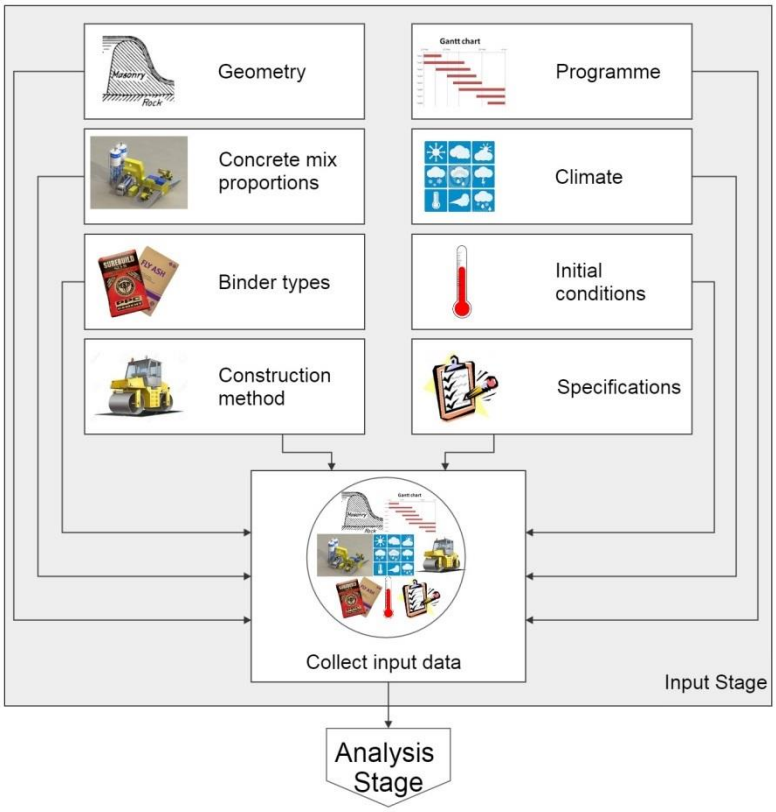

Figure 4-1 A schematic representation of the input stage

In selecting / estimating the above parameters, some engineering judgment to be applied by the analyst is inevitable. To use the temperature of fresh concrete as an example, it is up to the analyst to make a reasonable assumption with regards to which range of values to use throughout the construction period, based on site specific conditions.

4.3 Analysis stage

After all of the required input data has been assembled, a baseline temperature analysis can be performed. The proposed model makes use of finite element analysis to calculate the time-based temperature distribution in the concrete. The finite element analysis procedure is divided into three phases – pre-processing, solution and post processing (Amirouche, 2006).

Figure 4-2 provides an overview of the “Analysis stage” of the proposed model.

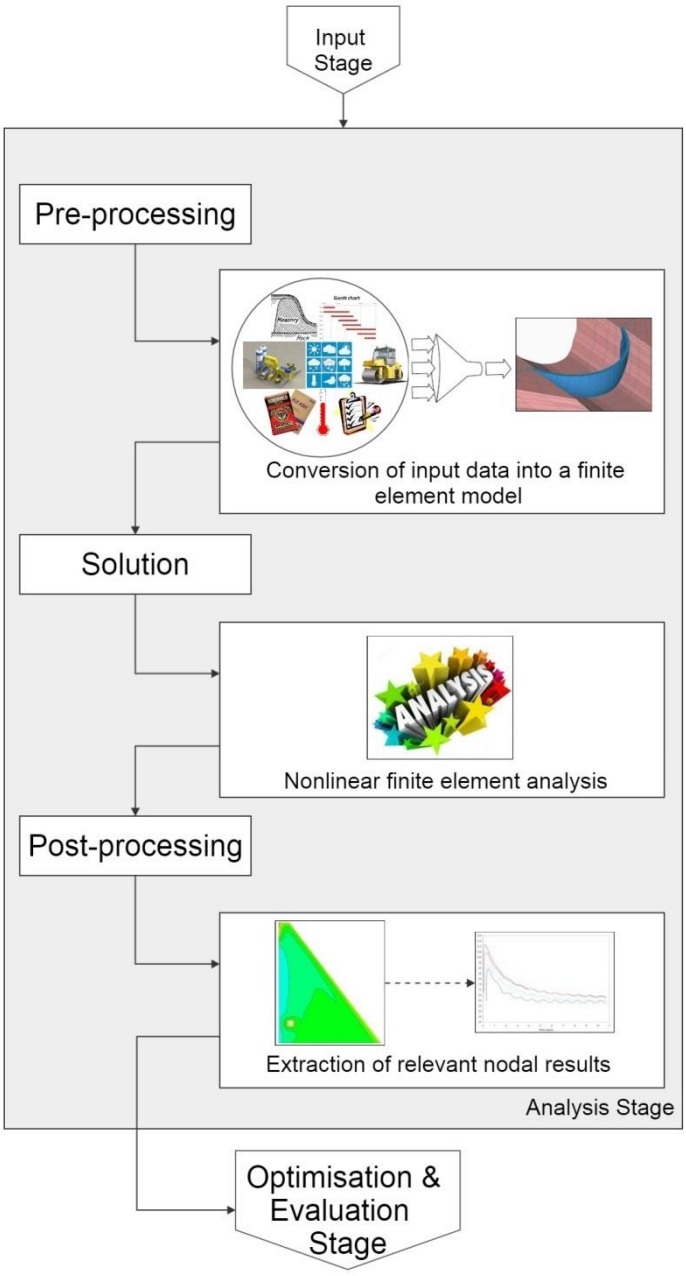

Figure 4-2 A schematic representation of the analysis stage

4.3.1 Pre-processing

The pre-processing phase entails converting the input data into usable values and formats, which is then implemented in a finite element model. As an example, knowledge of the thermal conductivity of unreacted Portland cement cannot be included in the finite element model directly. Conversely, thermal conductivity of concrete can be included directly in the finite element model, but it is not necessarily known from the input data. The calculation of the thermal conductivity of concrete from the thermal conductivity of its ingredients is done using one of the various methods and techniques forming part of the pre-processing procedure, as described below.

Mesh discretization: The first step in the pre-processing procedure entails discretizing the geometry of the dam and its foundation into finite elements. Mesh discretisation itself will not be discussed here, apart from stating that it is generally sufficient to model RCC dams in two dimensions, while mass concrete dams can either be modelled in two or three dimensions, depending on the dimensions of the dam being analysed. The interested reader is referred to one of several texts that deal with the theoretical basis underlying finite element analysis for more information on appropriate element size, type and shape selection (Amirouche, 2006; Cook et al., 2002; Van Rooyen, 2008).

Thermal conductivity: The thermal conductivity of concrete is not available directly and needs to be calculated. The approach suggested by Guo et al. (2011) has been adopted for use in the model. The Guo et al. approach simply entails calculating the weighted average of the thermal conductivities of the concrete mix constituents.

While there are other methods that are more accurate, they also require additional input that is not necessarily readily available. For instance, the approach proposed by Choktaweekarn et al. (2009b) requires knowledge on the amount of free water and gel water in the concrete at any given time. Including this amount of detail in the temperature control model would make the model too elaborate.

In the event that experimentally obtained thermal conductivity values are not available for some or all of the concrete mix constituents, literature based values are assumed where applicable. The thermal conductivity of the aggregate fraction of the concrete shown in Figure 2-2 can be used. Conductivities of other ingredients are summarised in Table 4-1.

Table 4-1 Thermal conductivity values used in the temperature control model for concrete ingredients other than the aggregate fraction (Choktaweekarn et al., 2009b).

Concrete ingredient	Thermal conductivity (W/m.K)
Portland cement	1.55
Fly ash	0.76
Water	0.59

Materials other than fresh concrete that are also included in the finite element model also need to be assigned thermal conductivities. For existing, hardened concrete the same approach used to calculate the conductivity of fresh concrete is utilized if its mix proportions are known. Alternatively values from Table 2-2 or other literature based values can be used.

The conductivity of the foundation is assumed to be the same as that of an aggregate of the same rock type and is also obtained from Figure 2-2.

Specific heat capacity: As is the case for thermal conductivity, the specific heat capacity of concrete needs to be calculated based on the proportions and the properties of mix constituents. A weighted average of the specific heat capacities of concrete mix's ingredients can be taken to calculate the specific heat capacity of the concrete.

Estimating the specific heat capacities of the concrete mix constituents in the absence of experimental data are done based on literature values. Table 2-3 is used to select the specific heat capacity of the aggregate fraction at different temperatures. Determining the specific heat capacity of the aggregates at temperatures other those tabled is done using linear interpolation between the tabled values. The specific heat capacities of the other concrete ingredients are selected from Table 4-2.

Mass density: The density of the concrete is simply taken as the mass weighted average of its unreacted ingredients. The densities of the ingredients can either be measured directly, or the values from Table 2-5 and Figure 2-5 could be used.

Hydration heat development: The model uses the adiabatic temperature rise of concrete as input. If only isothermal or maturity based data is available, it first needs to be converted to adiabatic data. This is done with the help of Equations 2.5.2 and 2.5.3. A reference temperature of 20 °C and default apparent activation energy of 33.5 kJ / mole are used as input as part of this process.

Table 4-2 Specific heat capacity values used in the temperature control model for concrete ingredients other than the aggregate fraction (Choktaweekarn et al., 2009a).

Concrete ingredient	Specific heat capacity (J/kg.K)
Portland cement	817[1]
Fly ash	711
Cement gel	419
Water	4187

Solar radiation & convection: Solar radiation heat flux is converted to an effective ambient temperature using a slightly modified version of Equation 2.6.6. Instead of taking the daily

[1] Average value from Gibbon et al. (1997) and Choktaweekarn et al. (2009a).

global solar radiation energy to calculate the average daily temperature lump sum from radiation, the equation is modified so that the lump sum temperature calculated corresponds to the length of the time-step used in the analysis:

$$\Delta T_{rad} = \frac{Q_{S,glob}}{c \cdot m} = \frac{\int_t^{t+1} q_{S,glob} dt}{c \cdot \rho \cdot \left(0.2 \times \frac{\Delta t}{24}\right)} \quad 4.3.1$$

Where: t = Clock-time at beginning of time-step (h)

$t + 1$ = Clock-time at end of time-step (h)

Δt = Length of time-step (h)

The effective ambient temperature for each time-step is then calculated using Equation 2.6.5, which is then applied to the model as a convection load in combination with the convection coefficient.

Care should be taken when using Eq. 3.2.1 instead of Eq. 2.6.6. By adjusting the characteristic penetration depth of the diurnal temperature cycle (0.2 m) to the characteristic penetration depth for a time-step specific temperature cycle, the characteristic penetration depth of the concrete will increase beyond 0.2 m for time-steps longer than 24 h. The minimum section thickness that is analysed should be greater than twice the characteristic penetration depth (0.2 m x 2 = 0.4 m for a 24 h time-step).

It should be noted that the global solar radiation heat flux is dependent on the angle between the surface normal vector and the sun. Horizontal surfaces and vertical surfaces (as well as different vertical or inclined surfaces with varying orientations) will consequently receive different amounts of solar radiation at the same moment in time. The effective ambient temperature needs to be calculated for each surface inclination.

The convection coefficient is calculated based on the climate input data (air temperature and wind velocity) as well as information on the type of shutter / insulation used and how long said shutters remain in place after concrete placement has taken place. Equations 2.6.2 - 2.6.3 are used for these calculations.

Initial temperature: The initial temperature of all the components included in the analysis needs to be specified. For the foundation it is recommended that a pre-analysis of sufficient length be performed. An initial temperature still needs to be specified for the foundation, but the pre-analysis will reduce the magnitude of the mistake made with the initial assumption. For fresh concrete the initial temperature that is specified needs to account for all of the factors discussed in Section 2.6.3.

4.3.2 Solution phase

The time-based temperature distribution in the concrete is obtained by implementing the analysis in commercially available finite element analysis software. The following user input is required in the solution phase:

- A phased analysis needs to be carried out. Elements corresponding to each construction lift are simply activated at a designated time period to simulate the construction process.
- Appropriate time-steps should be selected. The length(s) of the time-steps used should be short enough to accurately model climate and hydration effects, but long enough so as not to be too resource intensive. As a first approximation it is suggested that time-steps in the order of 6 hours in length be used during the first couple of days of hydration. Time-step lengths can be increased with an increase in maturity as the hydration rate decreases. A 6-hour time-step might be too long to accurately model the hydration of concrete with a high initial heat generation rate. Conversely, it might be unnecessarily long for concrete that releases its hydration heat slowly, and over a long period. Ultimately it is up to the user to determine the optimal time-step length that does not lead to a decrease in accuracy, but also does not result in ineffective resource use.
- A nonlinear analysis should be carried out. This allows evaluating the effects of hydration heat development as well as the temperature dependant behaviour of some material properties.

Care should be taken when selecting a software package to use for the analysis. The selected software package should have the following capabilities:

- It should be capable of carrying out phased analyses.
- It should have the capability to model nonlinear material properties.
- It should be able to model hydration heat production and concrete maturity. Preferably as a built-in function, or alternatively as a user defined sub-routine.

4.3.3 Post-processing phase

In the post-processing phase, the calculated nodal temperature results are extracted at relevant positions for use as input data during the evaluation stage of the temperature control model.

4.4 Evaluation & optimisation stage

During the “Evaluation & optimisation stage” of the temperature control model the results obtained from the initial baseline temperature analysis are evaluated and optimised. provides an outline of the process followed in this part of the model.

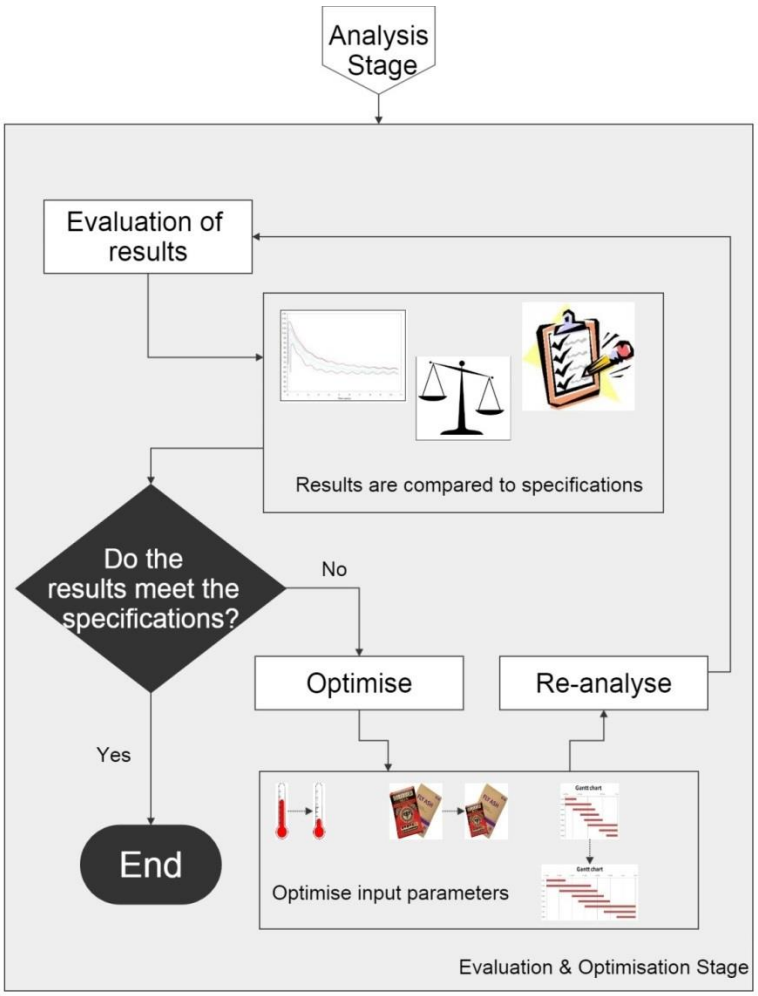

Figure 4-3 A schematic representation of the evaluation & optimisation stage

The calculated nodal temperatures calculated during the analysis phase are critically reviewed here. This review procedure starts by selecting nodes along the centreline of selected cross sections (or in the case of a 3-D analysis, the 2-D section). The temperature distribution along these points is taken to represent the maximum internal concrete temperature at any specific time during construction.

A review of the temperature distribution at the centre of the dam over time will reveal if the concrete temperature exceeds the pre-set maximum temperature specification. To evaluate whether the maximum temperature gradient specification has been exceeded, more lines of nodes can be selected at the downstream, upstream and (possibly) side faces. Comparing

the temperature difference between the exposed concrete faces with the maximum internal temperature will reveal if the maximum temperature gradient has been exceeded.

If the time-based concrete temperature distribution is acceptable as measured against the pre-set specifications, no further design changes are necessary. If this is not the case, optimisation of the design is required.

Optimisation is an iterative process. The input parameters are modified, implemented in the analysis module and the results evaluated. If the result is acceptable, the process ends. If not, the input parameters are modified, restarting the process.

Changes to the input parameters need to be made with care, though. Certain project specific circumstances may prohibit specific interventions to be made. Caution is advised when changing the mix design for a RCC dam, for instance. RCC mix design is a specialised field, with much care taken to ensure that a combination of the temperature, strength and workability requirements is met. It would be ill-advised to tamper with the mix without taking workability and strength requirements into consideration as well.

4.5 Limitations and applicability

The proposed temperature control model is subject to certain limitations to its accuracy and applicability. All of the calculation procedures (including equations, figures and tables) included in the proposed model were originally developed for specific applications under specific conditions. Consequently the limitations on the accuracy and applicability of the proposed model are derived from the conditions determining the accuracy and applicability of the calculation procedures used in the model.

Stating the limitations of the model not only illustrates under which conditions the model is not valid, but by implication it shows under which conditions it is valid. The accuracy and applicability limitations of the calculation procedures employed in the proposed temperature control model have been dealt with in the literature review. A summary of the limitations on the applicability of the model is given below:

- The calculation procedures for determining the thermal conductivity and specific heat capacity of concrete do not consider any other cementitious materials than Portland cement and fly ash. Future research would have to be done to develop robust and accurate methods to determine the thermal conductivity and specific heat capacity of blended Portland cement and slagment concrete mixes if the model were to be expanded to make provision for such blended concrete mixes.

The proposed temperature control model is consequently only applicable to situations where the concrete that is used contains 100% Portland cement or a blend of Portland cement and fly ash. The model's lack of functionality to deal with Portland cement / slagment concrete blends is not considered a major drawback, as most modern dams are constructed using Portland cement / fly ash blends.

If experimental data on the thermal conductivity and specific heat capacity of a blended Portland cement and slagment concrete mix is available, this data can be used as input into the model.

- Including cooling pipes as a temperature control intervention in the concrete body is not taken into account in the proposed model. The lack of ability of the model to take cooling pipes into account is not considered a major drawback, as cooling pipes are not widely used in South Africa.

- The method included to calculate the convection coefficient is based on air and not water. Convection from a water body is not considered, but convection from air at any wind velocity is. Water was not included, as impoundment normally only starts after the completion of a dam and would consequently not affect concrete temperatures during construction. For specific cases where partial impoundment is allowed, the reader is referred to the following references for procedures to determine the film coefficient (Lienhard IV & Lienhard V, 2000; Mills, 1992).

- The method used to take solar radiation into account assumes characteristic penetration depth of approximately 0.2 m, depending on the length of the time-step. Only sections thicker than twice the characteristic penetration depth should be analysed. Conventional concrete is normally placed in lifts thicker than 1.2 m, while RCC is placed in lifts up to 3 m thick. This limitation will therefore not have much practical influence if time-steps are kept short enough.

As demonstrated above, notwithstanding the limitations mentioned, the model can still be considered relatively versatile as it is applicable to most conditions encountered in practice.

Chapter 5: Case Study - Rehabilitation of the Stompdrift Dam

"*The only relevant test of the validity of a hypothesis is comparison of prediction with experience*"

Milton Friedman

5.1 Introduction

This chapter is used to demonstrate the accuracy of the analysis module included in the temperature control model. This is done by comparing data collected during the rehabilitation of the Stompdrift Dam to results obtained when replicating the construction process in the analysis module.

Stompdrift Dam is a multiple buttressed, double curvature arch dam with a curved gravity section at the right flank. It is located 40 km east of Oudtshoorn in the Western Cape province of South Africa. The dam was designed, built and is owned by the Department of Water and Sanitation (previously known as the Department of Water Affairs). Construction of the original dam was completed in 1965.

A rehabilitation project was undertaken between 2012 and 2015 to address certain dam safety and operational deficiencies. Part of the rehabilitation entailed converting the smallest of the dam's three dome shaped arches from a thin arch to a thick arch with a cylindrical downstream face. This was done by placing mass pumped concrete against the downstream face of the arch. The width (radial direction) of the rehabilitation works varied from approximately 12 m at foundation level to less than a metre at the crest of the dam. The height of the section where concrete was added ranged from nearly 30 – 33 m.

Figure 5-1 shows a downstream view of the dam before, during and after construction. Concrete was placed in leader and follower blocks. Only data collected from one of the central, leader blocks was analysed for this study. This is mainly due to the lack of in-situ concrete data collected from the other blocks.

To further elucidate the extent of the rehabilitation, Figure 5-2 shows a cross section drawing of a representative section of the rehabilitated tertiary arch.

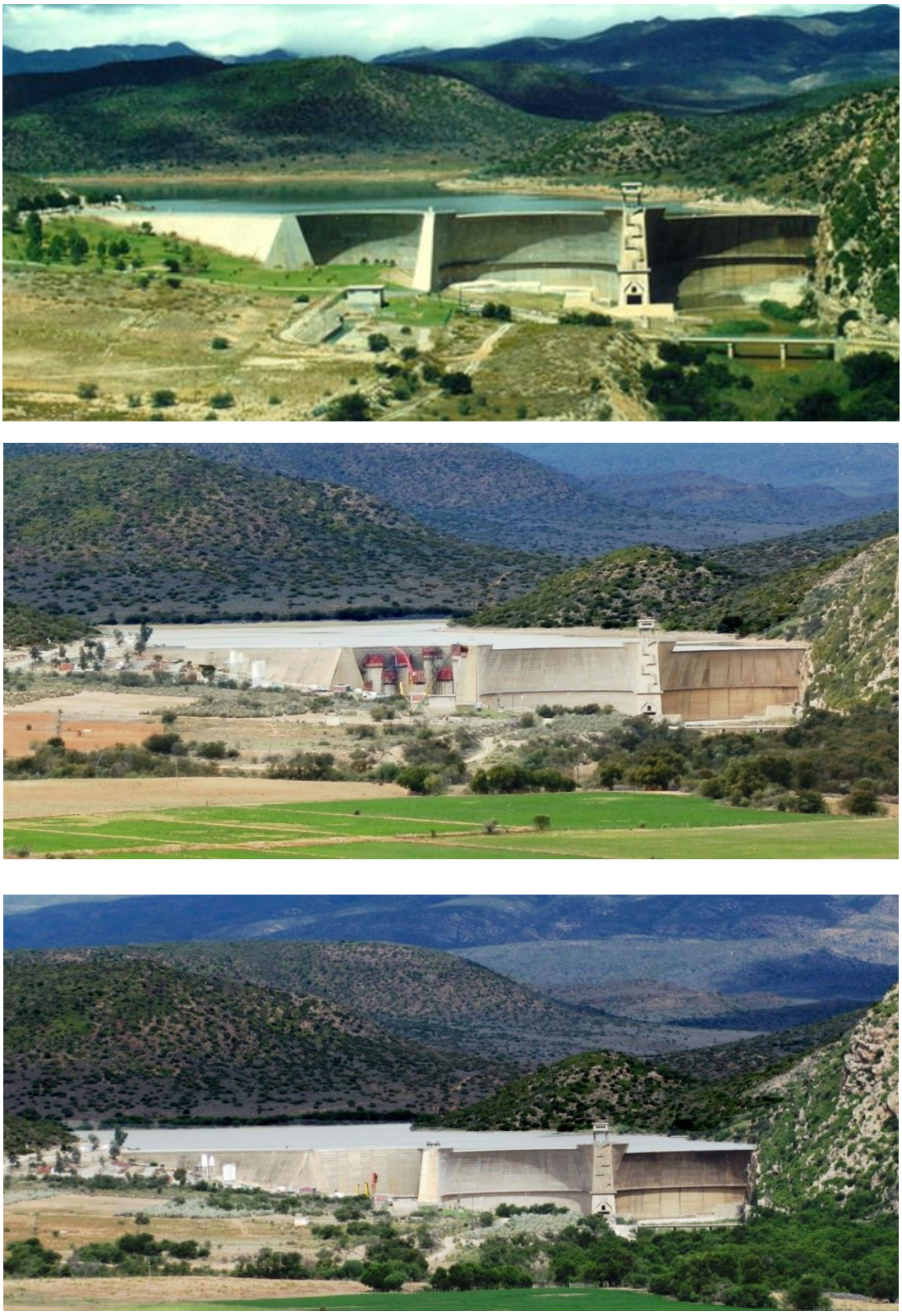

Figure 5-1 **A downstream view of the Stompdrift Dam prior to, during and after the dam safety rehabilitation (Schoeman & Oosthuizen, 2015).**

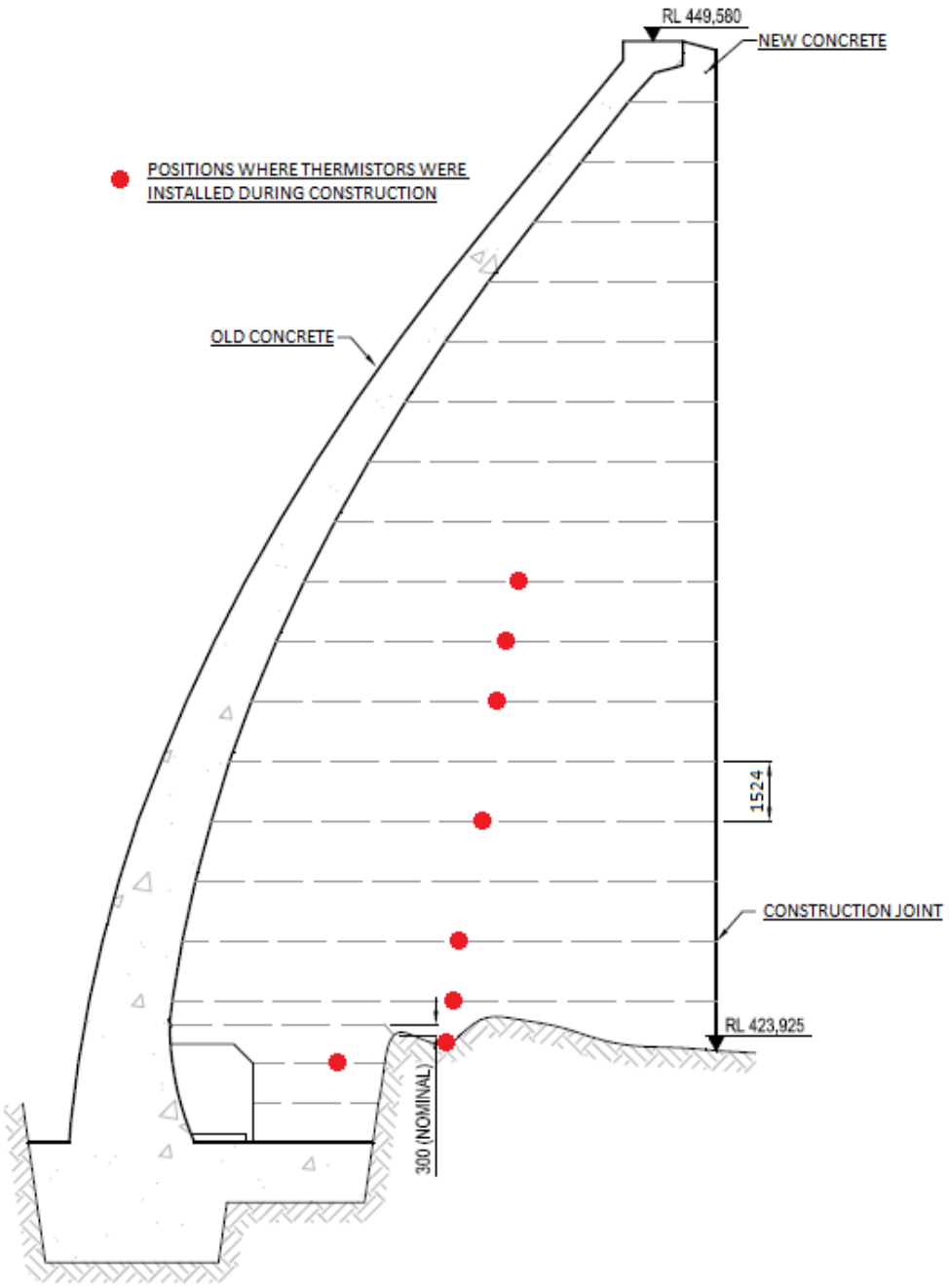

Figure 5-2 **A representative cross section of the rehabilitated arch showing the relative thickness of both the new and pre-existing concrete. Approximate positions of thermistors are also shown.**

5.2 Physical construction and data collection

The first concrete placed at the block analysed as part of this study was cast on 8 August 2012. Twenty lifts were placed in total for this block, with the final lift cast 373 days later on 16 August 2013. During construction, four types of data were collected:

- Climate data;
- Fresh concrete temperatures;
- In-situ concrete temperature; and

- Water level

The data collected is briefly discussed below.

5.2.1 Climate data

A weather station was installed on site during the construction period. A GRWS100 weather station was used as it was available for use without having to procure it. The GRWS100 is described by Campbell Scientific as a “research grade” weather station (2015). The installation position of the weather station was determined by the need to measure the difference between incoming and outgoing radiation on a horizontal plane, while causing as little disruption to the construction process as possible. The crest of the existing dam wall was consequently selected. The following climate related parameters were recorded:

- Air temperature;
- Wind speed;
- Wind direction;
- Relative humidity;
- Barometric pressure;
- Precipitation; and
- Solar radiation.

Placing the weather station on the crest did have adverse consequences. One of these is that the wind speed data that was collected is not equivalent to that experienced where the concrete was placed. This is because the existing dam wall acted as a wind barrier, reducing wind speeds dramatically.

Solar radiation was measured using a Q7.1L REBS net radiometer. This instrument has two receivers: one facing upwards and another facing downwards. The value that is recorded is the difference between the readings of the two receivers, which is equal to the amount of radiation absorbed by the concrete on a horizontal plane. As with the wind speed, the recorded radiation data is also not necessarily equal to the radiation imparted to the concrete placed downstream of the existing arch. As the dam wall is aligned such that the upstream-downstream direction approximately coincides with the east-west line, the existing dam wall blocked direct radiation during the early to late morning. However, in the afternoon radiation reflected from the downstream face of the arch was reflected onto the new concrete. As the effects described were not measured directly, it has been assumed for simplicity that the direct radiation that is blocked during the morning is equivalent to the reflected radiation in the afternoon.

The collected air temperature and radiation absorbed was used as boundary conditions for the analysis performed, as described in Section 5.3.

5.2.2 Fresh concrete temperature

The temperature of the fresh concrete was measured at the batching plant as part of the normal quality assurance procedure employed on site. The concrete temperature at the batching plant is assumed to be not much different to that of the concrete temperature at the final point of delivery. The recorded fresh concrete temperatures were consequently used as the initial concrete temperature at each construction lift during the finite element analysis that was subsequently performed.

It should be noted that the recorded fresh concrete temperature may not be entirely representative of all of the concrete placed in a specific construction lift. The recorded concrete temperature corresponds to a specific batch of concrete, randomly selected for quality control purposes. Some construction lifts required several loads of concrete, batched over a period of 7+ hours. Some temperature variation can be expected between different concrete batches under these circumstances, but this is not represented in the recorded data. The effect thereof, however, is not expected to be significant and has been ignored in the subsequent analysis.

5.2.3 In-situ concrete temperature

The RS Components 3 kΩ NTC thermistors installed at Stompdrift Dam is the standard temperature measurement device used by the Dam Safety Surveillance sub-directorate of the Department of Water and Sanitation. The reliability of the instruments themselves is acceptable. Measured values are within 0.9% of the actual values, according to the supplier's specifications.

According to the initial instrumentation design, all data was to be collected automatically using a Campbell Scientific datalogger system. However, procurement difficulties led to the datalogger system only being procured near the end of the construction period. Instruments were consequently initially measured and logged manually by an instrumentation assistant.

The design of the instrumentation system specified two sets of thermistors to be installed. Thermistors from the first set were to be installed at the centre (plan view) of every block of concrete cast as part of the rehabilitation of the tertiary arch, at the level of each construction joint. Thermistors from set two were to be installed in selected blocks at positions 500 mm from the edges of these blocks. The aim of the instrumentation layout was to monitor the

concrete temperature development during construction for both quality control, monitoring and research purposes. Figure 5-3 shows a schematic layout of a typical thermistor layout.

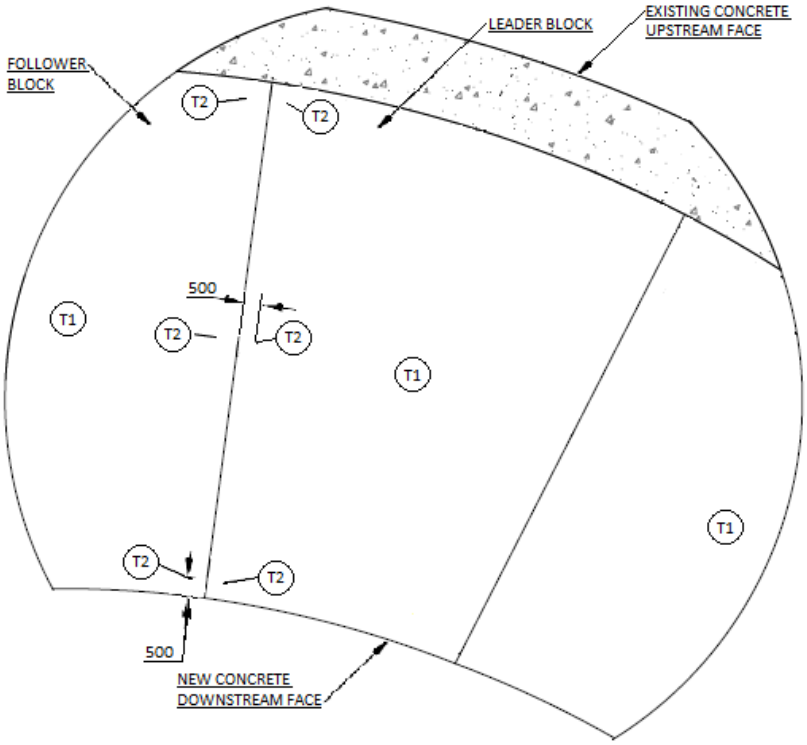

Figure 5-3 A plan view of the thermistor layout. Thermistors from set one are indicated by the label "T1" while thermistors from set two are labelled "T2."

Thermistors from set one were installed near the centres of construction lifts (plan view) because this position is the least influenced by atmospheric conditions. It is also likely that the maximum temperature that would occur during hydration would occur near the centre of the block. The instruments were installed at the bottom of lifts to minimise the effect of instrumentation on the construction process.

Only data collected from thermistor set 1 was used in the current analysis. This is due to the relatively low amount of data available for thermistor set 2. As data had to be collected manually, priority was given to data collection from instruments from set 1.

Unlike the other data collected, the in-situ concrete temperature data was not used as input into the finite element analysis performed. Instead it was used to compare the results obtained from the finite element analysis to the actual concrete temperatures, thereby showing whether or not the calculated concrete temperatures are correct / accurate.

5.2.4 Water level

The water level at Stompdrift Dam is continuously monitored by the Hydrological Services Directorate of the Department of Water & Sanitation. Data is collected at 12 minute intervals, and is available online (Department of Water & Sanitation, 2015).

5.3 Analysis stage: Pre-processing

The construction of one of the leader blocks was replicated in the analysis module. As per the developed model, the analysis stage starts by performing pre-processing features.

The commercially available software package Diana 9.5 was used to perform the finite element analysis, including some of the pre- and post-processing.

5.3.1 Mesh discretization

It was decided that, for simplicity, only a 2-D analysis would be performed. The geometry of a representative cross section, shown in Figure 5-2 above, was used to generate a finite element mesh. The developed mesh is partly shown in Figure 5-4. The mesh shown is applicable to the final construction lift modelled in the analysis – lift 15. Elements are activated and deactivated during the analysis to model the construction process. During the analysis of lift 14, for instance, the 2-D elements associated with lift 15 would still be de-activated, while a different combination of boundary elements would be active than is shown in Figure 5-4.

5.3.2 Thermal conductivity

Foundation: The foundation is composed of quartzite (Van Schalkwyk, 2013). According to Figure 2-2 the thermal conductivity of naturally occurring quartzite varies significantly - values between 3.0 and 6.8 W/m.K have been reported, with an average value of 5.3 W/m.K provided. The relatively wide band within which the thermal conductivity of quartzite varies makes it highly possible to over- or underestimate the thermal conductivity of the foundation. A conservative value of 3.5 W/m.K was adopted for the analysis. This value is conservative, as the higher the foundation's thermal conductivity is, the more it will tend to conduct heat away from the concrete, thereby reducing its temperature.

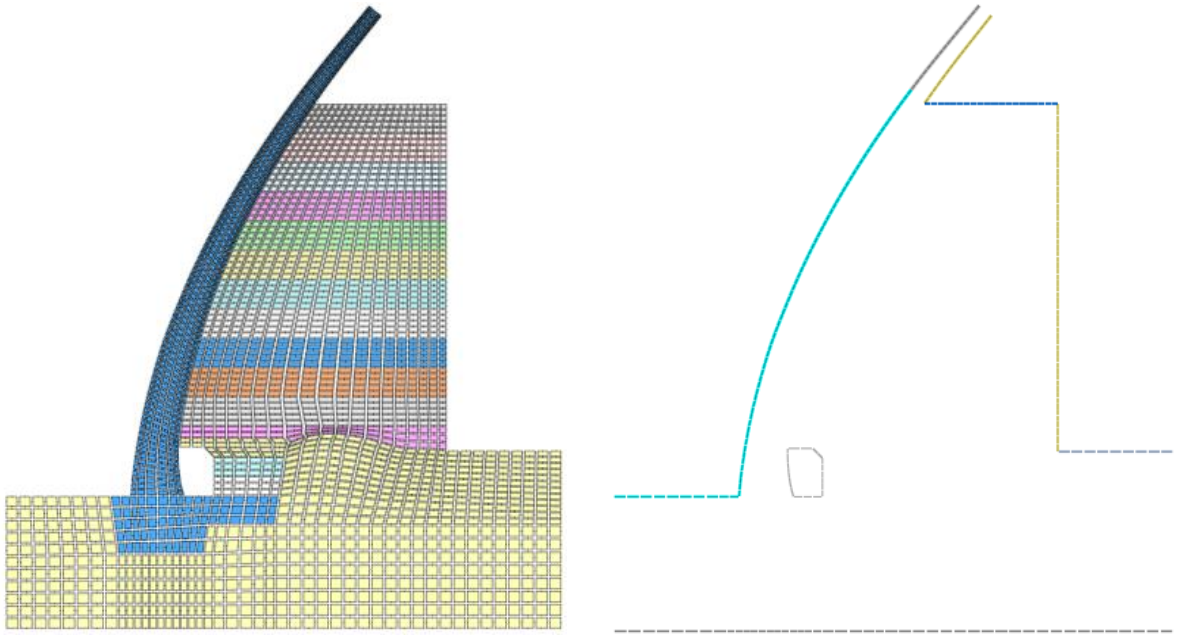

Figure 5-4 **A schematic layout of the finite element model during the final time-step of the analysis showing (a) 2-D quadrilateral elements used to model concrete and the foundation; and (b) 1-D boundary elements used to incorporate boundary conditions.**

Pre-existent concrete: The proportions and properties of the concrete mix used during the original construction of the dam are not known. Core drilling during construction revealed that the coarse aggregate used was in all probability mostly smooth and rounded sandstone or quartzitic sandstone rock - possibly obtained from the riverbed in what would later become the dam basin. Table 2-2 provides a rough guideline for the thermal conductivities of concrete made with a common range of aggregates. The value given for concrete made using quartzite is 3.5 W/m.K. No value is given for concrete made using sandstone or quartzitic sandstone aggregates. To find a representative value to use, the thermal conductivity of an arch dam constructed during the same era, using the same type of aggregate was used. The hungry Horse dam, completed in the USA in 1948, is such a dam (ACI Committe 207, 1997). The thermal conductivity of the concrete used for the construction of the Hungry Horse Dam was used to represent that of the pre-existent concrete at the Stompdrift Dam – 2.8 W/m.K.

New concrete: The new concrete that was placed had the mix proportions as shown in Table 5-1 (quantities shown are for 1 m^3 of concrete). As the mix proportions are known, the thermal conductivity of the concrete was determined from the weighted average of the thermal conductivities of its ingredients. The thermal conductivities of the components were obtained from Section 2.4. An average value of 2.95 was adopted for Greywacke. The finally calculated thermal conductivity of the concrete was 2.66 W/m.K.

Table 5-1 Mix proportions of the concrete mix used during the rehabilitation of the Stompdrift Dam

#	Ingredient	Mass (kg)
1	CEM I 52.5	132
2	Fly ash	132
3	Crusher sand - Greywacke	490
4	River sand – Sandstone / Quartzite	490
5	19mm aggregate - Greywacke	940
6	Superplasticiser - Chryso Fluid 423	1.9
7	Water	200

5.3.3 Specific heat capacity

Again, as for thermal conductivity, the specific heat capacity of the foundation, pre-existent concrete and new concrete needed to be determined. But unlike thermal conductivity, specific heat capacity is more temperature dependent.

Foundation: The specific heat capacity of the quartzite foundation was taken from Table 2-3, and is plotted in Figure 5-5.

Pre-existent concrete: No information is known regarding the original concrete used, apart from that it was placed in the 1960's and that sandstone or quartzitic sandstone was used as aggregate. Again, the properties of the concrete used during the construction of the Hungry Horse Dam was used in the analysis (ACI Committe 207, 1997). The values implemented in the analysis are plotted in Figure 5-5.

New concrete: The specific heat capacity of the concrete placed during the rehabilitation was calculated as suggested in Section 4.3.1. The calculated value is also shown in Figure 5-5.

Where the temperature that occurs in any one of the abovementioned components fell outside the range of specified values, the closest value was used instead of extrapolating outside the range of specified values.

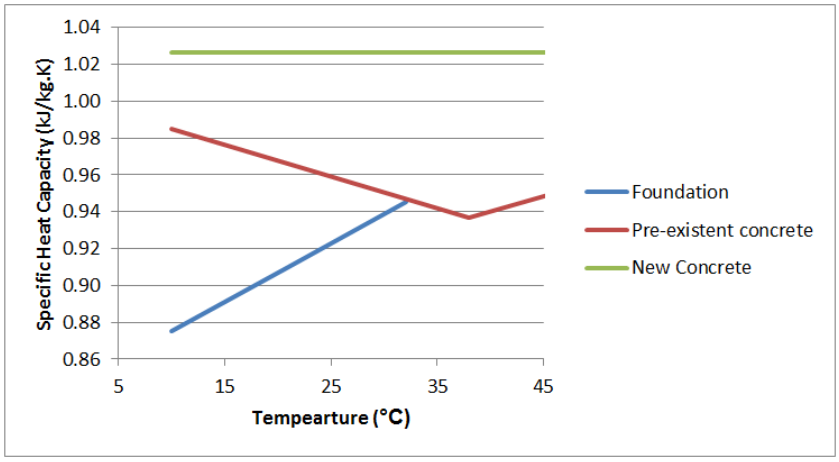

Figure 5-5 Specific heat capacities of the components included in the analysis over a range of temperatures.

5.3.4 Mass density

The mass densities of the components included in the analysis are summarised in Table 5-2. The software package used requires an input parameter called “capacity,” which is equal to the product of specific heat capacity and density. The calculated capacity values for components included in the analysis are included in Table 5-2.

Table 5-2 Mass densities and capacities of the components included in the analysis.

Component	Density (kg/m^3)	Capacity (kJ/m^3.K)				
		10 °C	21 °C	32 °C	38 °C	66 °C
Foundation	2650	2332	2412	2518		
Pre-existent concrete	2400	2376			2256	2352
New concrete	2387	2458				

5.3.5 Hydration heat development

Physical testing to determine the hydration characteristics of the concrete used during the rehabilitation was not performed. Consequently secondary data from Ballim & Graham (2009) was used. The hydration data published by Ballim & Graham is in the form of maturity heat rate over maturity time. The software package used for the finite element analysis, however, requires hydration data input in the form of adiabatic temperature rise over time. The data was converted into the required format using Equations 2.5.2 - 2.5.3. The resulting adiabatic temperature rise curve is shown in Figure 5-6.

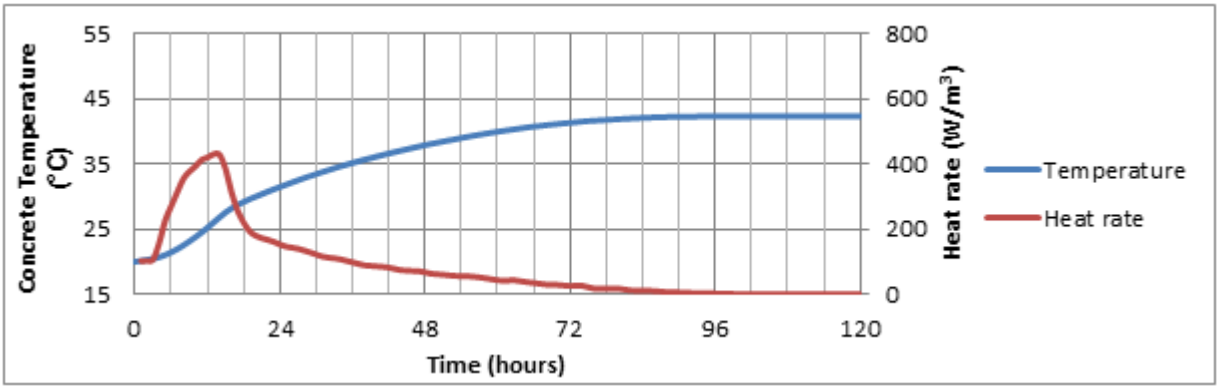

Figure 5-6 The calculated adiabatic temperature rise over time curve for the concrete used during the rehabilitation.

5.3.6 Solar radiation & convection

Solar radiation was taken into account as described in Section 4.3.1. The radiation data collected during construction was used as input in Equation 4.2.2 to calculate the lump sum temperature over time. The effective ambient temperature, calculated using Equation 2.6.5, was used as the external boundary temperature.

Different convection coefficients were used at various locations in the model, as deemed appropriate over the boundary area shown in Figure 5-4 (b).

Concrete – water: The developed temperature control model does not make provision for modelling convection between water and concrete, as most dams would not be in contact with the water of the reservoir during construction. As the current analysis relates to the rehabilitation of an existing dam which was not drained during construction, convection between the reservoir and the existing dam needs to be accounted for. Several engineering manuals describe methods to calculate the convection coefficient for laminar natural convection (Lienhard IV & Lienhard V, 2000; Mills, 1992). The method described by Lienhard IV & Lienhard V was used to calculate a convection coefficient of 40 W/m^2.K. A constant water temperature of 17.5 °C was used in the analysis. The water level was also kept constant during the analysis at the mean water level observed during construction.

Concrete – plastic sheets & gallery: After a new construction lift was placed during physical construction, plastic sheets were placed over the concrete to prevent drying shrinkage. It was assumed for the analysis that the plastic sheets prevented all air-flow, thereby reducing convective heat transfer. It was also assumed that there was no airflow in the gallery. Using Equation 2.6.3, the calculated film coefficient for zero wind velocity is 5.7 W/m^2.K.

The effective ambient temperature, that is the measured ambient temperature plus an increase / decrease in ambient temperature attributable to solar radiation, was used as the external temperature boundary. Both the effective and average ambient temperature is illustrated in Figure 5-7.

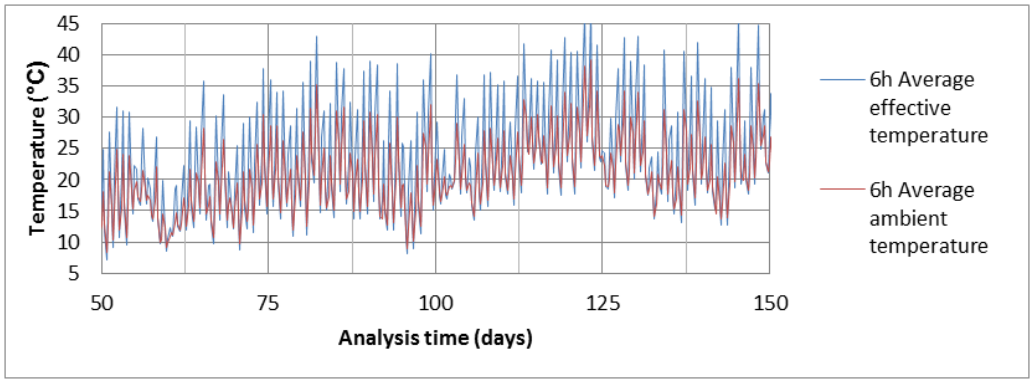

Figure 5-7 A representation of the 6-hour average ambient and 6-hour average effective temperatures.

Concrete – other: The film coefficient between air and concrete, whether covered with hessian or steel shutters or exposed directly to the atmosphere, was assumed to be the same. Assuming a mean wind speed over exposed surfaces of 4 km/h for the entire construction period, the calculated film coefficient is 10 W/m^2.K.

Foundation: The lower boundary of the model was modelled as a convection boundary. A convection coefficient equal to the thermal conductivity of the foundation was used. Specifying a convection boundary instead of a fixed temperature allows temperatures to rise or fall above the boundary temperature, which is considered to be more realistic than specifying a fixed temperature at an arbitrary depth below the surface.

5.3.7 Initial temperature

The finite element mesh shown in Figure 5-4 (a) represents three different materials – the foundation, pre-existent concrete and new concrete. The initial temperature of all three components needs to be specified.

For the foundation and pre-existent concrete an initial temperature of 17.5 °C was specified. A pre-analysis, 7 days in duration, was then performed using the same boundary conditions and material properties described below. The resulting temperature distribution in the foundation and pre-existent concrete is shown graphically in Figure 5-8

The initial temperature of the fresh concrete was specified based on the data collected during the construction of the dam. The temperatures used, as well as the cast date of each construction lift is summarised in Table 5-3.

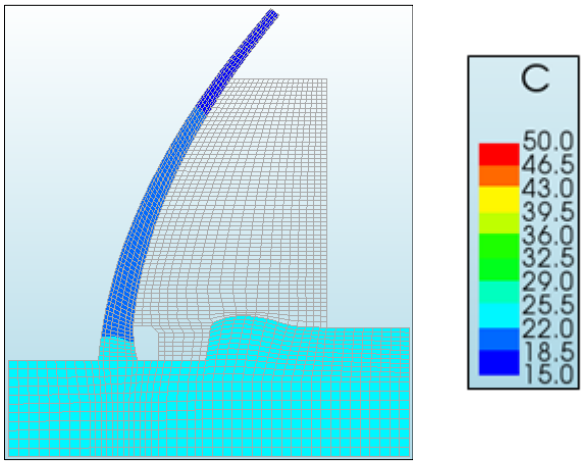

Figure 5-8 **A graphical representation of the initial temperature distribution used as input in the main analysis.**

Table 5-3 **A summary of the initial temperature and cast dates of the construction lifts included in the analysis.**

Lift #	Initial Temperature (°C)	Date Cast	Lift #	Initial Temperature (°C)	Date Cast
1	13.5	2012/08/20	9	24.6	2013/02/04
2	15.8	2012/09/15	10	26.1	2013/02/19
3	20.6	2012/10/03	11	24.8	2013/03/06
4	19.5	2012/10/16	12	24.3	2013/03/26
5	21.5	2012/11/07	13	16.2	2013/04/11
6	21.5	2012/11/22	14	20.9	2013/04/25
7	21.3	2012/12/05	15	20.3	2013/05/14
8	25.9	2013/01/16			

5.4 Analysis stage: Solution phase

During the solution phase, three aspects are dealt with:

- Determine adequate time-step durations;
- Set analysis phases;
- Perform a nonlinear finite element analysis.

After considering the adiabatic temperature rise curve shown in Figure 5-6, it was decided to use 6-hour time-steps for the initial stages of hydration. 6-hour time-steps were used for the first eight days after a new construction lift had been placed. If, after eight days, a new construction lift had not been placed, the time-step length would be increased to 24 hours.

The analysis performed aimed to replicate the construction of the first 15 construction lifts as close as possible. The analysis performed modelled the placement of these 15 lifts over a period of 273 day using 30 phases. Two phases were used per construction lift in order to differentiate between the convection coefficients assigned to plastic sheets and hessian cloth.

The analysis itself was performed using the software package Diana 9.5.

5.5 Analysis stage: Post-processing

5.5.1 Initial results

The calculated temperature profiles using the material properties and boundary conditions described in the previous section are shown in Figure 5-11. The temperature profiles shown represent the temperature distribution in the new concrete three days after every second construction lift was cast. The final temperature distribution over the whole model is also shown. From Figure 5-11 it can be seen that the maximum calculated concrete temperature throughout the construction period is between 39.5 and 43.0 °C.

After extracting the nodal temperatures at positions that correspond to locations where thermistor were installed, the calculated and measured temperature versus time profiles at these positions could be graphically compared. This is done in Figure 5-12. The temperature profiles at positions at the bottom of construction lifts 7 and 9 are also shown to provide a comprehensive representation of the results calculated by the model, even though thermistors were not installed at these positions.

It can be seen that both the calculated peak and longer term temperatures were significantly underestimated in the initial analysis.

5.5.2 Calibration – hydration data

To obtain a more realistic solution than the one presented in Figure 5-12, the previously calculated adiabatic temperature rise curve was scaled up by a best fit calibration factor of 1.6. More specifically, the maturity heat rate over maturity time was multiplied by 1.6 while keeping the maturity time constant. Figure 5-9 shows the newly calculated adiabatic temperature rise curve.

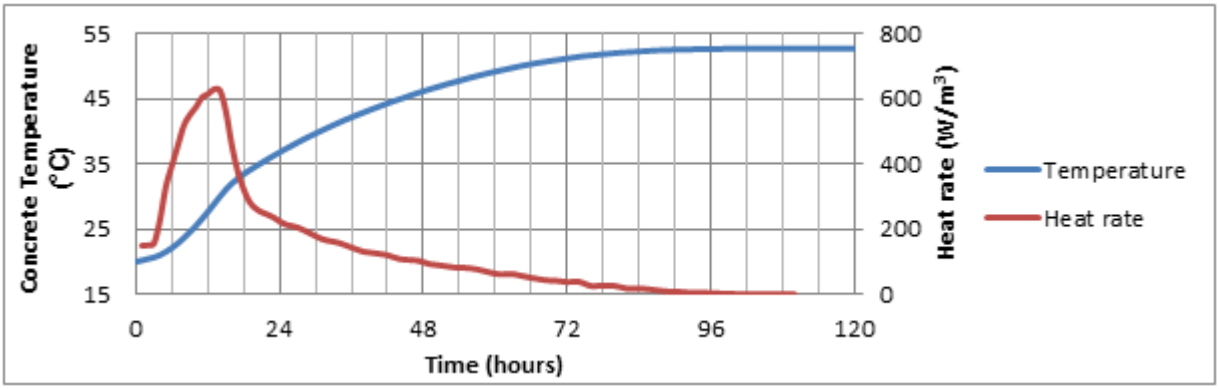

Figure 5-9 The calibrated adiabatic temperature rise curve used subsequent to the initial analysis.

The resulting temperature distribution over time is shown in Figure 5-13. Again, the temperature distribution is shown three days after every second construction lift is cast. The newly calculated temperature versus time at selected measuring points is shown in Figure 5-14.

5.5.3 Calibration – initial temperature in the foundation and lifts 3 & 4

The calculated temperatures for lifts 3 and 4 shown in Figure 5-14 are significantly lower than those measured. The low temperatures calculated at these lifts affects the temperature distribution in subsequently cast lifts, resulting in a reduction of the accuracy of the calculated values in the upper lifts.

A correction was made to the initially assumed foundation temperatures as well as to the temperatures previously calculated for lifts 1 - 4. The temperatures at these lifts were set equal to 30 °C (lifts 1 & 2), 31 °C (lift 4) and 32 °C (lift 3) respectively, in order to correspond to the measured temperatures. The foundation temperature was set equal to 30 °C in the upper part and 28 °C in the lower part. A new pre-analysis was subsequently performed to even out the discrete temperature levels specified in these construction lifts and the foundation. The temperature distribution at the start of the analysis is shown in Figure 5-10.

The start date of the analysis was moved to the instant when lift 5 was placed. Hydration heat development was not modelled in construction lifts 1 to 4, as further hydration in these lifts would be insignificant at this time. This assumption was confirmed by checking that the degree of reaction had reached 99% in all of these lifts prior the placement of lift 5. The degree of reaction is one of the variables calculated by Diana as part of hydration heat calculations.

The result of the adjusting the input temperature used is higher accuracy of the calculated temperatures in the upper lifts. The final temperature distribution is shown in Figure 5-15 and Figure 5-16.

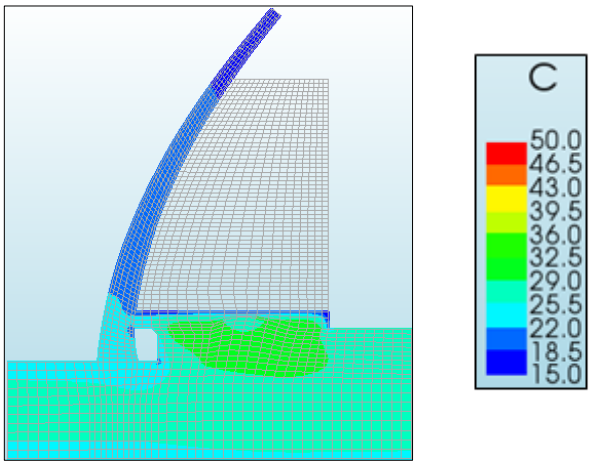

Figure 5-10 The adjusted temperature field used as input in the final analysis.

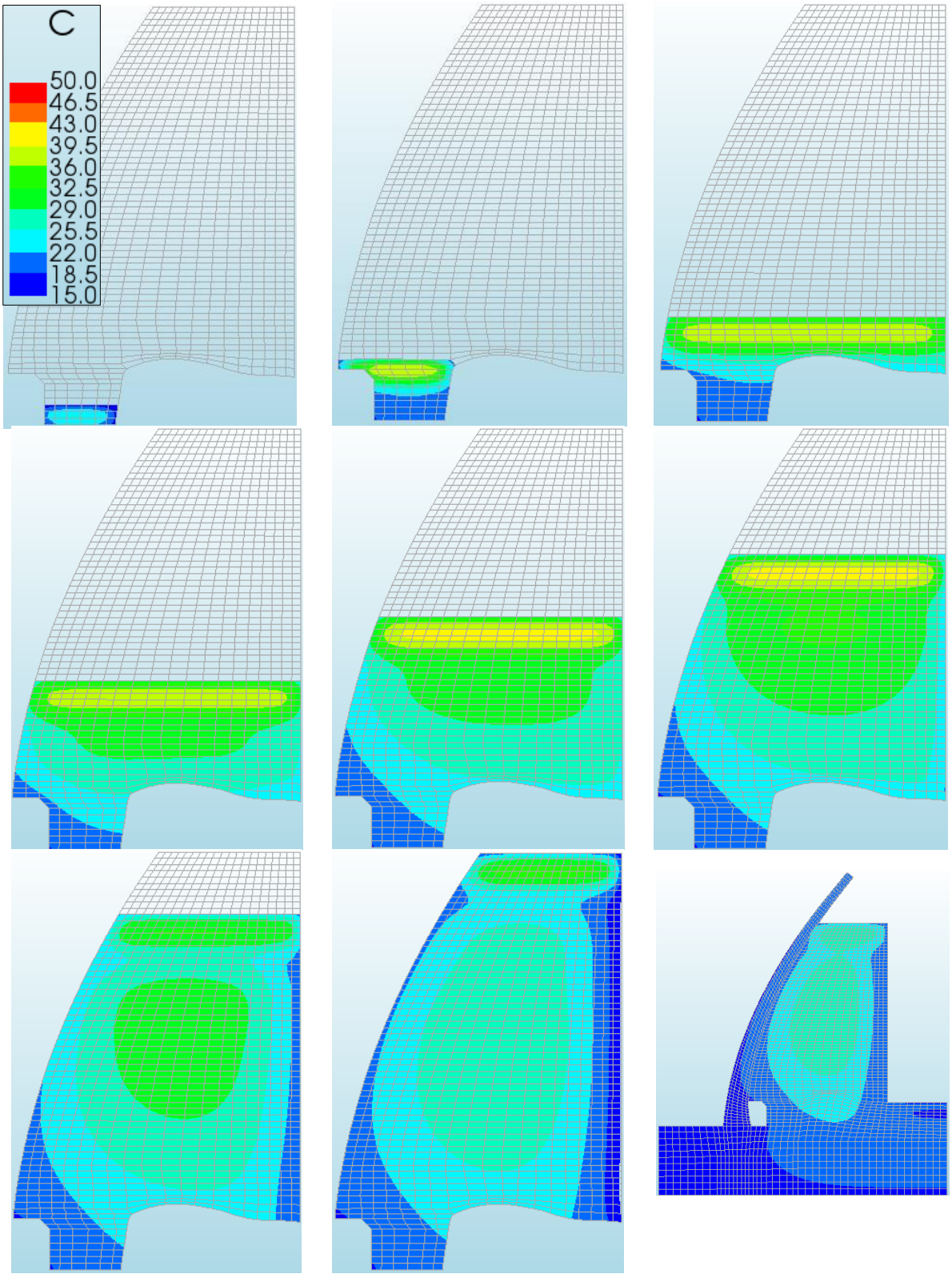

Figure 5-11 **A graphical representation of the temperature profile in the new concrete, as calculated in the initial analysis.**

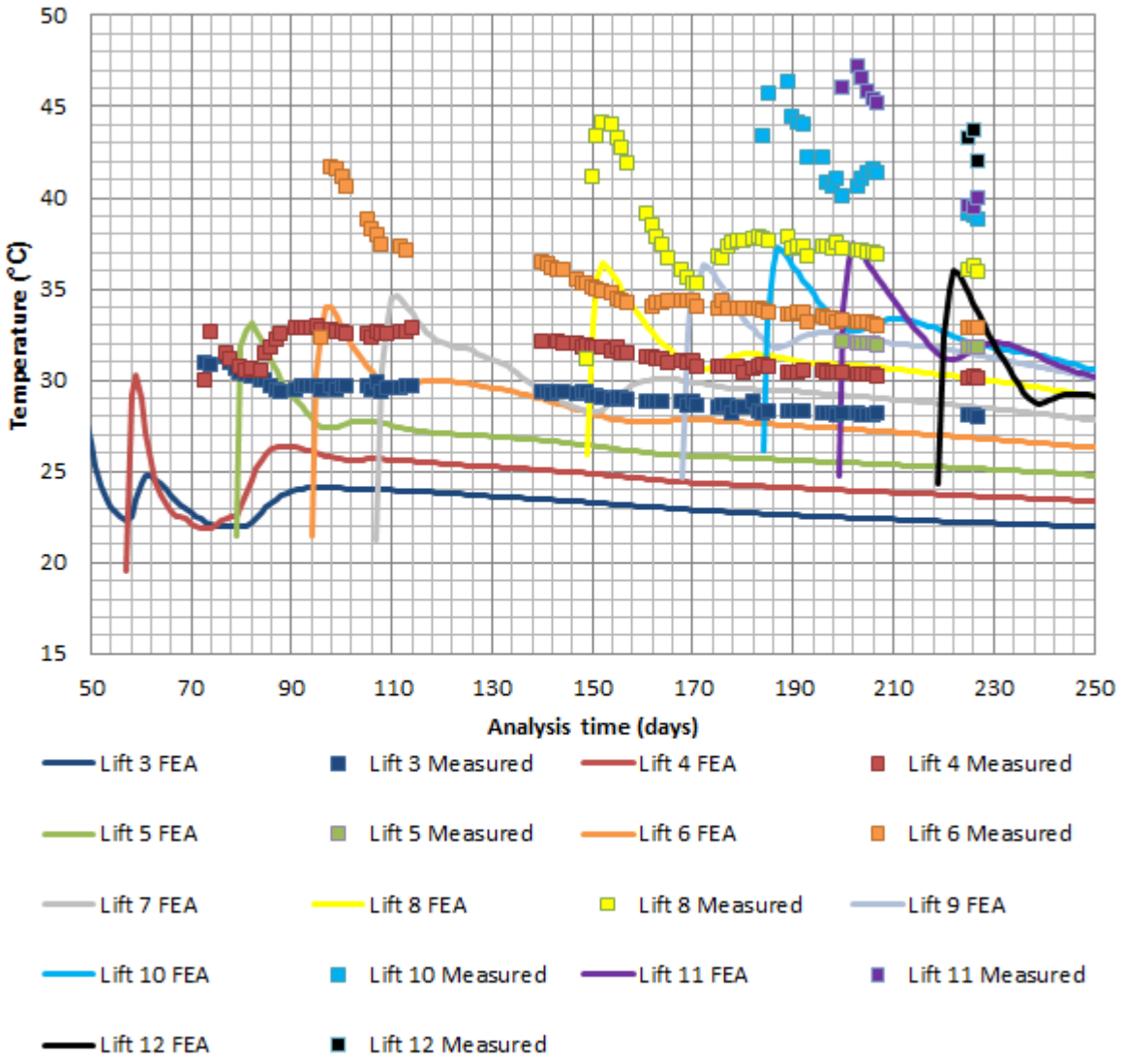

Figure 5-12 A comparison between the results calculated by the model and the data collected during construction.

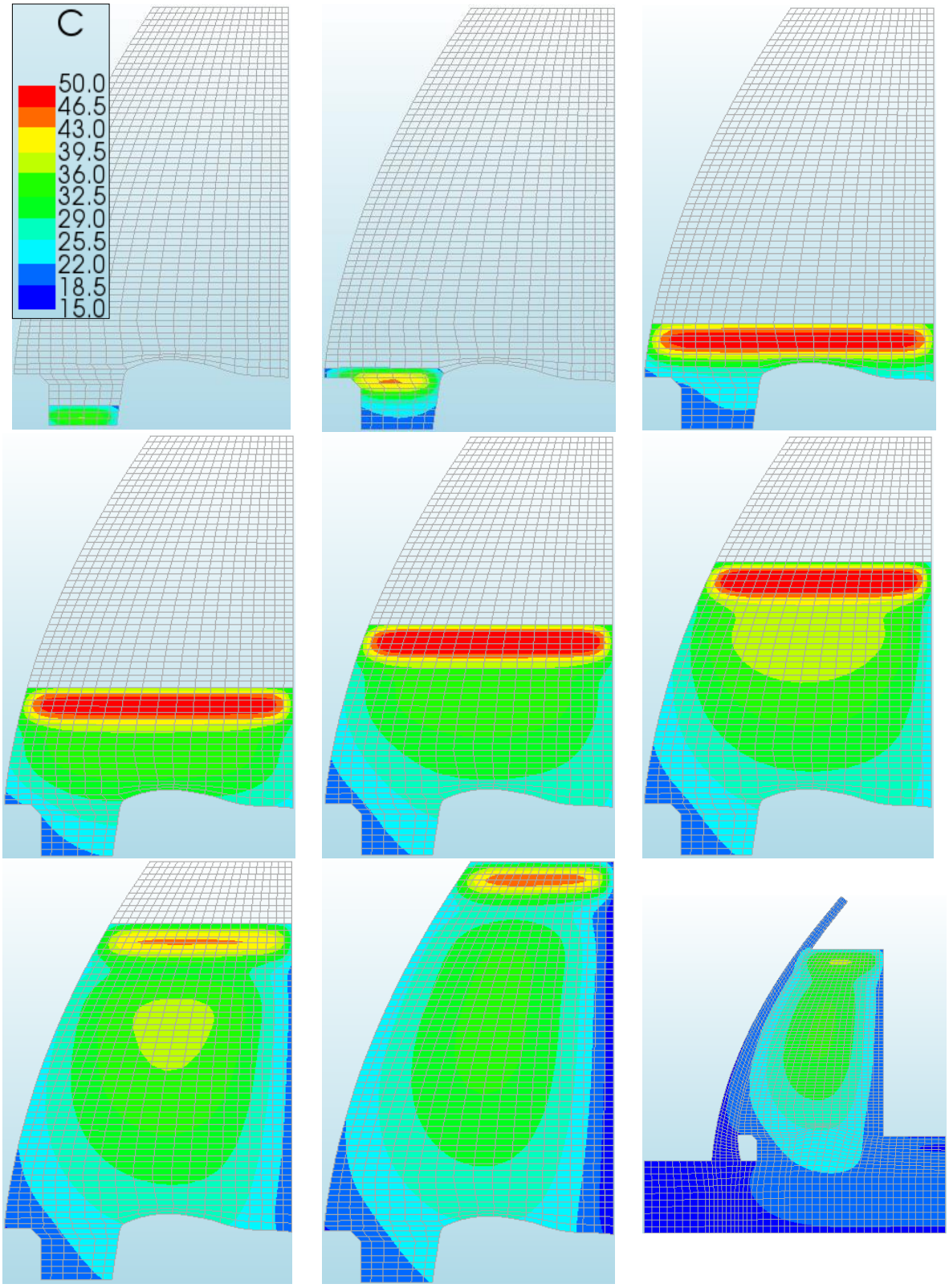

Figure 5-13 **A graphical representation of the calculated temperature profile in the new concrete, after the hydration characteristics were calibrated.**

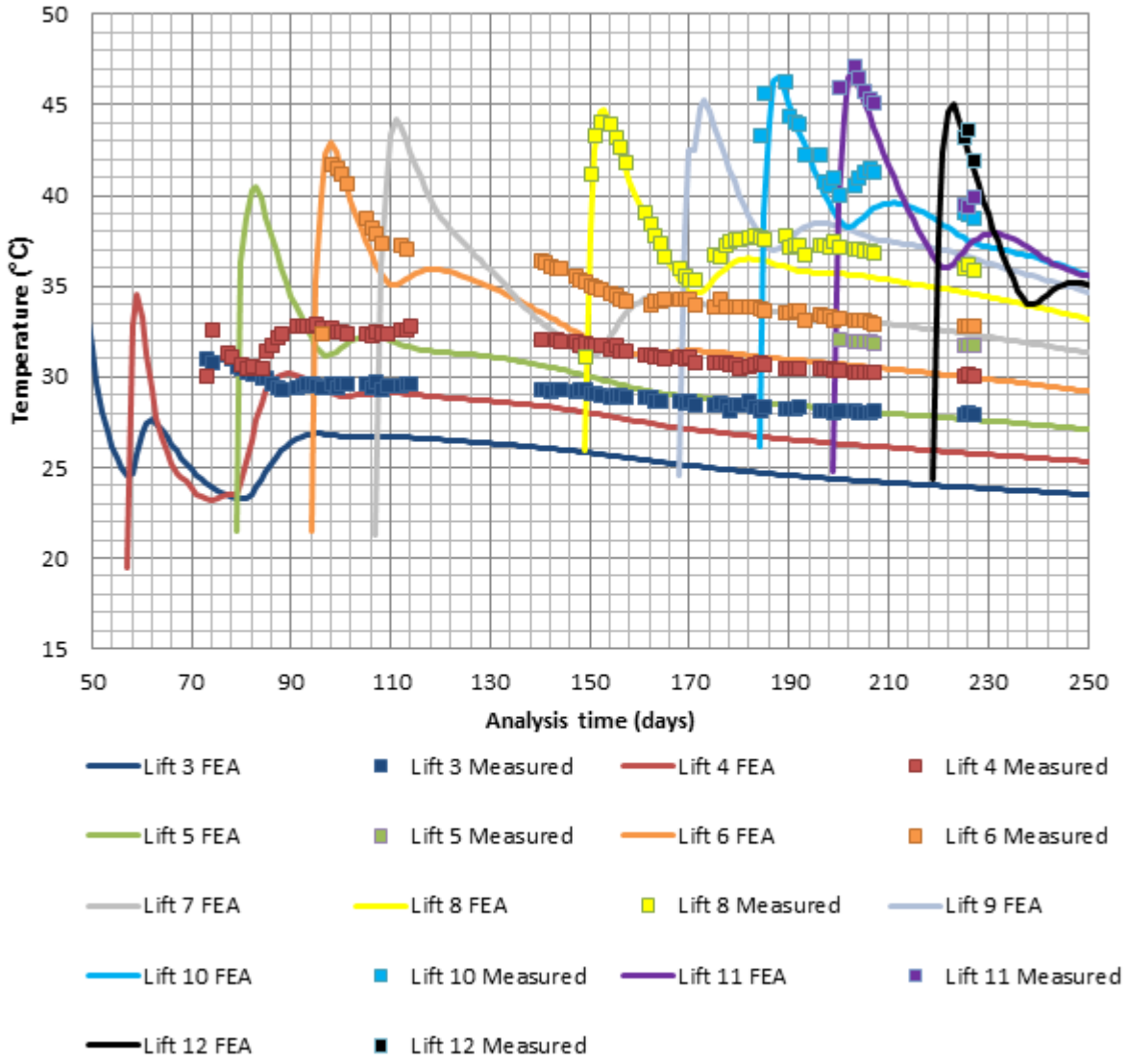

Figure 5-14 A comparison between the calculated and measured temperatures using the calibrated hydration characteristics.

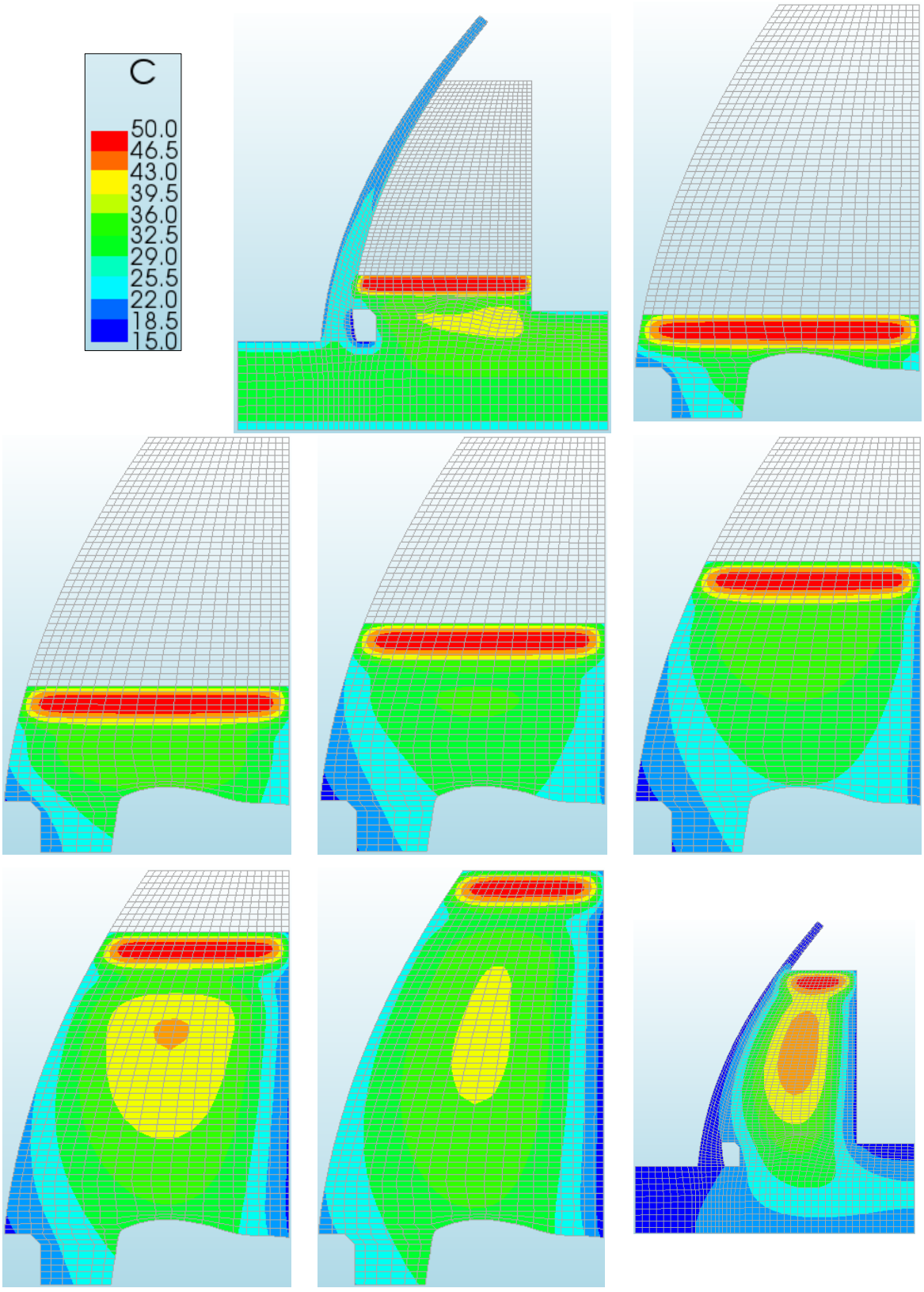

Figure 5-15 A graphical representation of the temperature profile in the new concrete using calibrated hydration data and corrected foundation temperatures.

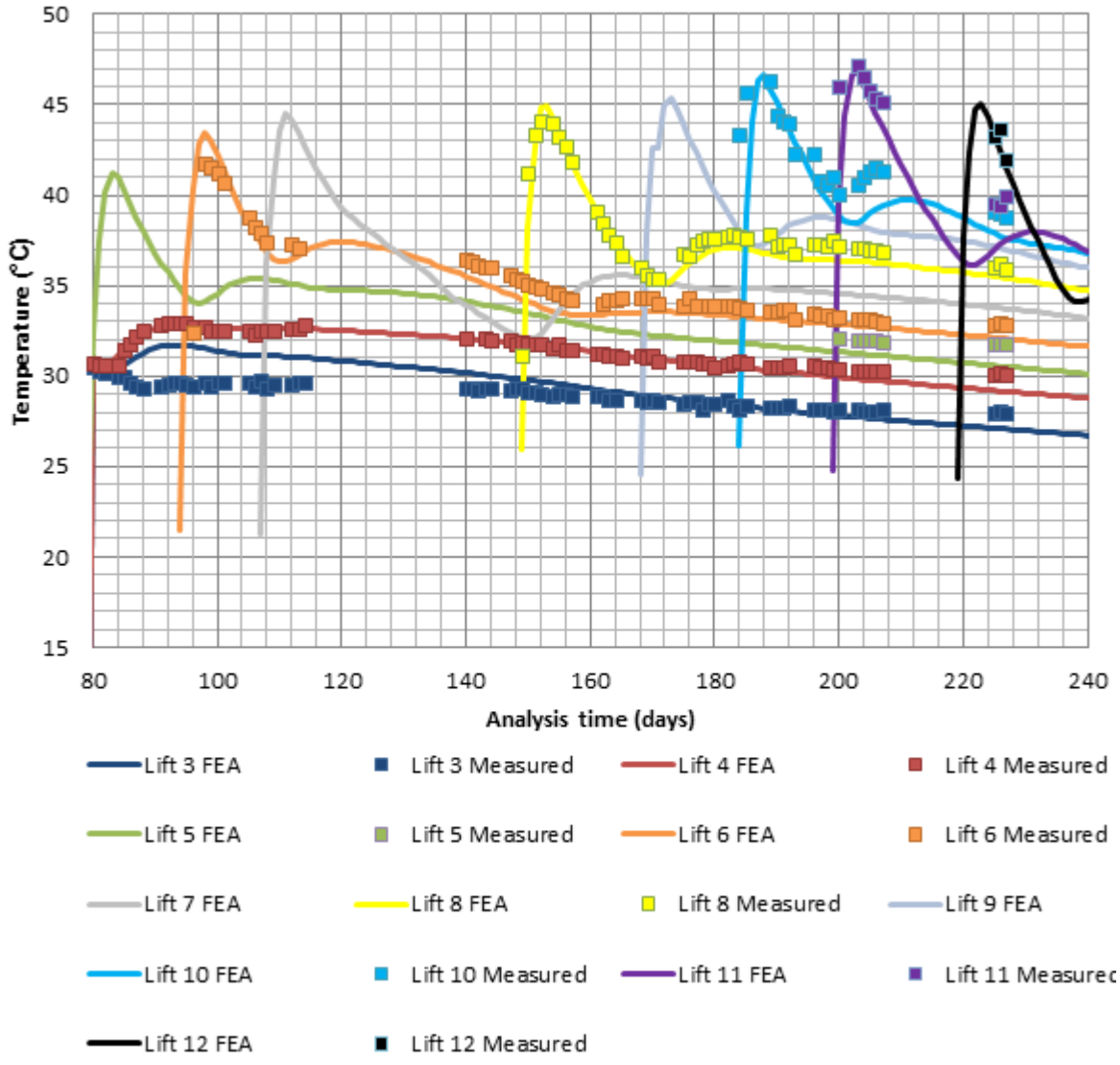

Figure 5-16 A final comparison between measured and calculated concrete temperatures. Both the calibrated hydration rate input and the correction made to the initial foundation temperature are reflected in the calculations.

5.6 Discussion of results

5.6.1 Initial analysis

The temperature distributions shown in Figure 5-11 are generally equivalent to what can be expected in terms of the distribution of temperature throughout the cross section. The temperature within a construction lift generally peaks approximately three days after a construction lift is placed causing a localised “hot spot.” The heat generated in a construction lift is then conducted to the layers below, existing concrete and the foundation, or across

convective boundaries. Ultimately the temperature at the centre of the concrete mass has a higher temperature than the concrete closer to the edges.

It is clear from the data presented in Figure 5-12 that the results calculated by the initial analysis was generally much lower than the concrete temperatures measured. This is primarily considered to be an indication that the hydration characteristics of the binder used in the analysis was significantly different to that of the binder used during construction. Other contributing factors could be that convective heat transfer was overestimated, conduction was overestimated or capacity was underestimated.

The data used to approximate the hydration characteristics of the binder used was published by Ballim & Graham in 2009. The research by these two authors was done at a time when CEM I 42.5 was widely used throughout South Africa. During the rehabilitation of Stompdrift Dam, the more finely ground variant, CEM I 52.5, was used. It is not clear from Ballim & Graham (2009) which cement variant was used in their research, but it is considered likely that CEM I 42.5 was used to generate their data.

In Chapter 2 it was shown that, in addition to how finely the cement clinker is ground, the location where either fly ash or cement is sourced from has a significant effect on the total amount of heat liberated as well as the rate of heat liberation. It is possible that both the cement and fly ash used during the rehabilitation are more reactive than that used by Ballim & Graham to generate their data. This could account for the lower than expected calculated temperatures.

It should be noted that the accuracy of the data used to model hydration should not be viewed as a reflection of the model's ability to model hydration.

5.6.2 Calibration: hydration data

As was the case for Figure 5-11, the temperature distributions shown in Figure 5-13 are generally equivalent to what can be expected in terms of the general temperature distribution over the cross section with a change over time. The calculated temperatures are higher than what was shown in Figure 5-11, but this is to be expected when modelling a binder that generates more heat.

From Figure 5-14 it can be concluded that hydration heat is modelled adequately. The difference between the peak temperatures reached during construction and that calculated in the analysis are within 1.5 °C. Expressed as a percentage of the total adiabatic temperature rise, the error in the calculation peak value is 4.1%.

It is possible that the error percentage of 4.1% is artificially low. As mentioned in section 4.6.1, overestimation of convection or conduction, or underestimation of capacity could also have contributed to the lower than expected temperature values shown in Figure 5-11. The calibrated hydration characteristics might therefore be exaggerated.

The concrete temperatures calculated subsequent to the initial peak are generally lower than those measured. This observation is more pronounced at the lower lifts. One explanation for this could be that the modelled foundation temperature is much lower than the actual foundation temperature. When the first lift is placed, more heat is transferred into the foundation because of an artificially high temperature gradient. This effect forms a chain reaction, affecting each new construction lift in turn. One would expect the effect to become less prevalent with increasing height, due to the low thermal conductivity of the concrete.

The above theory is supported by the data shown in Figure 5-14. Initially, a temperature difference of 8.5 °C can be observed between the measured and calculated temperature at 4. Once lift 5 is placed, the calculated temperature in lift 4 rises more relative to the measured temperature in lift 4. This indicates that more energy is transferred into lift 4 in the analysis than in real life, leading to lower long term values calculated in lift 5.

A calibration factor of 1.6 was applied to the maturity heat rate for this analysis. The factor was obtained by a trial and error process where the aim was to minimise the difference between the calculated and measured peak temperature values. The potential user of the model for other cases would not have this luxury. Adiabatic testing of the binder characteristics should form part of the design process. It is advised against the use of literature based values in this case.

5.6.3 Calibration: foundation temperature

High foundation temperatures (higher than 36 °C) can be observed in Figure 5-15. This is considered to be an overestimation of the actual conditions, but there is no way to definitively verify what the actual foundation temperature was during construction. Apart from the foundation temperature, the distribution of the temperature over the cross section appears to be realistic. Higher long term temperatures are observed near the centre of the new concrete than was the case for Figure 5-13. This is consistent with less heat being conducted to the foundation.

A comparison between the measured and calculated values shown in Figure 5-16 reveals that measured and calculated values are now reasonably similar. The calculated peak

temperatures are still accurate to within 4.1%, while the longer term temperatures are within 2 °C of the measured values.

Modelling only a 2-D cross section appears not to have had a significant effect on the results shown in Figure 5-16. If 3-D effects were significant, one would expect to see measured temperatures reducing faster than values calculated using a 2-D method, as a 3-D model would have more convection surfaces. As this is not the case, the approximation made by only modelling a 2-D case appears to be sufficient for this application.

Chapter 6: Parameter study

6.1 Introduction

In this chapter the temperature control model was used to optimise the construction design of the rehabilitation works to Stompdrift Dam - after the fact. The data that was available prior to the construction of the rehabilitation works is implemented in the model. The model is then used to optimise the construction design. The result is a solution that ensures that concrete temperatures are kept within specified limits during construction.

In section 6.6 it is demonstrated that the construction design determined by the temperature control model would have resulted in a temperature field that is within the specified limits during the actual construction conditions. This is done by a further analysis incorporating both the optimised construction design and climate data collected during the construction period.

6.2 Input stage

Most of the input into the model is the same as was described in section 5.3. This includes the geometry, concrete mix proportions, binder types and hydration characteristics (calibrated) and the construction method used. To avoid duplication only input parameters different to those described in section 5.3 are described below.

6.2.1 Construction programme

The initial design of the rehabilitation works to Stompdrift Dam specified that the construction lift immediately above the gallery, lift 3, was to be placed during the month of August. It was also initially planned that one construction lift would be placed every seven days. The programme for construction lift placement is included in Table 6-3.

6.2.2 Site climate conditions

Monthly minimum and maximum temperatures applicable to region were obtained from World Weather Online (2015). These values are shown in Figure 6-1. Solar radiation maps that show the average daily irradiation during each month of the year were published by the Schulze (1997). The values shown in Table 6-1 were obtained from these maps.

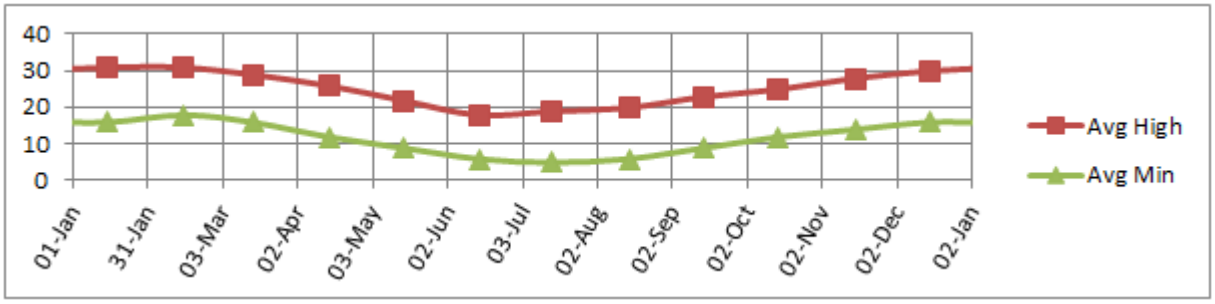

Figure 6-1 **Minimum and maximum average monthly temperatures over a one year cycle (World Weather Online, 2015).**

Table 6-1 **Average daily irradiation on a horizontal plane at Stompdrift Dam (Schulze, 1997).**

Month	Solar Radiation ($MJ.m^{-2}.day^{-1}$)	Month	Solar Radiation ($MJ.m^{-2}.day^{-1}$)	Month	Solar Radiation ($MJ.m^{-2}.day^{-1}$)
January	34	May	16	September	23
February	32	June	13	October	29
March	26	July	13	November	33
April	20	August	17	December	35

6.2.3 Initial conditions

According to Ballim & Graham (2009) the temperature of fresh concrete can be calculated as the mass weighted average of the temperature of its ingredients. To simplify the problem of determining the temperature of the ingredients it has been assumed that all of the concrete ingredient would be at the same temperature, and that this temperature can be calculated as a mass weighted average of the effective ambient over the three days preceding concrete placement.

6.2.4 Specifications

For the purpose of the simulation performed, a simple specification has been set: The maximum temperature during the hydration of the new concrete should not exceed 38 °C.

6.3 Analysis stage: Pre-processing

To avoid duplicating the overlapping parts between the current simulation and that which has already been addressed in Chapter 5, some steps in the pre-processing stage are not shown in this sub-section. These steps are (i) mesh discretization, (ii) thermal conductivity, (iii) specific heat capacity and (iv) mass density.

6.3.1 Hydration heat development

To avoid obtaining results that are too low it was decided to use the calibrated adiabatic temperature development curve shown in Figure 5-9 as input in the finite element model.

6.3.2 Solar radiation & convection

Solar radiation: The solar radiation data in in Table 6-1 was converted into lump sum temperatures (LST) from daily radiation using Equation 2.6.6. Additionally, it was estimated that only 5% of the radiation would be absorbed by the concrete. The calculated monthly values are shown in Figure 6-2.

To validate the approach followed to predict the calculated monthly lump sum temperatures these values were compared to the average monthly lump sum temperatures calculated from the data collected during construction. Comparison between the two datasets shown in Figure 6-3 reveals that there is some correlation between the values, and that the values calculated from the Schulze (1997) data is generally slightly more conservative than that calculated from the data collected during construction.

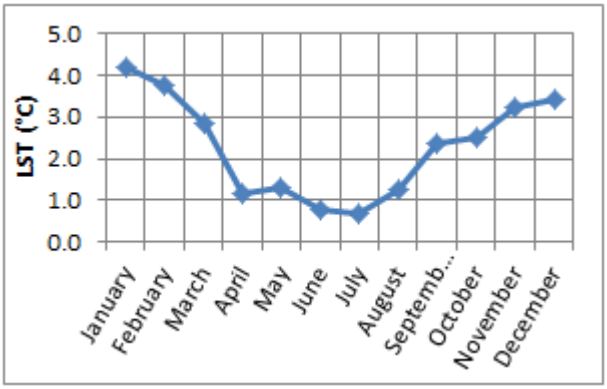

Figure 6-2 **Calculated monthly LST from Schulze (1997) data.**

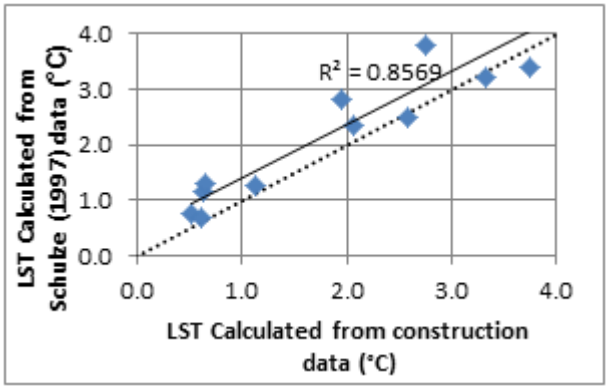

Figure 6-3 **Comparison between daily LST as calculated from Schulze (1997) and construction data.**

Convection: Sinusoidal temperature oscillations were assumed to occur between the daily ambient temperature and lump sum temperature.

The effective ambient temperature was calculated by adding the lump sum temperature. The calculated effective ambient temperature for an arbitrary three day period is shown in Figure 6-4.

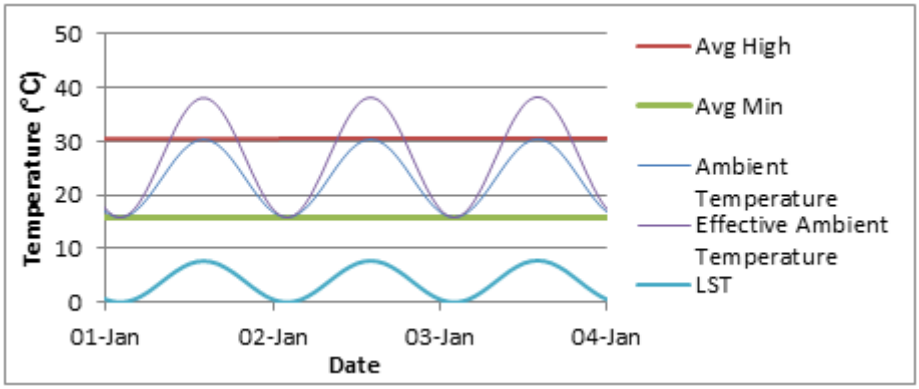

Figure 6-4 The calculated ambient and effective ambient temperatures occurring over a three day period.

The convection coefficients described in section 5.3.6 were used in the analyses presented in this chapter as well.

6.3.3 Initial temperature

The weight factors used in the calculation of the initial concrete temperatures used in the simulation are shown in Table 6-2.

Table 6-2 Weight factors used to calculate the initial temperature of fresh concrete.

Time before placement of construction lift (hours)	Weight factor
-72 to -48	0.20
-48 to -24	0.35
-24 to 0	0.45

The initial concrete temperatures were calculated based on a construction rate of one lift per 7 days, the relationship between effective ambient temperature and initial concrete temperature described in Table 6-2 and the effective ambient temperature calculated in section 6.3.2. Table 6-3 shows the calculated values for the baseline analysis.

Table 6-3 A summary of the calculated initial temperature and cast dates of the construction lifts included in the analysis.

Lift #	Initial Temperature (°C)	Date Cast	Placement rate (days between lifts)	Lift #	Initial Temperature (°C)	Date Cast	Placement rate (days between lifts)
1	12.8	2012/07/18	7	**9**	18.1	2012/09/12	7
2	13.2	2012/07/25	7	**10**	18.8	2012/09/19	7
3	13.5	2012/08/01	7	**11**	19.4	2012/09/26	7
4	13.9	2012/08/08	7	**12**	20.0	2012/10/03	7
5	14.5	2012/08/15	7	**13**	20.6	2012/10/10	7
6	15.4	2012/08/22	7	**14**	21.3	2012/10/17	7
7	16.3	2012/08/29	7	**15**	22.0	2012/10/24	N/A
8	17.2	2012/09/05	7				

The initial temperature of the foundation and pre-existent concrete was assumed to be 17.5 °C. The temperature field used as the initial temperature in the main analysis was obtained by performing a pre-analysis. The pre-analysis, 7 days in length, was performed using the effective temperature calculated in section 6.3.2 as the ambient temperature boundary.

6.4 Analysis stage: Solution & post-processing baseline

To be consistent with the analysis performed in Chapter 5 it was decided to use the same time-step regime. In the Chapter 5 analysis 6-hour time-steps were used for the initial period after a construction lift had been cast. The time-step length throughout the analysis was kept constant at 6 hours.

The construction of the first 15 lifts was modelled over a period of 108 days. 30 phases were used in order to account for the difference between the convection coefficients assigned to plastic sheets and hessian cloth. The non-linear finite element analysis was performed in Diana 9.5. A summary of the results obtained is shown in Figure 6-5.

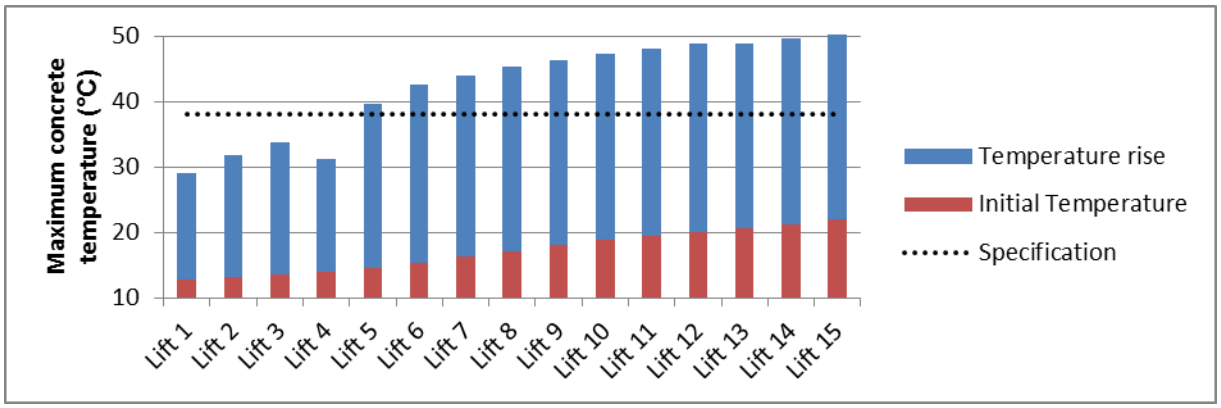

Figure 6-5 The maximum temperature that occurs in each lift for the baseline case.

6.5 Evaluation & optimisation stage

The results displayed in Figure 6-5 show that temperatures outside of the specified limit occur from the placement of lift 5 and onwards. Intervention is required to keep the temperature within specified limits. The types of interventions considered are summarised in Table 6-4.

Table 6-4 Summary of the interventions considered to keep temperatures within specified limits.

#	Intervention	Discussion
1a	Reduce cementitious content	The quality control data collected during the construction of Stompdrift Dam showed that the characteristic strength of the concrete was 22.3 MPa at 90 days. As the specified strength was 15 MPa, optimisation of the mix would have resulted in a lower total cementitious content.
1b	Change aggregate type	Quartzite occurs naturally around the construction site. A quarry could have been opened and aggregate and crusher dust be manufactured on site. The thermal conductivity of quartzite is higher than that of greywacke and would allow more heat to dissipate from the concrete during hydration, thereby lowering the ultimate temperature reached.
2a	Construction season	The initial concrete temperature can be effectively controlled by only placing concrete during winter months. The consequence of this is that there would be a seasonal construction break during the warmer months.
2b	Construction rate	By speeding up the construction rate during cooler periods, more lifts can be placed during the cooler part of the year. Slowing down the construction rate allows more heat to dissipate before a subsequent lift is placed, which results in a lower ultimate concrete temperature.
3	Cooling plant	If a cost-benefit analysis shows that it would be more economic to cool concrete ingredients to a predetermined temperature rather than having to include a construction break during the warmer months, this could be a viable option.

6.5.1 Concrete mixture

The water / cement ratio of the concrete used during the rehabilitation of the Stompdrift Dam was 0.76. It is estimated that increasing this ratio to 0.85 would still have resulted in a concrete mixture that reached the specified characteristic strength. If the water content is kept constant, the total binder content can be reduced from 264 to 236 kg/m^3 – an 11% reduction in cementitious materials.

Replacing the greywacke crusher dust and coarse aggregate with quartzite affects the thermal conductivity and specific heat capacity of the concrete. The newly calculated concrete diffusivity characteristics are shown in Table 6-5.

Using the values shown in Table 6-5 and the same scale factor used to determine the calibrated adiabatic temperature rise curve shown in Figure 5-9, a new adiabatic temperature rise curve was determined. This is shown in Figure 6-6.

Table 6-5 Diffusivity characteristics of the optimised concrete mix.

#	Parameter	Value(s)			Unit
1	Density	2387			Kg/m^3
2	Thermal conductivity	3.0			W/m.K
3	Specific heat capacity	10 °C	21 °C	32 °C	kJ/kg.K
		1.14	1.17	1.20	

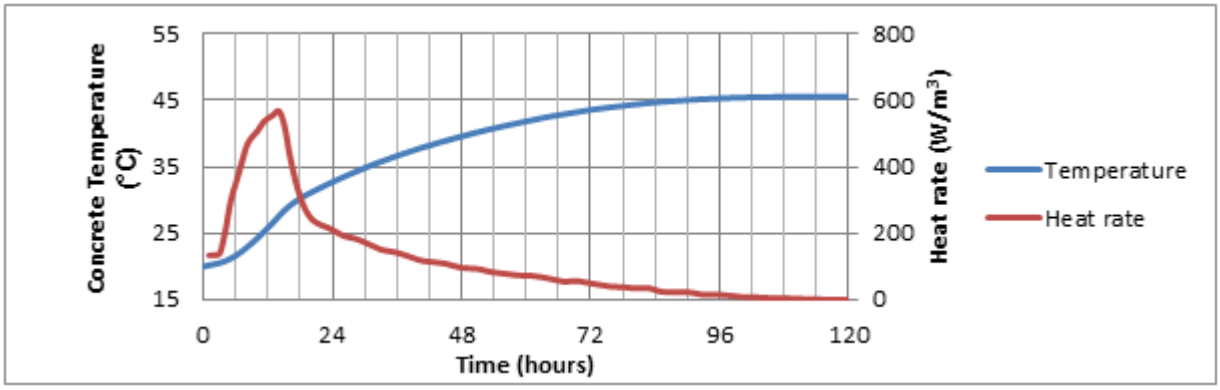

Figure 6-6 The adiabatic temperature rise curve calculated for the optimised concrete mix.

The above input parameters were used in the model. The resulting maximum concrete temperatures are shown in Figure 6-7

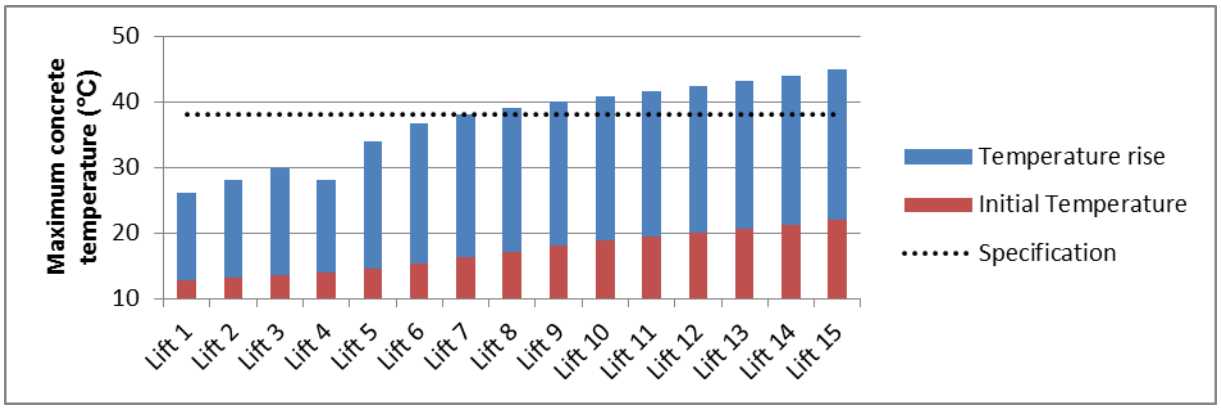

Figure 6-7 The maximum concrete temperature reached at each construction lift when using an optimised concrete mix.

The results presented in Figure 6-7 show marked improvement over those shown in Figure 6-5. By optimising the concrete mix, the first time that the specified maximum temperature is exceeded is at lift 7. But more needs to be done to keep the maximum concrete temperature within specified limits at all construction lifts.

6.5.2 Construction schedule

It can be inferred from the results shown in Figure 6-7 that concrete temperatures exceed the specified limit when the initial concrete temperature becomes too high. To prevent this, a limit can be placed on the initial concrete temperature. This would require that construction is halted in the warmer months, and recommenced in a subsequent cooler season.

Inspection of the maximum concrete temperatures shown in Figure 6-7 reveals that there is some margin of safety regarding the maximum temperature reached at lifts 1 – 5. The construction rate can thus be increased during the placement of these lifts. Speeding up the placement rate would enable additional lifts to be placed during the cooler months. Table 6-6 shows the optimised construction schedule, which was determined by a trial and error method.

Table 6-6 A summary of the initial temperature and cast dates of the construction lifts when using an optimised construction schedule.

Lift #	Initial Temperature (°C)	Date Cast	Placement rate (days between lifts)	Lift #	Initial Temperature (°C)	Date Cast	Placement rate (days between lifts)
1	12.6	2012/07/22	5	**9**	16.3	2012/09/06	268
2	12.9	2012/07/27	5	**10**	15.1	2013/06/01	5
3	13.1	2012/08/01	5	**11**	14.4	2013/06/06	5
4	13.4	2012/08/06	6	**12**	13.8	2013/06/11	5
5	13.7	2012/08/12	6	**13**	13.1	2013/06/16	5
6	14.0	2012/08/18	6	**14**	12.6	2013/06/21	5
7	14.6	2012/08/24	6	**15**	12.6	2013/06/26	N/A
8	15.4	2012/08/30	7				

The result obtained from model when the above initial temperatures and construction program are implemented is shown in Figure 6-8. The calculated results are within specified limits.

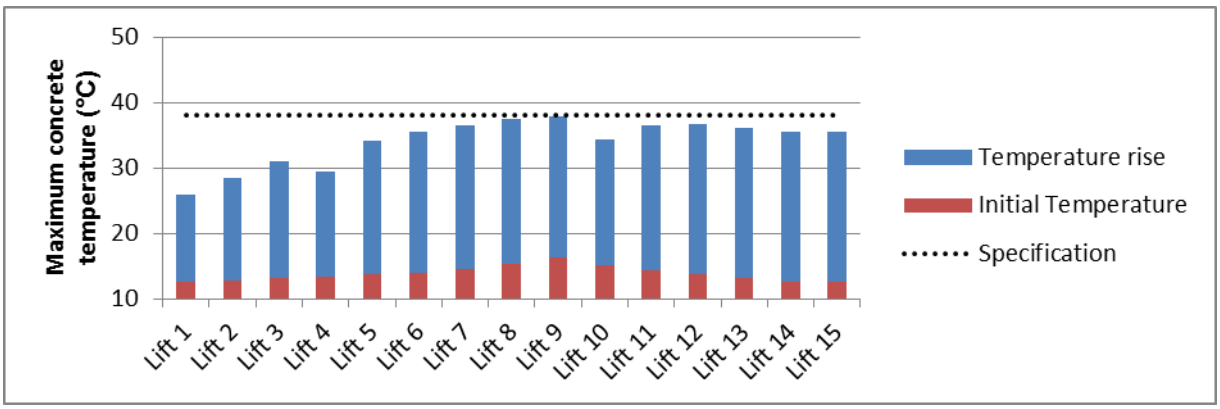

Figure 6-8 The maximum concrete temperature reached at each construction lift when using an optimised construction schedule and concrete mix.

6.5.3 Initial temperature

The solution presented in section 6.5.2 requires a lengthy construction break. Economic analysis might show that it is more feasible to pre-cool fresh concrete using a cooling plant, and implement a continuous placement schedule. Using the placement schedule shown in Table 6-3 and limiting the concrete placement temperature to 13 °C yields the results shown in Figure 6-9.

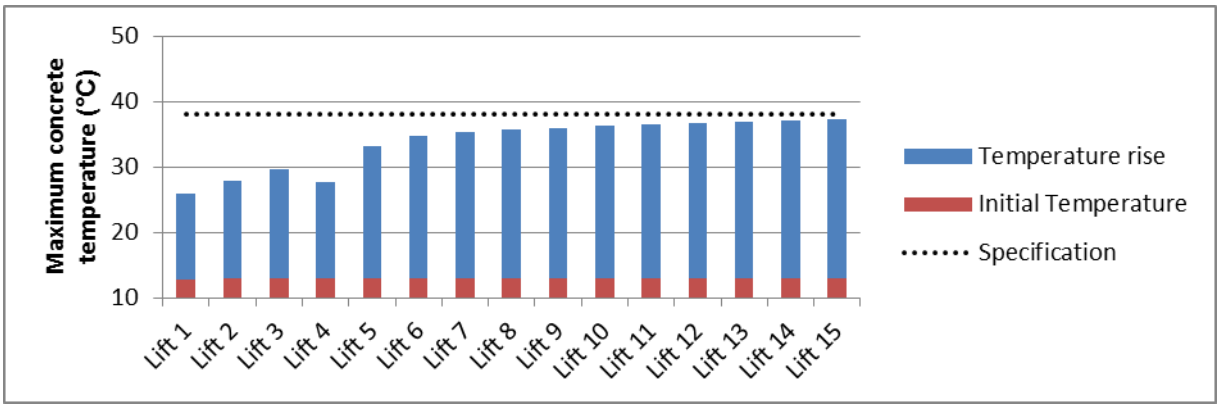

Figure 6-9 The maximum concrete temperature reached at each construction lift when using an optimised concrete mix and a cooling plant to limit the concrete placement temperature to 13 °C.

6.6 Demonstration of model performance using collected climate data

To demonstrate that the results provided by the model can be used to keep concrete temperatures within specified limits during actual construction conditions, the scenario in section 6.5.2 was re-analysed using the climate data collected during the construction of the Stompdrift Dam. Initial concrete temperatures were also re-calculated using the method described in section 6.2.3. Actual concrete temperatures were not used, as these were not available for all of the days where concrete was scheduled to be placed in the simulation. Note

that the calculated initial temperatures are generally conservative (higher) when compared to measured temperatures.

A summary of the initial concrete temperatures used in the analysis is given in Table 6-7. The results obtained from the analysis are shown in Figure 6-10.

Table 6-7 A summary of the initial concrete temperatures calculated using actual climate data.

Lift #	Initial Temperature (°C)	Lift #	Initial Temperature (°C)	Lift #	Initial Temperature (°C)
1	14.2	**6**	14.5	**11**	11.4
2	12.9	**7**	14.0	**12**	13.0
3	11.1	**8**	15.2	**13**	11.0
4	12.6	**9**	14.1	**14**	15.8
5	12.1	**10**	14.4	**15**	15.1

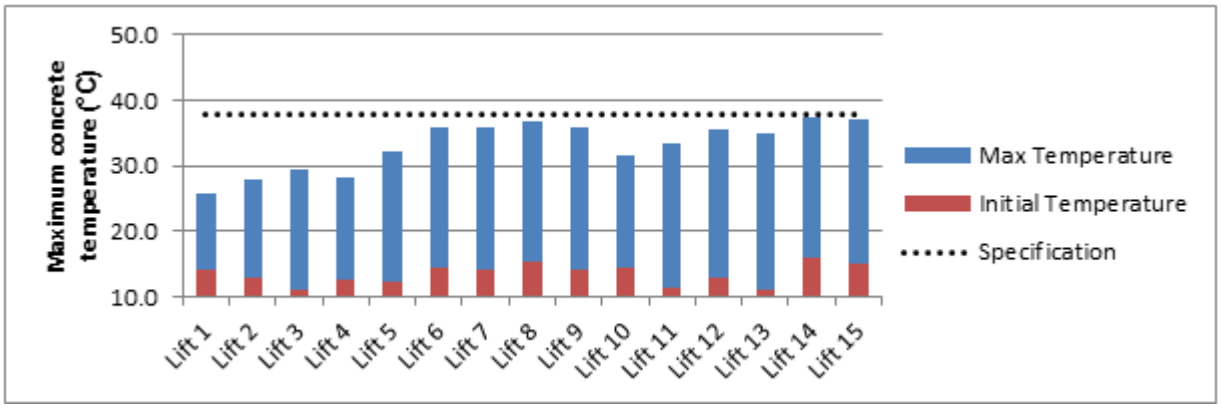

Figure 6-10 The maximum concrete temperature reached at each construction lift when using an optimised concrete mix and construction programme as well as recorded climate data.

6.7 Discussion of results

6.7.1 Baseline results

The baseline results shown in Figure 6-5 reveals that a maximum temperature of 50.4 °C occurs at the end of the simulation. The specified maximum temperature is thus exceeded by 12.4 °C. This is in line with what can be expected, given that the maximum observed temperature during the actual construction period was 47 °C, and that the simulated construction rate was significantly faster.

6.7.2 Optimised concrete mix

In section 0 the same construction schedule was used as for the baseline analysis, but the aggregate type and the cementitious content were changed. These changes resulted in a reduction in the maximum achieved temperature – 44.9 °C. This is still 6.9 °C higher than the

specified limit, but the result demonstrates the combined effect of selecting an appropriate aggregate type and optimising cementitious content.

6.7.3 Optimised construction schedule

In section 6.5.2 the optimised concrete mix developed in section 0 was implemented in the model along with an optimised construction schedule. The combination of these two interventions led to the specification being met. The maximum calculated temperature was 37.9 °C – only 0.1 °C below the limit value.

To determine an optimal construction schedule, several analyses were carried out until a solution was found that maximised the amount of construction lifts that could be placed during the first of the two construction seasons. Only the results of the final, optimised schedule are shown above. However, the process followed to determine the optimised schedule revealed that the results obtained are sensitive to ambient conditions. As average maximum and minimum temperatures and average solar radiation values were used to model ambient conditions, it is 50% likely that the conditions encountered during construction would be warmer than modelled, which might lead to the specified limit being exceeded if there is no margin for error. The model is not equipped to deal with this uncertainty. A probabilistic approach would need to be followed to obtain a more robust solution.

6.7.4 Pre-cooling of fresh concrete

By using the baseline schedule, optimised concrete mix and limiting the maximum concrete placement temperature to 13 °C, a solution was obtained with a maximum temperature of 37.2 °C. Pre-cooling aggregate is considered to be more robust than making use of seasonal temperature variations to control concrete temperature. This is because the result obtained is less sensitive to the highly variable climate conditions.

6.7.5 Demonstration of model performance

In the final analysis performed, the optimised concrete mix and construction schedule was used as input along with the climate data collected during the construction of the rehabilitation works. The maximum temperature calculated in the analysis was 37.5 °C: 0.5 °C below the specified limit. This result demonstrates that the model can be used to ensure that concrete temperatures are kept within specified limits – if one accept that the model provides accurate results to begin with.

6.8 Chapter conclusion

This chapter dealt with the implementation of the developed model. A baseline scenario was used as input into the model. The input data was processed and analysed. It was shown that implementation of the baseline scenario would lead to the specified temperature limit being exceeded.

Changes were subsequently made to the baseline scenario to find a technically feasible solution. It was shown that, by optimising both the concrete mix design and the construction schedule, a solution could be obtained that conformed to the specification. It was also shown that concrete temperatures could be kept below the specified limit by artificially cooling fresh concrete to a specified value before concrete placement when using the optimised concrete mix and baseline construction schedule.

Finally a demonstration was done to show that concrete temperatures could be kept within specified limits by optimising the concrete mix and construction schedule, even when climate data collected during construction is incorporated into the analysis.

Chapter 7: Conclusions and Recommendations

7.1 Introduction

The aim of this research was to develop a combined model to calculate and control concrete temperatures during the construction of concrete dams, that incorporates several tools and techniques developed by other researchers. Three objectives were set to meet this aim:

- Develop a temperature control model from the work of other researchers.
- Show that the analytical module included in the proposed model can be used to accurately model concrete temperature development.
- Demonstrate the model by showing that it can be used to ensure that concrete temperatures remain within specified limits during construction.

This chapter is used to discuss conclusions that can be drawn following the research carried out. Recommendations for future work are also discussed.

7.2 Conclusions

7.2.1 Objective 1: Develop the model

A generic model to ensure that concrete temperatures are kept within specified limits during construction was developed by amalgamating the work of other scholars into a combined model. Through the use of a variety of techniques, eight sets of input parameters are incorporated into a finite element analysis. An iterative process follows whereby the results from the finite element analysis are evaluated, input parameters are optimised and the optimised input parameters are again incorporated into a finite element analysis. The final result is a solution that should ensure that concrete temperatures are kept within specified limits during construction.

7.2.2 Objective 2: Accuracy of the analysis module

Modelling hydration heat development using literature based data has been shown to be inaccurate – a confirmation of the view held by Ballim & Graham (2009). It has been shown that accurate results can be obtained if literature based data is calibrated from data collected during construction. It has been shown in this investigation that peak concrete temperatures can be modelled to within 5% of the total adiabatic temperature rise when using calibrated literature based hydration data.

The investigation has shown that inaccurate modelling of foundation temperatures can lead to underestimation of concrete temperatures over the longer term. The effect of imprecisely modelled foundation temperatures on the accuracy achieved throughout the rest of the analysis appears to be limited to the longer term temperature distribution – peak concrete temperatures are still modelled accurately. Nonetheless, it has also been shown that longer term effects can be accurately modelled if foundation temperatures are accurately modelled as well.

In the light of the fact that the final aim of the research is to develop a model that can be used to keep concrete temperatures within specified limits and that peak temperatures are accurately modelled, limitations related to the model's ability to model foundation temperature is not considered to be of major concern.

7.2.3 Objective 3: Demonstration of the model

It was shown that the developed model is capable of delivering an optimised construction design that ensures that concrete temperatures remain within specified limits when using a synthesised climate record as input. It was then shown that the solution is credible by showing that concrete temperatures could be kept within specified limits by re-analysing the optimised construction design, but using actual instead of synthesised climate data as the ambient temperature boundary.

The model has only been shown to be valid through the simulation of a single case, backed up by actual climate data. Its applicability can, however, be generalised based on the validity of the model itself. In Chapter 4 it was shown that the model is not valid for (i) applications where concrete other than portland cement / fly ash blends is used, (ii) applications that include cooling pipes and (iii) applications where convection between concrete and a water body has a significant effect. By implication it is applicable to any other concrete dam application, insofar as that the application was explicitly addressed in the model.

7.3 Suggestions for future research

The model in its present form is adequate for the purpose which it was developed for, but improvements to the model are possible through future research:

- The results calculated by the model is only as good as the quality of the input used to generate them. There is a general shortage of thermal diffusivity related data that is directly applicable to the South African context. Future research could focus on compiling such data for aggregates commonly found in South Africa.

- Including the use of cooling pipes in the model could further extend the range of the model's applicability.
- Incorporating other cementitious materials, such as slagment or metakaolin, into the model can expand its applicability.
- Provision could also be made in the model to incorporate coupled thermo-structural analysis instead of using simplistic temperature specifications.
- The robustness of the final construction design determined by the model can be improved by incorporating probabilistic analysis into the model.

References

ACI Committe 207. (1993). *Cooling and Insulating Systems*. Farmington Hills.

ACI Committe 207. (1997). *Mass Concrete*. Farmington Hills.

Acquaye, L. (2006). *Effect of High Curing Temperatures on Strength, Durability and Potential of Delayed Ettreingite Formation In Mass Concrete Structures*. University of Florida.

Addis, B., & Goodman, J. (2009). Concrete mix design. In G. Owens (Ed.), *Fulton's Concrete Technology* (9th ed.). Midrand: Cement & Concrete Institute.

American Concrete Institute. (1999). *Manual of Concrete practice, Part 1: Materials and general properties of concrete*. Detroit: American Concrete Institute.

Amirouche, F. (2006). Introduction to the finite-element method. In E. A. Avallone, T. Baumeister III, & A. M. Sadegh (Eds.), *Mark's Standard Handbook for Mechanical Engineers* (11th ed.). McGraw-Hill Professional.

Ballim, Y. (2004a). A numerical model and associated calorimeter for predicting temperature profiles in mass concrete. *Cement and Concrete Composites*, *26*, 695–703. http://doi.org/10.1016/S0958-9465(03)00093-3

Ballim, Y. (2004b). Temperature rise in mass concrete elements - model development and experimental verification using concrete at Katse dam. *Journal of the South African Institution of Civil Engineering*, *46*(1), 5.

Ballim, Y., & Graham, P. C. (2004). A numerical model for predicting time-temperature profiles in concrete structures due to the heat of hydration of cementitious materials. *Research Monograph No. 8*. Cape Town: University of Cape Town, Department of Civil Engineering. Retrieved from http://www.csirg.uct.ac.za/Downloads/Mono 8.pdf

Ballim, Y., & Graham, P. C. (2009). Thermal properties of concrete and temperature development at early ages in large concrete elements. In G. Owens (Ed.), *Fulton's Concrete Technology* (9th ed.). Midrand: Cement & Concrete Institute.

Bartolucci, A. A., & Hillegass, W. B. (2010). Overview, Strengths, and Limitations of Systematic Reviews and Meta-Analyses. In F. Chiappelli (Ed.), *Evidence-Based Practice: Toward Optimizing Clinical Outcomes* (pp. 1–251). Berlin Heidelberg: Springer Berlin Heidelberg. http://doi.org/10.1007/978-3-642-05025-1

Berodier, E., & Scrivener, K. (2012). Impact of filler on hydration kinetics. In *32nd Cement and Concrete Science Conference*. Belfast: Queen's University Belfast.

Berodier, E., & Scrivener, K. (2014). Understanding the Filler Effect on the Nucleation and Growth of C-S-H. *Journal of the American Ceramic Society*, *97*(12), 3764–3773. http://doi.org/10.1111/jace.13177

Beushausen, H., Alexander, M., & Ballim, Y. (2012). Early-age properties, strength

development and heat of hydration of concrete containing various South African slags at different replacement ratios. *Construction and Building Materials*, *29*, 533–540. http://doi.org/10.1016/j.conbuildmat.2011.06.018

Brown, T. D., & Javaid, M. Y. (1970). The thermal conductivity of fresh concrete. *Matériaux et Construction*, *3*(18), 411–416. http://doi.org/10.1007/BF02478765

Campbell Scientific. (2015). GRWS100. Retrieved July 29, 2015, from Campbell

Cervera, M., Oliver, J., & Prato, T. (1999). Thermo-Chemo-Mechanical Model for Concrete. I: Hydration and Aging. *Journal of Engineering Mechanics*. http://doi.org/10.1061/(ASCE)0733-9399(1999)125:9(1018)

Cervera, M., Oliver, J., & Prato, T. (2000). Simulation of Construction of RCC Dams. I: Temperature and Aging. *Journal of Structural Engineering*, *126*(9), 1053–1061. Retrieved from http://cedb.asce.org/cgi/WWWdisplay.cgi?123232

Chen, Y. L., Wang, C. J., Li, S. Y., & Chen, L. J. (2003). The effect of construction designs on temperature field of a roller compacted concrete dam — a simulation analysis by a finite element method. *Canadian Journal of Civil Engineering*, *30*(April), 1153–1156. http://doi.org/10.1139/l03-076

Cheng, A. H. D., & Cheng, D. T. (2005). Heritage and early history of the boundary element method. *Engineering Analysis with Boundary Elements*, *29*(3), 268–302. http://doi.org/10.1016/j.enganabound.2004.12.001

Choktaweekarn, P., Saengsoy, W., & Tangtermsirikul, S. (2009a). A model for predicting the specific heat capacity of fly-ash concrete. *ScienceAsia*, *35*, 178–182. http://doi.org/10.2306/scienceasial513-1874.2009.35.178

Choktaweekarn, P., Saengsoy, W., & Tangtermsirikul, S. (2009b). A model for predicting thermal conductivity of concrete. *Magazine of Concrete Research*, *61*(4), 271–280. http://doi.org/10.1680/macr.2008.00049

Conrad, M. (2006). *A contribution to thermal stress behaviour of Roller-compacted-concrete (RCC) gravity dams: Field and Numerical Investigations*. Technischen Universitat Munchen, Munich.

Cook, R. D., Malkus, D. S., Plesha, M. E., & Witt, R. J. (2002). *Concepts and applications of finite element analysis* (4th ed.). Hoboken: John Wiley & Sons.

Czernin, W. (1980). *Cement Chemistry and Physics for Civil Engineers* (2nd ed.). Wiesbaden: Bauverlag.

da Silva, W. R. L., Šmilauer, V., & Štemberk, P. (2015). Upscaling semi-adiabatic measurements for simulating temperature evolution of mass concrete structures. *Materials and Structures*, *48*, 1031–1041. http://doi.org/10.1617/s11527-013-0213-3

Demirboğa, R., Türkmen, İ., & Karakoç, M. B. (2007). Thermo-mechanical properties of concrete containing high-volume mineral admixtures. *Building and Environment*, *42*(1),

349–354. http://doi.org/10.1016/j.buildenv.2005.08.027

Department of Water & Sanitation. (2015). Station J3R002. Retrieved July 10, 2015, from https://www.dwa.gov.za/hydrology/HyDataSets.aspx?Station=J3R002

Dooley, K. (2002). Simulation research methods. In J. Baum (Ed.), *Companion to organizations* (pp. 829–848). London: Blackwell.

Folliard, K., Juenger, M., Schindler, A., Whigham, J., Meadows, J., Riding, K., … Slatnick, S. (2008). *Prediction Model for Concrete Behavior*. Austin.

Fowkes, N., Mamboundou, H., Makinde, O., Ballim, Y., & Patini, A. (2004). Maturity effects in concrete dams. In *Mathematics in Industry Study Group South Africa 2004* (pp. 1–9).

Gaspar, A., Lopez-Caballero, F., Modaressi-Farahmand-Razavi, A., & Gomes-Correia, A. (2014). Methodology for a probabilistic analysis of an RCC gravity dam construction. Modelling of temperature, hydration degree and ageing degree fields. *Engineering Structures*, *65*, 99–110. http://doi.org/10.1016/j.engstruct.2014.02.002

Gawin, D., Pesavento, F., & Schrefler, B. a. (2006). Hygro-thermo-chemo-mechanical modelling of concrete at early ages and beyond. Part II: Shrinkage and creep of concrete. *International Journal for Numerical Methods in Engineering*, *67*(3), 332–363. http://doi.org/10.1002/nme.1615

Gibbon, G., & Ballim, Y. (1996). Laboratory test procedure to predict the thermal behaviour of concrete - Gibbon & Ballim (1996).pdf. *SAICE Journal*, *38*(3), 21–23.

Gibbon, G., Ballim, Y., & Grieve, G. (1997). A Low-Cost, Computer-Controlled Adiabatic Calorimeter for Determining the Heat of Hydration of Concrete. *Journal of Testing and Evaluation*, *25*(2), 261. http://doi.org/10.1520/JTE11488J

Graham, P. C. (2003). The heat evolution characteristics of South African cements and the implications of mass concrete structures. *Unpublished Phd Thesis*.

Graham, P. C., Ballim, Y., & Kazirukanyo, J. B. (2011). Effectiveness of the fineness of two South African Portland cements for controlling early-age temperature development in concrete. *Journal of the South African Institution of Civil Engineering*, *53*(1), 39–45.

Grieve, G. (2009). Cementitious materials. In G. Owens (Ed.), *Fulton's Concrete Technology* (9th ed.). Midrand: Cement & Concrete Institute.

Guo, L., Guo, L., Zhong, L., & Zhu, Y. (2011). Thermal conductivity and heat transfer coefficient of concrete. *Journal of Wuhan University of Technology, Materials Science Edition*, *26*(4), 791–796. http://doi.org/10.1007/s11595-011-0312-3

Hagemann, K. (2013). South Africa's Wind Power Potential. Cape Town: South African National Energy Association. Retrieved from http://www.sanea.org.za/CalendarOfEvents/2013/SANEALecturesCT/Feb13/KilianHagemann-G7RenewableEnergiesAndSAWEA.pdf

Hansen, K. D., & Forbes, B. A. (2012). Thermal Induced Cracking Performance of RCC Dams. In *6th International Symposium on Roller Compacted Concrete Dams* (pp. 23–25). Zarogoza.

Hodkinson, P., & Hodkinson, H. (2001). The stregths and limitations of case study research. In *Learning and Skills Development Agency conference*. Cambirdge: University of Leeds.

Hofstee, E. (2006). *How to construct a good disseration*. Sandton: EPE.

Hooton, R. D., Boyd, A. J., & Bhadkamkar, D. (2004). *Effect of cement fineness and C3S content on properties of concrete: A literature review*. *Portland Cement Association Research & Development*. Portland Cement Association.

Husein Malkawi, A. I., Mutasher, S. a., & Qiu, T. J. (2003). Thermal-Structural Modeling and Temperature Control of Roller Compacted Concrete Gravity Dam. *Journal of Performance of Constructed Facilities*, *17*(4), 177–187. http://doi.org/10.1061/(ASCE)0887-3828(2003)17:4(177)

Illstone, J. M., & Domone, P. L. J. (2010). *Construction materials: their nature and behaviour - 4th edition* (3rd ed.). London; New York: Spon Press. http://doi.org/10.1016/S0141-0296(02)00088-3

Kellerman, J., & Crosswell, S. (2009). Properties of fresh concrete. In G. Owens (Ed.), *Fulton's Concrete Technology* (9th ed.). Midrand: Cement & Concrete Institute.

Khan, M. I. (2002). Factors affecting the thermal properties of concrete and applicability of its prediction models. *Building and Environment*, *37*(6), 607–614. http://doi.org/10.1016/S0360-1323(01)00061-0

Kim, K.-H., Jeon, S.-E., Kim, J.-K., & Yang, S. (2003). An experimental study on thermal conductivity of concrete. *Cement and Concrete Research*, *33*(3), 363–371. http://doi.org/10.1016/S0008-8846(02)00965-1

Kim, S. G. (2010). *Effect of heat generation from cement hydration on mass concrete placement*. Iowa State University.

Klemczak, B., & Knoppik-Wróbel, A. (2011). Early age thermal and shrinkage cracks in concrete structures–description of the problem. *Architecture Civil Engineering Enviroment*, *3*, 55–70.

Koenders, E. A. B., & Van Breugel, K. (1995). *Direct solar radiation on inclined surfaces*. Delft.

Kuzmanovic, V., Savic, L., & Stefanakos, J. (2010). Long-term thermal two- and three-dimensional analysis of roller compacted concrete dams supported by monitoring verification. *Canadian Journal of Civil Engineering*, *37*, 600–610. http://doi.org/10.1139/L10-004

Lienhard IV, J. H., & Lienhard V, J. H. (2000). *A Heat Transfer Textbook* (Third). Cambridge,

Massachusetts: J.H. Lienhard V.

Liu, X., Duan, Y., Zhou, W., & Chang, X. (2012). Modeling the Piped Water Cooling of a Concrete Dam Using the Heat-Fluid Coupling Method. *Journal of Engineering Mechanics*, (September). http://doi.org/10.1061/(ASCE)EM.1943-7889.0000532

Luna, R., & Wu, Y. (2000). Simulation of Temperature and Stress Fields during RCC Dam Construction. *Journal of Construction Engineering and Management*, *126*, 381–388.

Martinelli, E., Koenders, E. A. B., & Caggiano, A. (2013). A numerical recipe for modelling hydration and heat flow in hardening concrete. *Cement and Concrete Composites*, *40*, 48–58. http://doi.org/10.1016/j.cemconcomp.2013.04.004

Merriam, S. B. (2009). *Qualitative research: A guide to design and implementation*. San Francisco: John Wiley & Sons.

Mills, A. (1992). *Heat transfer*. Burr Ridge: Irwin.

Nikishkov, G. (2010). *Programming Finite Elements in Java*. London: Springer-Verlag.

Noorzaei, J., Bayagoob, K. H., Thanoon, W. a., & Jaafar, M. S. (2006). Thermal and stress analysis of Kinta RCC dam. *Engineering Structures*, *28*(13), 1795–1802. http://doi.org/10.1016/j.engstruct.2006.03.027

Nzuza, M. H. S. (2012). *Thermo-mechanical modelling of arch dams for performance assessment*. *CoMSIRU*. University of Cape Town.

Owens, G. (Ed.). (2009). *Fulton's concrete technology*. *Fulton's Concrete Technology* (9th ed.). Midrand: Cement & Concrete Institute.

Reyes, A. G. (2007). *A preliminary evaluation of sources of geothermal energy for direct heat use*. *GNS Science Report SR2007/16*.

Riding, K., Poole, J., Schindler, A., Juenger, M., & Folliard, K. (2007a). Evaluation of Temperature Prediction Methods for Mass Concrete Members. *ACI Materials*, *103*(103), 357–365.

Riding, K., Poole, J., Schindler, A., Juenger, M., & Folliard, K. (2007b). Temperature boundary condition models for concrete bridge members. *ACI Materials Journal*, *104*(4), 379–387.

Schindler, A. (2004). Effect of temperature on hydration of cementitious materials. *ACI Materials Journal*, *101*(101), 72–81. http://doi.org/10.14359/12990

Schindler, A., & Folliard, K. (2003). Influence of Supplementary Cementing Materials. *Advances in Cement and Concrete IX Conference Colorado*, 1–10.

Schindler, A., & McCullough, F. (2002). Importance of Concrete Temperature Control During Concrete Pavement Construction in Hot Weather Conditions. *Transportation Research Record*, *1813*(January), 3–10. http://doi.org/10.3141/1813-01

Schoeman, J., & Oosthuizen, C. (2015). Monitoring the behaviour changes of an unreinforced multi domed buttress arch during rehabilitation. *Unpublished Conference Paper*.

Schulze, R. (1997). *South African Atlas of agrohydrology and -climatology*. Pretoria: Water Research Commision.

Sheibany, F., & Ghaemian, M. (2004). Three Dimensinal Thermal Stress Analysis of Concrete Arch Dams Including Earthquake Effect. *13th World Conference on Earthquake Engineering*, (488).

Swamy, R. N. (Ed.). (1986). *Cement Replacement Materials*. London: Surrey University Press. http://doi.org/10.1007/978-3-642-36721-2

Theart, P. J. (2014). *Development of a multi-criteria assessment tool to choose between housing systems for the low cost housing market*. Stellenbosch University.

Thomas, J. J. (2012). The instantaneous apparent activation energy of cement hydration measured using a novel calorimetry-based method. *Journal of the American Ceramic Society*, *95*(31489), 3291–3296. http://doi.org/10.1111/j.1551-2916.2012.05396.x

TNO DIANA BV. (2014). Diana Finite Element Analysis. Delft: TNO DIANA BV.

Townsend, C. (1981). Control of Cracking in Mass Concrete Structures. *Water Resources Technical*. Denver: United States Department of the Interior Bureau of Reclamation.

Trench, W. F. (2013). *Elementary Differential Equations with Boundary Value Problems* (1st ed.). San Antonio: Trinity University, Department of Mathematics.

U.S. Army Corps of Engineers. (1997). *Thermal Studies of Mass Concrete Structures*. *Engineering*. Washington, D.C.

Van Rooyen, G. C. (2008). *Objek modellering van fisiese probleme*. Stellenbosch: Universiteit Stellenbosch, Departement van Siviele Ingenieurswese.

Van Schalkwyk, A. (2013). *Report on Geotechnical Mapping of Foundation Excavations*. Pretoria.

Wang, R., & Aki, K. (Eds.). (1996). *Mechanics problems in geodynamics Part II*. *Tectonophysics* (Vol. 271). Basel: Birkhauser Verlag. http://doi.org/10.1016/S0040-1951(97)88192-9

World Weather Online. (2015). Oudtshoorn Monthly Climate Average, South Africa. Retrieved October 16, 2015, from http://www.worldweatheronline.com/Oudtshoorn-weather-averages/Western-Cape/ZA.aspx

Zajac, M., & Ben Haha, M. (2013). Experimental investigation and modeling of hydration and performance evolution of fly ash cement. *Materials and Structures*, *47*, 1259–1269. http://doi.org/10.1617/s11527-013-0126-1

Zeng, Q., Li, K., Fen-Chong, T., & Dangla, P. (2012). Determination of cement hydration and

pozzolanic reaction extents for fly-ash cement pastes. *Construction and Building Materials*, *27*(1), 560–569. http://doi.org/10.1016/j.conbuildmat.2011.07.007

Zill, D. G., & Cullen, M. R. (2006). *Advanced Engineering Mathematics* (3rd ed.). Sudbury: Jones and Bartlett Publishers.